



LIBRARIES

UNIVERSITY OF WISCONSIN-MADISON

Tracer study for characterization of groundwater movement and contaminant transport in fractured dolomite. [DNR-101] 1998

Muldoon, Maureen A.; Bradbury, K. R.

Madison, Wisconsin: Wisconsin Geological and Natural History Survey, 1998

<https://digital.library.wisc.edu/1711.dl/QNF727QNJKVV382>

<http://rightsstatements.org/vocab/InC/1.0/>

For information on re-use see:

<http://digital.library.wisc.edu/1711.dl/Copyright>

The libraries provide public access to a wide range of material, including online exhibits, digitized collections, archival finding aids, our catalog, online articles, and a growing range of materials in many media.

When possible, we provide rights information in catalog records, finding aids, and other metadata that accompanies collections or items. However, it is always the user's obligation to evaluate copyright and rights issues in light of their own use.

**TRACER STUDY FOR CHARACTERIZATION OF GROUNDWATER MOVEMENT
AND CONTAMINANT TRANSPORT IN FRACTURED DOLOMITE**

Final Report to the Wisconsin Department of Natural Resources

by

Maureen A. Muldoon
Kenneth R. Bradbury

Wisconsin Geological and Natural History Survey

WATER RESOURCES INSTITUTE
LIBRARY
UNIVERSITY OF WISCONSIN
1975 WILLOW DRIVE
MADISON, WI 53706-1103
608-262-3069

WOFR 98-2

May, 1998

ABSTRACT

Fractured-carbonate aquifers are important, but vulnerable, sources of drinking water in Wisconsin. This study was designed to 1) provide a better understanding of the advective flow rates and hydraulic conductivity distributions of shallow, fractured-dolomite aquifers; 2) generate a data set for use in evaluating existing fracture-flow computer codes; 3) evaluate whether it is appropriate to approximate the fractured dolomite as an equivalent porous medium at site-specific scales; and 4) test the effectiveness of monitoring wells in fractured-rock settings.

The authors characterized and instrumented a small (125 x 75 ft) study site located in an active dolomite quarry in Door County, WI. The quarry floor was cleared of sediment and vertical fractures were mapped and digitized. Eighteen boreholes, including five coreholes, were drilled to a depth of 35 ft. Borehole geophysical logs revealed several laterally extensive horizontal fractures and dissolution zones. Flowmeter and short-interval packer testing identified which of these features were hydraulically important. The monitoring system, consisting of multi-level samplers installed in 11 of the boreholes, was designed to monitor four horizontal fractures and two dissolution zones. Data on the hydraulic conductivity of the fracture network were obtained from a multi-well pumping test conducted with eight 35-ft open boreholes, a second pumping test conducted after the multi-level samplers had been installed, and packer tests conducted with a 0.75-ft straddle interval. The distribution of hydraulic head was monitored in both open boreholes as well as in the discrete intervals of the multi-level samplers. Several controlled-gradient and one natural-gradient tracer tests completed at the site yielded horizontal and vertical groundwater velocities on the order of 10's to 100's of ft/day. A two-dimensional discrete fracture flow model was used to simulate one of the controlled-gradient tracer tests. Using measured data on fracture characteristics, the model reproduced data from the tracer experiment relatively well.

This study has important implications for the design of groundwater monitoring systems in fractured-carbonate settings. Results suggest that standard investigative and monitoring techniques may not be appropriate to characterize transport at site-specific scales in fractured-carbonate aquifers. Hydraulic conductivity values determined from the open-hole pumping test under-predicted tracer velocity by several orders of magnitude. Comparing the head data from the open boreholes with the more complex distribution of head determined from the multi-level samplers, it is clear that choice of monitoring method significantly influences measured head distributions. Tracer results indicate that hydraulic data alone are poor predictors of transport at small scales; transport appears to be dominated by fracture channels and small variations in fracture and matrix characteristics. Tracer distributions and model results suggest that contaminants will be difficult to detect in these settings and that monitoring systems designed to monitor the high-permeability pathways are more likely to intercept contaminants.

Detailed characterizations of fracture networks and other aquifer heterogeneities are necessary for accurate monitoring, assessment, and modeling of groundwater movement in fractured carbonate rocks. Fracture-network models are more appropriate than porous-medium models for simulating flow and transport in these environments; future investigations should collect appropriate data for the use of these models.

ACKNOWLEDGEMENTS

Many people have contributed to this project. We'd like to thank Ivan Bissen for granting permission to conduct this research in the Sturgeon Bay Sand and Gravel quarry and his continued cooperation with ongoing research at the site. This project has been quite field-work intensive and many people have assisted with various aspects of the fieldwork including Bruce Brown, Dave Johnson, Fred Madison, and Walter Hall for assistance with coring. Fred Madison endured a miserably cold day of piezometer and datalogger installation. Jamie Robertson assisted with caliper logging. Peter Roffers and Reed Ruck mapped fractures on the quarry floor. The 1993 and 1994 Field Hydrogeology class assisted with a pumping test, water sampling, scanline mapping, and slug tests. A crew of folks assisted with the "multi-level" pumping test including Michelle Bridson, Jeremy Craven, Tom Dueppen, Sheila Haskins, Dave Johnson, Huckle Kuhner, Dave Misky, Bill Orr, Todd Rayne, Nils Richardson and Pete Roffers. The tracer tests presented technical as well as logistical challenges. We'd like to thank Richelle Allen-King for designing "manifold" samplers capable of pulling several samples at once. These tests were quite labor intensive, requiring many helpers including Jeremy Craven, Dave Misky, Brian Parsons, Pete Roffers, and Sue Swanson. Special thanks go to Tom Dueppen who helped with two separate tests including a week of sample collection for the natural-gradient test.

As this project generated many data, there was also considerable office work to be completed and again many folks have helped in various ways. We'd like to thank Chris Zahm for preliminary core descriptions and Toni Simo for providing more detailed analysis. Jill Maliszewski cut many feet of core so that it could be described in detail. Kris Lund, her students, and Jeremy Craven completed the majority of the ion-selective electrode analyses. Subsequent ion chromatography analyses were conducted in Jim Bockheim's laboratory in the Soil Science Department. Jay Peterson was instrumental in getting the ion chromatograph functional. Jodi VanderVelden, Bill Batten, Kathy Larson, and Kate Griffin completed much of the ion chromatography work. Pete Roffers provided much assistance including reduction of slug-test data, digitizing the fracture map, and entering all the fracture attribute data. Several former and current members of the Survey staff have assisted in variety of ways and we'd like to thank Mike Bohn, Nils Richardson, and Mike Czechanski.

The Wisconsin Department of Natural Resources provided funding for this project through the Groundwater Management Practice Monitoring Program, which receives appropriations from the Groundwater Account.

WATER RESOURCES INSTITUTE
 LIBRARY
 UNIVERSITY OF WISCONSIN
 1975 WILLOW DRIVE
 MADISON, WI 53706-1103
 608-262-3069

CONTENTS

| | <u>Page</u> |
|---|-------------|
| ABSTRACT | ii |
| ACKNOWLEDGEMENTS | iii |
| CONTENTS | iv |
| Chapter 1. INTRODUCTION | 1 |
| Project Background | |
| Purpose and Scope | 2 |
| Hydrogeologic Setting | 2 |
| Chapter 2. HYDROGEOLOGIC CHARACTERIZATION | 5 |
| Site Selection | 5 |
| Geology | 7 |
| Core Description | 10 |
| Geophysical Logs | 12 |
| Heat-pulse Flowmeter Logging | 12 |
| Fracture Distribution | 15 |
| Vertical Fractures | 15 |
| Horizontal Fractures | 19 |
| Monitoring System | 19 |
| Hydraulic Conductivity Testing | 23 |
| Open-hole Pumping Test | 23 |
| Multi-level Pumping Test | 25 |
| Packer Tests | 25 |
| Correlation Between Hydraulic Conductivity Distribution and Geologic Data | 28 |
| Head Distribution | 28 |
| Open Boreholes | 28 |
| Multi-level Samplers | 32 |
| Implications for Monitoring | 35 |
| Chapter 3. TRACER TESTS | 38 |
| Test Design and Methodology | 38 |
| Test Configuration | 38 |
| Natural-gradient Tests | 38 |
| Controlled-gradient Tests | 39 |
| Choice of Tracer | 40 |
| Tracer Injection | 41 |
| Monitoring Method and Frequency | 41 |

| | |
|---|----|
| Sample Analysis | 43 |
| Ion-selective electrode analyses | 45 |
| Ion-chromatography analyses | 45 |
| Background Chemistry | 45 |
| Description of Tracer Tests and Results | 46 |
| Controlled-gradient Bromide Test | 46 |
| Controlled-gradient Temperature Tests | 49 |
| Controlled-gradient Iodide Test | 54 |
| Controlled-gradient Chloride Test | 54 |
| Natural-gradient Chloride and Bromide Test | 60 |
| Chloride Results | 61 |
| Bromide Results | 68 |
| Discussion | 68 |
| Implications for Monitoring | 70 |
| | |
| Chapter 4. APPLICATION OF A FRACTURE-FLOW MODEL | 71 |
| Purpose | 71 |
| Model Selection | 71 |
| Model Objectives | 71 |
| Model Configuration | 72 |
| Location of Section | 72 |
| Boundary Conditions | 72 |
| Input Parameters | 72 |
| Modeling Procedure | 74 |
| Model Results | 74 |
| Synthetic Fracture Network | 74 |
| Groundwater Velocities and Particle Pathways | 74 |
| Simulated Tracer Concentrations | 76 |
| Discussion | 76 |
| | |
| Chapter 5. CONCLUSIONS | 79 |
| | |
| REFERENCES | 81 |

FIGURES

| | <u>Page</u> |
|---|-------------|
| 1. Location of study area. | 3 |
| 2. Summary of Door County bedrock stratigraphy. | 4 |
| 3. Location of quarries examined as possible research sites. | 6 |
| 4. Map showing location of Bissen Quarry in southern Door County. | 8 |
| 5. Photograph of detailed study site in Bissen Quarry. | 8 |
| 6. Diagram of study site showing location of boreholes. Fractures > 5 ft length are also shown. | 10 |
| 7. Stratigraphic log from hole 5. | 11 |
| 8. Geophysical logs for hole 5 with neutron log for hole 11. | 14 |
| 9. Heat-pulse flowmeter logs for hole 13. | 16 |
| 10. Map of quarry floor showing all fractures greater than 1 ft length. | 17 |
| 11. Fracture orientation and length data. | 18 |
| 12. Schematic block diagram of site. | 22 |
| 13. Block diagram of open intervals of monitoring system. | 22 |
| 14. Drawdown map for open-hole pumping test. | 24 |
| 15. Set-up and drawdown curves for multi-level pumping test. | 26 |
| 16. Fence diagram of hydraulic conductivity profiles of eight holes. | 29 |
| 17. Histogram of hydraulic conductivity values measured with short-interval packer device. | 29 |
| 18. Correlation between hydraulic conductivity distribution and stratigraphic data. | 30 |
| 19. Hydraulic head distribution in open boreholes. | 31 |
| 20. Water-levels versus time for piezometers in hole 6 and multi-level ports in hole 14. | 33 |
| 21. Hydraulic head distribution for specific fracture and dissolution zones. | 34 |
| 22. Time of travel comparison | 36 |
| 23. Manifold sampler used in tracer tests. | 44 |
| 24. Set-up for controlled-gradient bromide tracer test. | 48 |
| 25. Breakthrough curves for controlled-gradient bromide tracer test. | 50 |
| 26. Background temperature fluctuations at port 12-4. | 52 |
| 27. Results of first temperature tracer test. | 52 |
| 28. Results from second temperature tracer test. | 53 |
| 29. Results from tracer test using both temperature and bromide. | 53 |
| 30. Set-up for controlled-gradient chloride test. | 55 |
| 31. Breakthrough curves for holes 15 and 16 during the chloride tracer test. | 58 |
| 32. Breakthrough curves for holes 17 and 18 during the chloride tracer test. | 59 |
| 33. Set-up for controlled-gradient tracer test. | 61 |
| 34. Hydraulic head distribution measured 8/9/94. | 62 |
| 35. Chloride breakthrough curves for hole 15 during the natural-gradient test. | 64 |
| 36. Chloride breakthrough curves for the upper ports in hole 12. | 65 |
| 37. Chloride breakthrough curves for the lower ports in holes 12. | 66 |
| 38. Chloride and bromide breakthrough curves for ports in holes 14 and 16. | 67 |
| 39. Bromide breakthrough curves for monitoring ports in hole 15. | 69 |
| 40. Location of SDF model cross section. | 73 |

| | | |
|-----|---|----|
| 41. | Field-measured heads along the model cross section. | 73 |
| 42. | Boundary conditions for SDF model. | 75 |
| 43. | One realization of the simulated fracture network showing simulated hydraulic head. | 75 |
| 44. | One realization of particle pathways generated by SDF model. | 77 |
| 45. | Concentration probabilities based on stochastic particle paths. | 77 |
| 46. | Simulated breakthrough at the withdrawal well. | 78 |

TABLES

| | <u>Page</u> | |
|-----|---|----|
| 1. | Summary of construction data for open boreholes at Bissen Quarry. | 9 |
| 2. | Logs collected from boreholes prior to installation of monitoring system. | 13 |
| 3. | Summary of construction data for multi-level sampling systems at Bissen Quarry. | 20 |
| 4. | Summary of construction data for piezometers at Bissen Quarry. | 23 |
| 5. | Results from the open-hole pumping test. | 24 |
| 6. | Results from the pumping test monitored with multi-level samplers. | 27 |
| 7. | Comparison of measured hydraulic conductivity values and calculated travel times. | 36 |
| 8. | Background Cl ⁻ and Br ⁻ values from Bissen Quarry. | 47 |
| 9. | Summary of results from controlled-gradient bromide tracer test. | 49 |
| 10. | Summary of controlled-gradient temperature tracer tests. | 51 |
| 11. | Summary of results from controlled-gradient chloride tracer test. | 57 |
| 12. | Summary of results from natural-gradient tracer test. | 63 |
| 13. | Fracture input data for the SDF model. | 72 |

CHAPTER 1

INTRODUCTION

Project Background

Fractured-carbonate aquifers, including the Silurian dolomite of eastern Wisconsin and the Sinnipee and Prairie du Chien (dolomite and limestone) in southern and western Wisconsin are important sources of drinking water for the state. In places, thin soils and numerous fractures near the land surface combine to make these aquifers particularly susceptible to contamination.

Predicting groundwater movement and contaminant transport in fractured carbonates can be difficult. Groundwater flow in these aquifers is typically characterized by rapid flow through inter-connected fractures, while lower-permeability matrix blocks provide the majority of storage for the aquifer. Dissolution enhances both primary and secondary porosity and may lead to the development of well-integrated preferential flow paths.

Hydrogeologic investigations in these aquifers usually fall somewhere between two very different approaches to aquifer characterization. The continuum approach utilizes "averaged" parameters measured over some representative volume of rock. This approach assumes that the fractured aquifer approximates an equivalent porous medium at some working scale and that the properties of individual fractures are not as important as the properties of large regions or volumes of fractured material. At the opposite end of the continuum, the fracture network approach attempts to characterize the geometry of the fracture system and various properties of discrete fractures such as length, orientation, and aperture. The appropriateness of each of these approaches to aquifer characterization is largely a function of the type and scale of the problem.

The Silurian dolomite of the Door Peninsula has traditionally been treated as an equivalent porous medium and several regional models of groundwater flow have been constructed and successfully calibrated using this assumption (Bradbury 1982; Nauta, 1987; and Cherkauer and others, 1992). While this approach has been successfully employed to predict flow at regional scales, it may be inadequate to predict groundwater flowpaths or travel times at site-specific scales. Recent research by the Wisconsin Geological and Natural History Survey (WGNHS) has included efforts to determine at what scales the porous-medium approximation may be valid in the Silurian dolomite (Bradbury and others, 1991; Bradbury and Muldoon, 1994). Recently, several fracture-network models capable of characterizing two- and three-dimensional fracture geometries have been developed (Rouleau, 1988; Dershowitz and others, 1993). Fracture-network models have been successfully applied to research problems at site-specific scales in fractured-crystalline rock settings (Dershowitz and others, 1989; Cacas and others, 1990a,b). These models have not been tested in fractured-carbonate aquifers.

Tracer experiments have long been used as a tool for understanding groundwater movement (Slichter, 1905). Recently, detailed tracer studies in relatively homogeneous granular aquifers

(e.g., Garabedian and others, 1991; Hess and others, 1992; Moltyaner and others, 1993; Mackay and others, 1986; Sudicky, 1986) have contributed to a better understanding of groundwater flow processes and the important role that heterogeneities play in solute transport. If one views fractures and dissolution zones as discrete heterogeneities, the challenge of predicting transport in fractured carbonates may depend on characterization of these discrete features. This study combines detailed hydrogeologic characterization, tracer studies, and modeling experiments in an effort to gain a better understanding of groundwater movement in fractured carbonates.

Purpose and Scope

The primary goal of this project was to obtain a better understanding of groundwater movement in a shallow, fractured-carbonate aquifer. Specifically, the study was designed to 1) provide a better understanding of the hydrogeology of the Silurian dolomite in terms of advective flow rates, effective porosity, and hydraulic conductivity distributions; 2) generate a data set that can be used to evaluate existing fracture-flow computer codes; 3) help determine whether it is appropriate to approximate the fractured dolomite as an equivalent porous medium at site-specific scales; and 4) test the effectiveness of monitoring wells in a fractured-rock setting.

In order to meet these objectives, the project was conducted in a phased approach outlined below.

Phase 1. Identify an abandoned quarry in the fractured dolomite of Door County, Wisconsin for tracer tests. Perform a detailed hydrogeologic site characterization, and install instrumentation.

Phase 2. Perform a series of tracer tests to define groundwater flow paths, advective flow rates, and monitor tracer distribution.

Phase 3. Determine if existing two- and three-dimensional discrete fracture computer codes can be calibrated to site conditions and used to predict tracer distributions.

Phase 4. Draw conclusions about the applicability of a porous-media model of the fractured dolomite at site-specific scales.

Hydrogeologic Setting

The Silurian dolomite forms an important regional aquifer along the western flank of the Michigan Basin from Canada to northeastern Illinois (figure 1). In Door County, the dolomite lies beneath a thin cover of unlithified Pleistocene sediment and forms a prominent escarpment along the western edge of the county, adjacent to Green Bay. The Silurian strata dip gently into the Michigan basin to the east-southeast at approximately 0.5 degrees or 40-50 ft per mile. Erosion has beveled the dolomite aquifer into an eastward thickening wedge that thickens from 25 ft along the shore of Green Bay near Little Sturgeon Bay to more than 550 ft near Whitefish Dunes State Park on the eastern shore of the peninsula.

The Silurian aquifer provides the primary source of groundwater for Door county residents. The area receives about 76.5 cm/yr of precipitation, including both rain and snow. Due to the thin soils and permeable bedrock of the study area, runoff is negligible and approximately 24.1 cm/yr recharges the groundwater (Bradbury, 1989). Groundwater recharge does not occur uniformly

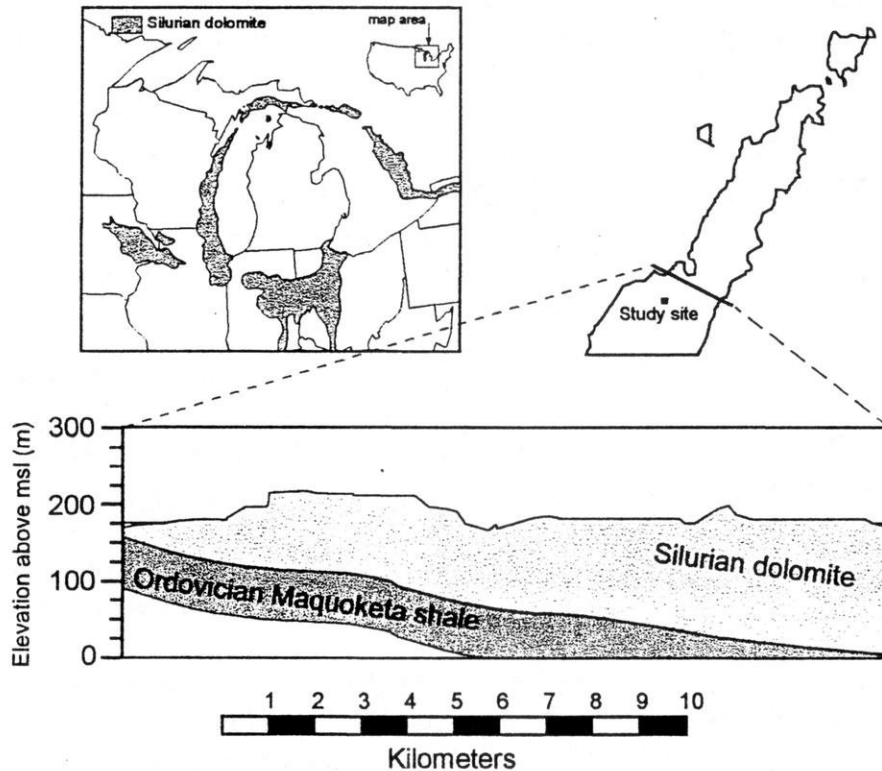


Figure 1. Location of study site including map of generalized Silurian subcrop and generalized geologic cross-section of southern Door County.

throughout the year; the primary recharge period is during spring snowmelt and additional recharge usually occurs in the fall of the year when vegetation has gone quiescent. Groundwater flow is characterized by recharge through vertical fractures and rapid lateral movement along horizontal high-permeability zones (Sherrill, 1978; Bradbury and Muldoon, 1992) that appear to be laterally continuous on the scale of miles (Gianniny and others, 1996).

Previous hydrogeology studies in Door County have generally divided the dolomite into the Upper Niagaran and Lower Alexandrian Series and included all the Silurian carbonate rocks in the "Dolomite Aquifer System" (Sherrill, 1978; Bradbury, 1982; Nauta, 1987). Finer scale divisions of stratigraphic formations within these series have been long recognized (Chamberlin, 1877; Shrock, 1940; Sherrill, 1978). Figure 2 summarizes the bedrock stratigraphy of Door County. Because the stratigraphic units are somewhat difficult to distinguish and because it was assumed that fracture zones (Sherrill, 1978) rather than lithologies controlled groundwater movement, stratigraphy has not been incorporated into many groundwater investigations. Recent work in southeastern Wisconsin (Rovey and Cherkauer, 1994) and in Door County (Muldoon and Bradbury, 1990; Gianniny and others, 1996) suggests that lithologies and horizontal stratigraphic discontinuities in the Silurian dolomite play a more important role in groundwater movement than was previously assumed. Silurian stratigraphy consists of predictable alternations of two characteristic facies: restricted marine cyclic facies deposited in supratidal to shallow tidal

environments and open marine, fossil-rich facies deposited in subtidal environments. The vertical lithologic succession shows horizontal stratigraphic discontinuities such as depositional bedding planes, diagenetic surfaces, cycle and sequence boundaries, and stylolites, some of which have been enlarged by dissolution, and preferred flow pathways have developed.

| SERIES | GROUP | FORMATION | MEMBER |
|--------------------------------------|---------------------------------|------------|---------|
| N I A G A R A N | | Engadine | |
| | | Manistique | Cordell |
| | Schoolcraft | | |
| | B B u l r u n f t f | Hendricks | |
| | | Byron | |
| ALEX-ANDRIAN | | Mayville | |
| | | Maquoketa | |

Figure 2. Summary of Door County bedrock stratigraphy (from Bradbury and Muldoon, 1992).

CHAPTER 2

HYDROGEOLOGIC CHARACTERIZATION

Designing reliable and efficient site characterization procedures and monitoring systems in fractured-carbonate settings is challenging due to the complex flow and transmission characteristics of these aquifers in which discrete heterogeneities (such as bedding planes, fractures, and dissolution zones) provide rapid flowpaths and the matrix portion of the aquifer provides most of the storage. Accurate predictions of groundwater movement and contaminant transport depend on adequate characterization of aquifer heterogeneities; if one views fractures as discrete heterogeneities, the challenge of predicting transport in fractured rocks is one of characterizing aquifer properties at a scale that captures the variability of these discrete heterogeneities.

Standard hydrogeologic field techniques, including standard monitoring wells, may not be capable of providing useful information in fractured-rock environments. The monitoring well is the standard measuring point for both obtaining representative ground-water samples and determining aquifer properties. Implicit in the design of a monitoring well is the idea that the volume of aquifer material encompassed by the open portion of the well will provide representative measures of water-levels, aquifer properties (such as hydraulic conductivity, porosity, and storativity), and water chemistry. In aquifers where flow is primarily through widely-spaced discrete high-permeability features, the standard monitoring well may not provide representative data.

At Bissen Quarry, the geology, fracture distributions and characteristics, as well as hydraulic properties have been determined in great detail and provide the data necessary to evaluate numerical models of fracture flow. We have measured aquifer properties using both standard monitoring techniques (*i.e.* "open-hole" pumping tests) as well as "short-interval" hydraulic tests to help determine which methods would yield hydraulic conductivities that could adequately predict groundwater or contaminant travel times at site-specific scales.

Site Selection and Description

When considering a location to conduct this research, we chose to look for sites in quarries for the following reasons: the depth to groundwater would be minimized, resulting in lower drilling and monitoring costs; and an exposed bedrock surface would facilitate characterization of the fracture pattern. We evaluated quarries throughout Door County, and chose four sites for coring based upon estimated depth to water, location near discharge areas, and number of downgradient domestic wells. Drill sites are shown in figure 3; one to three holes were drilled at each site and the resulting boreholes were abandoned. The core from these holes is stored in the WGNHS core repository and have the following Geologic Log Numbers: Spring Road DR401, DR402, DR403; Little Quarry DR404; Bissen Quarry DR421, DR422, DR423, DR424, DR425. Lilly Bay Road had an unexpectedly thick cover of unlithified sediment and no core was recovered from this site.

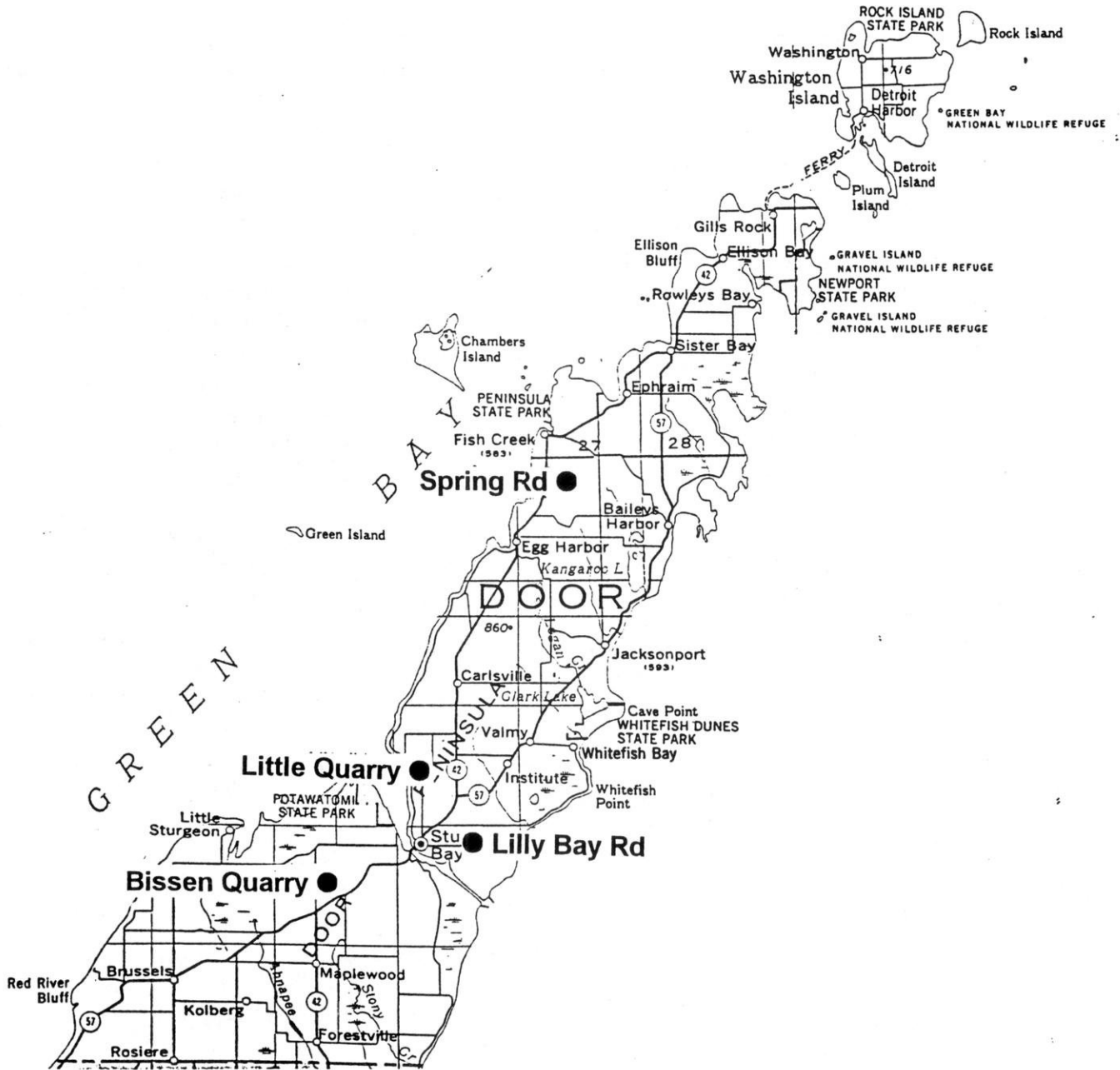


Figure 3. Location of quarries examined as possible research sites. Bissen Quarry was selected as the study site; it is located approximately 4.5 miles southwest of the city of Sturgeon Bay.

Bissen Quarry was selected as the research site because it has 1) a shallow water table, 2) variable porosity with depth, 3) proximity to a discharge area, and 4) few downgradient domestic wells.

Sherrill's (1978) water-table map suggests that the site lies approximately 3/4 mile west of a groundwater divide and that flow is primarily to the west (figure 4). A small creek located approximately 1/2 mile west of the site may intercept shallow flow, regional discharge is to Green Bay.

A small site, on the northern edge of the quarry was chosen for detailed characterization. The study site (figure 5) measures approximately 125 x 75 ft; in this area, we cleared the quarry floor of sediment and installed 18 boreholes. These include five coreholes (DR421 to DR425), three large-diameter (6-inch) boreholes (DR426 to DR428), and ten small-diameter (3-inch) boreholes (DR429 to DR438) installed using air-rotary drilling methods. Figure 6 is a map of the study site showing boreholes locations. Construction information and geophysical logs are on file at the WGNHS and are referenced to the Geologic Log numbers DR421 to DR438. In this report, we will refer to the holes as simply holes 1 to 18. Table 1 summarizes data on borehole identification numbers, diameter, casing stick-up, measuring point elevation, total depth, and drilling method. Measuring-point elevations, determined by-rod-and-level surveying, are relative to the top of well 5 which was arbitrarily set at 100 ft.

All holes are approximately 35 ft deep and were cased to approximately 2 ft depth prior to installation of the monitoring system. Figure 6 shows location of the boreholes relative to the mapped vertical fractures at the site. The five coreholes (holes 1-5) are widely spaced in order to better characterize the geology at the site. The small-diameter boreholes (holes 9-18) were placed in a grid pattern with holes approximately 15 ft apart. Five of the small-diameter holes were drilled along vertical fracture traces (holes 10, 12, 15, 16, 17); hole 18 was drilled off the vertical fracture approximately 4 ft from hole 17. We had hoped that this configuration would allow us to examine movement from the vertical fracture into a matrix block, however, hole 18 also appears to intersect a sub-vertical fracture at depth.

Geology

Recent work on the Silurian dolomite in southeastern Wisconsin (Rovey and Cherkauer, 1994) and in Door County (Muldoon and Bradbury, 1990; Waldhuetter, 1994; Gianniny and others, 1996; Hegrenes, 1996; Muldoon, 1996) suggests that lithologies and horizontal stratigraphic discontinuities control both the distribution of preferred flowpaths and storage capacity. Dissolution along horizontal stratigraphic discontinuities such as depositional bedding planes, diagenetic surfaces, cycle and sequence boundaries, and stylolites has led to the development of preferred flowpaths. From Gianniny and others' (1996) work, it is apparent that high-conductivity zones in the Silurian dolomite aquifer are laterally continuous at regional scales and appear to follow and be controlled by the stratigraphy. Matrix porosity, which varies following depositional environments and diagenesis, provides the majority of storage for the aquifer.

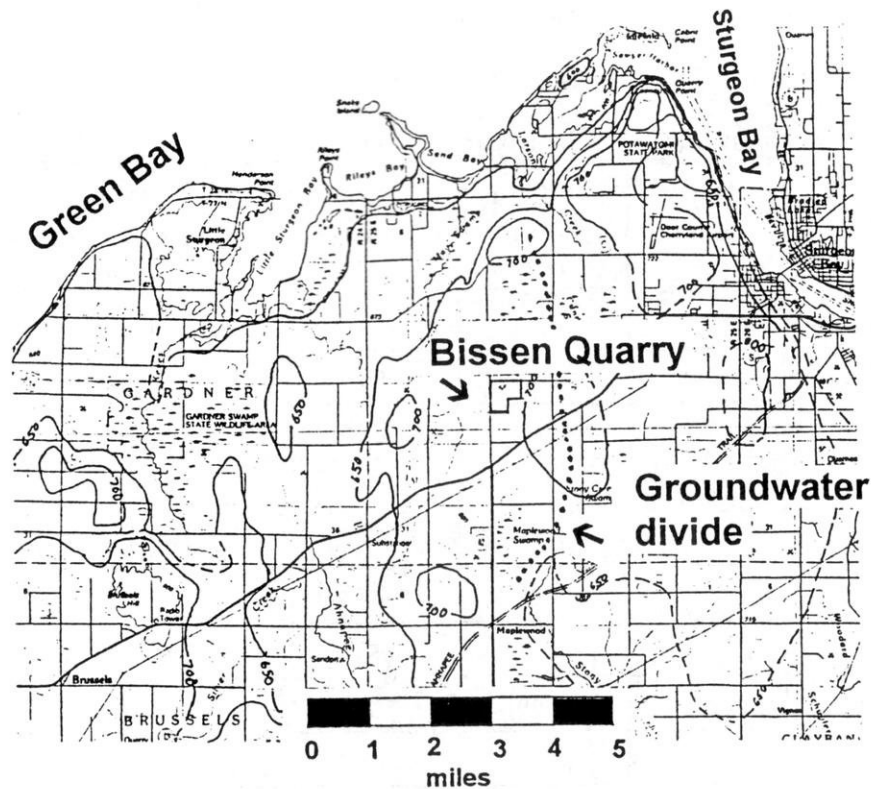


Figure 4. Map showing location of Bissen Quarry in southern Door County. Contours have been copied from Sherrill's (1978) regional water-table map, The dotted line indicates a local groundwater divide; Green Bay to the west, Sturgeon Bay to the north, and Lake Michigan to the east are regional discharge areas.

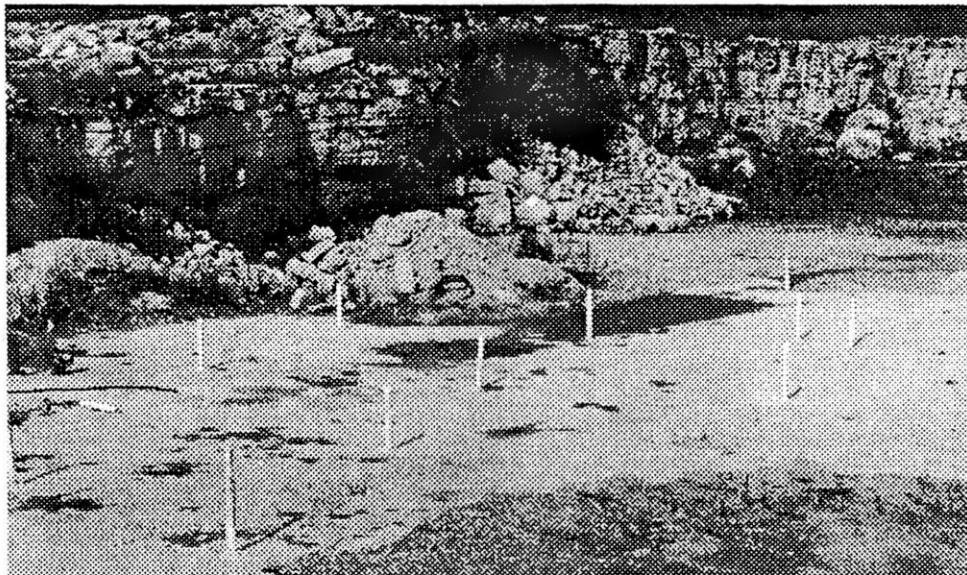


Figure 5. Photograph of detailed study site in Bissen Quarry. Holes are spaced approximately 15 ft apart. Note prominent bedding planes on back wall of quarry and area where quarry floor has been cleared of sediment.

Table 1. Data for open boreholes at Bissen Quarry

| Hole | WGNHS ID | Hole diam (in) | TOC to ground (ft) | Meas Point Elev (ft) | Hole Depth (ft) rel to TOC | Drilling method |
|------|----------|----------------|--------------------|----------------------|----------------------------|-----------------|
| 1 | DR-421 | 3 | 2.9 | 99.495 | 36.31 | coring |
| 2 | DR-422 | 3 | 2.98 | 99.21 | 35.735 | coring |
| 3 | DR-423 | 3 | 3.135 | 99.069 | 38.555 | coring |
| 4 | DR-424 | 3 | 3.2 | 99.07 | 38.325 | coring |
| 5 | DR-425 | 3 | 3.57 | 100.0 | 39.715 | coring |
| 6 | DR-426 | 6 | 1.9 | 98.42 | 37.73 | air rotary |
| 7 | DR-427 | 6 | 2.14 | 98.40 | 38.34 | air rotary |
| 8 | DR-428 | 6 | 2.039 | 98.419 | 38.15 | air rotary |
| 9 | DR-429 | 3 | 2.555 | 99.01 | 36.05 | air hammer |
| 10 | DR-430 | 3 | 2.92 | 99.285 | 37.75 | air hammer |
| 11 | DR-431 | 3 | 2.634 | 98.999 | 37.12 | air hammer |
| 12 | DR-432 | 3 | 2.573 | 98.778 | 37.80 | air hammer |
| 13 | DR-433 | 3 | 2.475 | 98.561 | 37.47 | air hammer |
| 14 | DR-434 | 3 | 2.652 | 98.847 | 37.35 | air hammer |
| 15 | DR-435 | 3 | 2.658 | 98.653 | 36.75 | air hammer |
| 16 | DR-436 | 3 | 2.752 | 98.667 | 37.5 | air hammer |
| 17 | DR-437 | 3 | 2.564 | 98.909 | 37.68 | air hammer |
| 18 | DR-438 | 3 | 2.595 | 98.84 | 37.58 | air hammer |

The rocks in the subsurface Bissen Quarry belong to the Byron Formation; while the Hendricks Formation is exposed in the quarry walls. The Byron Formation, ranging in thickness from 75 to 82 ft (Waldhuetter, 1994), was deposited in subtidal to supratidal environments and is characterized by cyclic alternations of bioturbated mudstones and very fine-grained, laminitic mudstones. Mudcracks and interclastic lenses suggest repeated instances of intermittent sub-aerial exposure throughout this formation. A measured section for Bissen Quarry summarizes the lithologies, interpreted lithofacies, and estimated porosity distribution for rocks exposed in the quarry walls (Waldhuetter, 1994; p. 202-204). While Waldhuetter classifies the quarry walls as Byron Formation; geophysical logs suggest that the Hendricks/Byron contact is approximately at the level of the quarry floor.

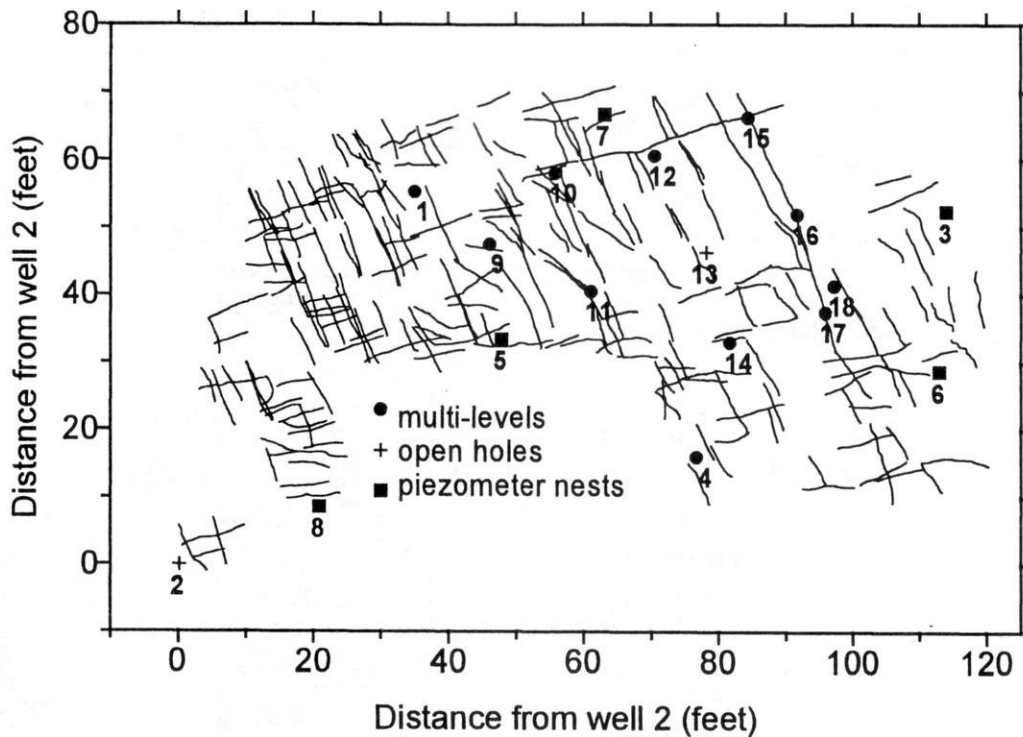


Figure 6. Diagram of study site showing location of boreholes. Fractures > 5 ft length are also shown.

Core Description

A description of the core recovered from hole 5, completed by Dr. J.A. Simo (UW-Madison) is summarized in figure 7. The upper 14 ft of core consists of medium bedded coarse dolomite with open marine fauna (corals, stromatoporids, brachiopods and gastropods). There is a minor laminite at 5-6 ft depth. The lower part of the core (25.5 - 36.5 ft depth) also belongs to the open marine facies.

The middle portion of the core (14-25.5 ft depth) belongs to the restricted marine cyclic facies characterized by shallowing-upward cycles consisting of an initial marine flooding followed by sediment filling. Complete cycles contain a lower part with mudstones, and an upper part characterized by algal lamination; most of the cycles are capped by a diagenetic cap and overlain by a surface with depositional relief. The basal mudstones may be bioturbated, often contain fenestral porosity, and discontinuous brecciated horizons may occur within the mudstones. The upper part of the cycles consist of laminated facies, which may contain domal stromatolites at the base, and thinly and crinkly laminites at the top. These laminated lithologies are typically very well-cemented and may have a brownish color. The diagenetic cap varies in thickness and occasionally is truncated by the overlying surface. Cemented sheet-cracks, and vertical cracks are very common and occasional micro-karst affects the diagenetic cap. Cycle boundaries separate the very well cemented laminite/diagenetic cap and the overlying less cemented mudstones. At

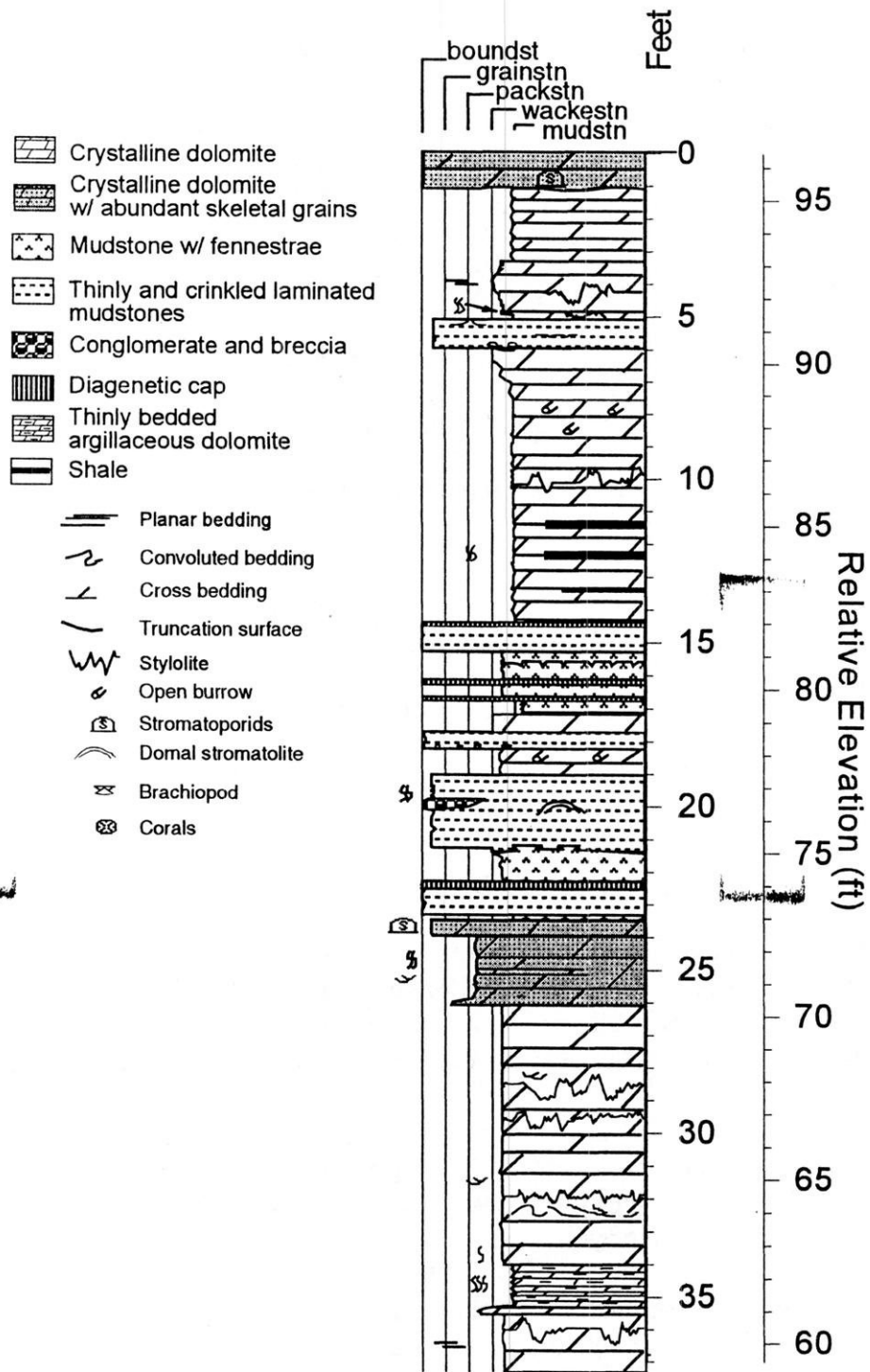


Figure 7. Stratigraphic log from hole 5 showing rock textures and lithofacies (log measured, described, and drafted by J.A. Simo, UW-Madison). Legend is shown to left; on the right side of the diagram, multiple axes show depth in both feet below ground surface and elevation (relative to an arbitrary datum).

these contacts, thin and discontinuous organic-rich mudstones may occur and often represent a horizontal discontinuity.

Rock textures range from mudstones to boundstones (Dunham's, 1962 classification). Dolomite crystal size varies from 500 microns (very coarse) to 60 microns (very fine) and controls the amount of matrix or intercrystalline porosity. Secondary minerals are calcite partially filling molds and vugs, and pyrite that predates the calcite, concentrates along stylolites, and coats vugs.

Geophysical Logs

Geophysical logs can be used to correlate stratigraphy between holes, provide qualitative estimates of porosity, and help identify fracture zones and other horizontal discontinuities. Logs run on most holes include caliper, which measures borehole diameter and can help identify fractures and dissolution zones; natural gamma, which measures natural radiation and can be used to identify zones with shale, or clay; single-point resistivity and spontaneous potential, which are useful for stratigraphic correlation; and temperature, which can sometimes be used to identify horizontal fractures or solution features where water is leaving or entering the borehole. Most holes were also televised prior to installation of the monitoring system. Additional logs run on selected holes include neutron (holes 1, 2, 3, 11), which provides a qualitative estimate of porosity; and electrical conductivity (holes 2, 4, 5, 9, 10, 13, 14), which identifies differences in total dissolved solids of the water in the hole. Table 2 summarizes the logs run on the various holes; all geophysical and television logs are on file at the WGNHS.

Figure 8 summarizes logs for hole 5, as well as the neutron log from hole 3. Horizontal fractures (approximate elevations 92.2, 89.5, 85.5, 82.5, 78, and 75.5 ft) are shown as dotted lines. The natural gamma log (left-most graph) indicates an argillaceous zone (5-15 ft) but does not provide much indication of the presence of horizontal fractures. The temperature, single-point resistivity, caliper, and electrical conductivity logs all provide indications of one or more of these fractures. The neutron log (right-most graph) provides a qualitative estimate of porosity. Neutron logging is usually performed in the unsaturated zone. Neutrons are slowed by the presence of hydrogen molecules. If neutron counts have been correlated to water content, a neutron log can provide a measurement of moisture content. We extended the logs into the saturated zone by lowering 2-inch PVC with an endcap to the bottom of the hole and then lowering the probe into the dry pipe. In the saturated portion of the aquifer, pores contain only water and no air. Changes in neutron counts therefore indicate changes in porosity. We do not have an independent measure of porosity and so the neutron log in figure 8 indicates relative changes in porosity. In general, there is not much variation in the neutron counts, porosity seems generally low, especially within the laminated restricted marine facies. Increases in neutron counts between 77 and 78.5 ft elevation and at 71.5 ft elevation correspond to vuggy zones developed in the higher-porosity crystalline dolomite. The sharp peak at approximately 94.7 ft elevation may correspond to a large fracture.

Heat-pulse Flowmeter Logging

Flowmeter logging is a useful tool for determining which fractures are significant in terms of groundwater flow. Traditional spinner flowmeters measure vertical flow within a borehole and

Table 2. Logs collected from Bissen boreholes prior to installation of monitoring system

| Hole | WGNHS ID | Gamma | SP/ resistivity | Caliper | Neutron | Elec Cond | Fluid Temp | Tele- vision |
|------|----------|-------|--------------------|---------|---------|--------------|---------------|-----------------|
| 1 | DR-421 | X | X | X | X | | X | X |
| 2 | DR-422 | X | X | X | X | X | | X |
| 3 | DR-423 | X | X | X | X | | X | |
| 4 | DR-424 | X | X | X | | X | X | X |
| 5 | DR-425 | X | X | X | | X | X | X |
| 6 | DR-426 | | | | | | | X |
| 7 | DR-427 | X | X | X | | | X | X |
| 8 | DR-428 | | | X | | | X | X |
| 9 | DR-429 | X | X | X | | X | X | X |
| 10 | DR-430 | X | X | X | | X | X | X |
| 11 | DR-431 | X | X | X | X | | X | X |
| 12 | DR-432 | X | X | X | | | X | X |
| 13 | DR-433 | X | X | X | | X | X | X |
| 14 | DR-434 | X | X | X | | X | X | X |
| 15 | DR-435 | X | X | X | | | X | X |
| 16 | DR-436 | X | X | X | | | X | X |
| 17 | DR-437 | X | X | X | | | X | X |
| 18 | DR-438 | X | X | X | | | X | X |

are only sensitive to relatively large flow rates (*i.e.* in the tens of gpm range). Newly developed heat-pulse flowmeters also measure vertical flow, however, these tools are designed to be measure the low flow rates (*i.e.* in the 0.01 gpm range) that are typically encountered in fractured low-permeability rocks (Paillet, 1996). The heat-pulse meter consists of a heating element with two thermistors; one located above the heating element and one below it. A flexible rubber centralizer, located near the heating element, serves to center the tool in the borehole and focus flow through the meter. A heat pulse is generated and as the water flows either up or down the borehole, it is detected by one of the thermistors. The time from generation of pulse, until it is recorded by one of the two thermistors, is then used to calculate a flow rate. Measurements are taken at specific depths and any change in flow rate or flow direction from one measurement point to the next indicates water either entering or leaving the borehole over that distance.

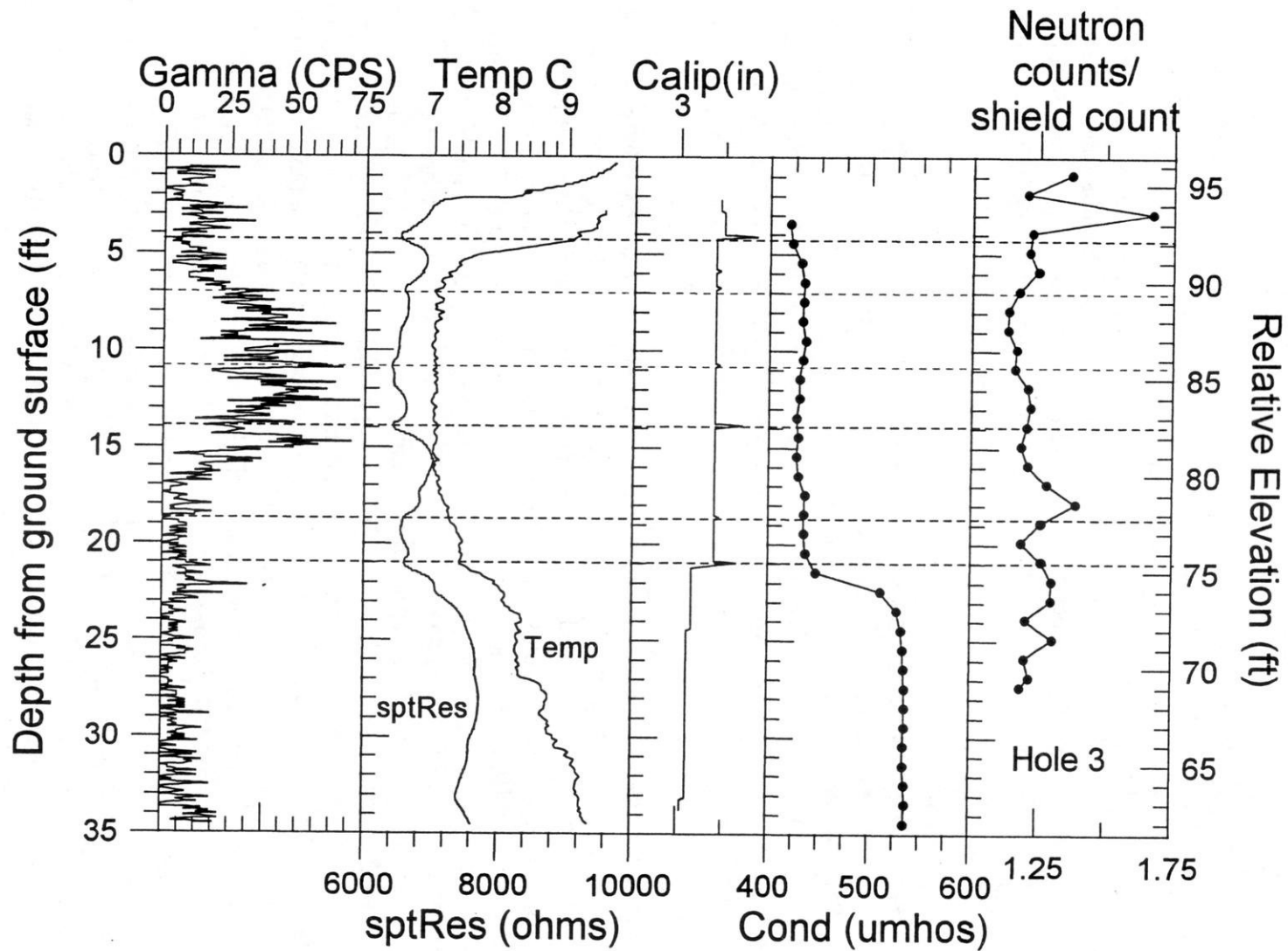


Figure 8. Geophysical logs for hole 5 with neutron log for hole 3. Dashed horizontal lines indicate horizontal fractures.

Heat-pulse flow logs were run on holes 7 and 13. Figure 9 shows the flowmeter logs for hole 13 under both static (left side) and pumping conditions (right side). Under static conditions, water moves down and exits the hole through the fracture at an elevation of approximately 75.5 ft. Flow increases with depth in the hole. There is a slight increase in flow between measurements taken at 88.5 and 83.5 ft; we assume the fracture at 85.5 ft is contributing the flow. Flow also increases between measurements at 80.5 and 81.5 ft elevation. Flow decreases sharply between 75 and 76 ft elevation as most water exits the large, highly conductive fracture at 75.5 ft. The second log was run while pumping 1.5 gpm from the top of the borehole; under these conditions, all flow was upward (note difference in horizontal scale). Below an elevation of 73.5 ft, the flow rate is zero indicating that flow into the hole is negligible. Going up the hole, sharp increases in flow rate between 74.5 and 75.5 ft, between 78.5 and 80.5 ft, and between 85 and 86.5 ft elevation indicate that fractures in those intervals contribute the bulk of the water being pumped from the hole.

Fracture Distribution

Fracture-network models require statistical descriptions of fracture characteristics including orientation, dip, length, and density. Scan-lines and areal mapping (Laslett, 1982; LaPointe and Hudson, 1985) are the standard methods for obtaining statistical descriptions of fracture characteristics. Both methods have been used to characterize the three sets of fractures at the site. Two near-vertical sets are oriented approximately 075° and 155° ; bedding-plane fractures constitute the third set.

Vertical Fractures

Characterization of the vertical fracture pattern included clearing the quarry floor of sediment, photographing 10 x 10 ft grid squares from a vertical lift truck. The lift truck allowed us to take photos while centered over each grid square, thus minimizing parallax. The resulting photos were used to map and digitize all fractures greater than 1 ft in length. The map of all fractures at the site, shown in figure 10, clearly shows the dominant fracture sets as well as fractures caused by blasting during the quarrying operation. Evidence in quarry walls and from the boreholes suggest that the blast-influenced fractures do not penetrate far into the rock. Therefore we did not wish to include those fractures in the datasets developed as input for the fracture-flow models. We characterized the fracture sets by a variety of methods in order to develop representative fracture statistics for the flow models. The methods include the following: 1) hand-editing the fracture map to remove blast-influenced fractures, 2) using a sub-set of data from a block in the northeast corner of the site where there is little to no evidence of blasting (x-coord 70 to 120 ft, y-coord 30 to 70 ft), and 3) performing scanline mapping on the bench above the quarry floor; this area was relatively free of sediment and glacial striations indicated that no rock had been removed by quarrying. The surveys were conducted in June 1994 by the UW-Madison Hydrogeology Field Class. The survey teams laid out one 142-ft horizontal scanline oriented 135° and a second 64-ft scanline oriented 045° and then recorded the location, length, orientation, fracture type, termination type, censoring, as well as qualitative estimates of aperture, roughness and planarity for every fracture crossing the scanlines. Figure 11 compares length and orientation statistics developed by these methods.

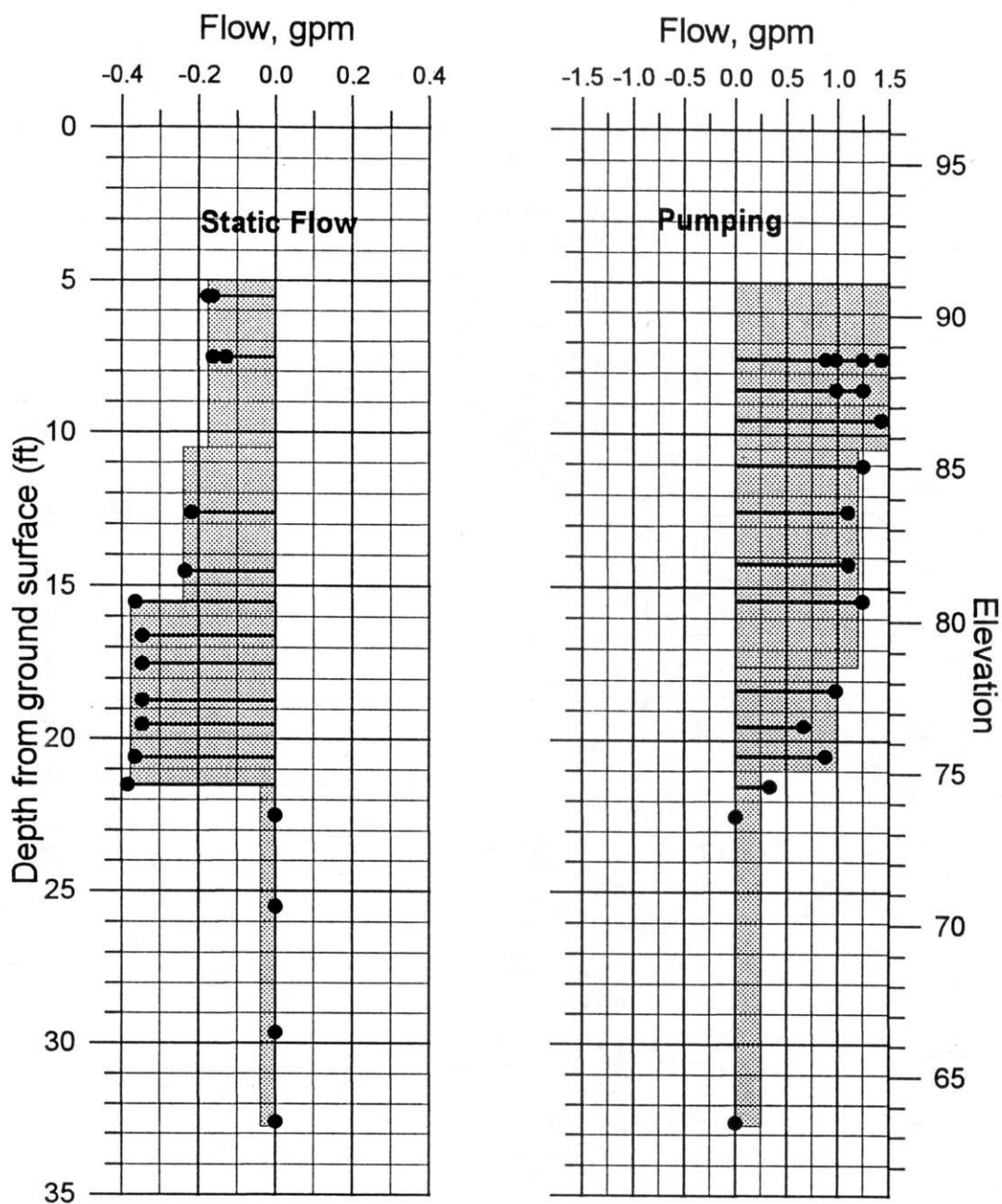


Figure 9. Heat-pulse flowmeter logs from hole 13 run under static (left log) and pumping (right log) conditions. Negative flows are downward and positive flows are upward; note difference in flow scale for the two logs.

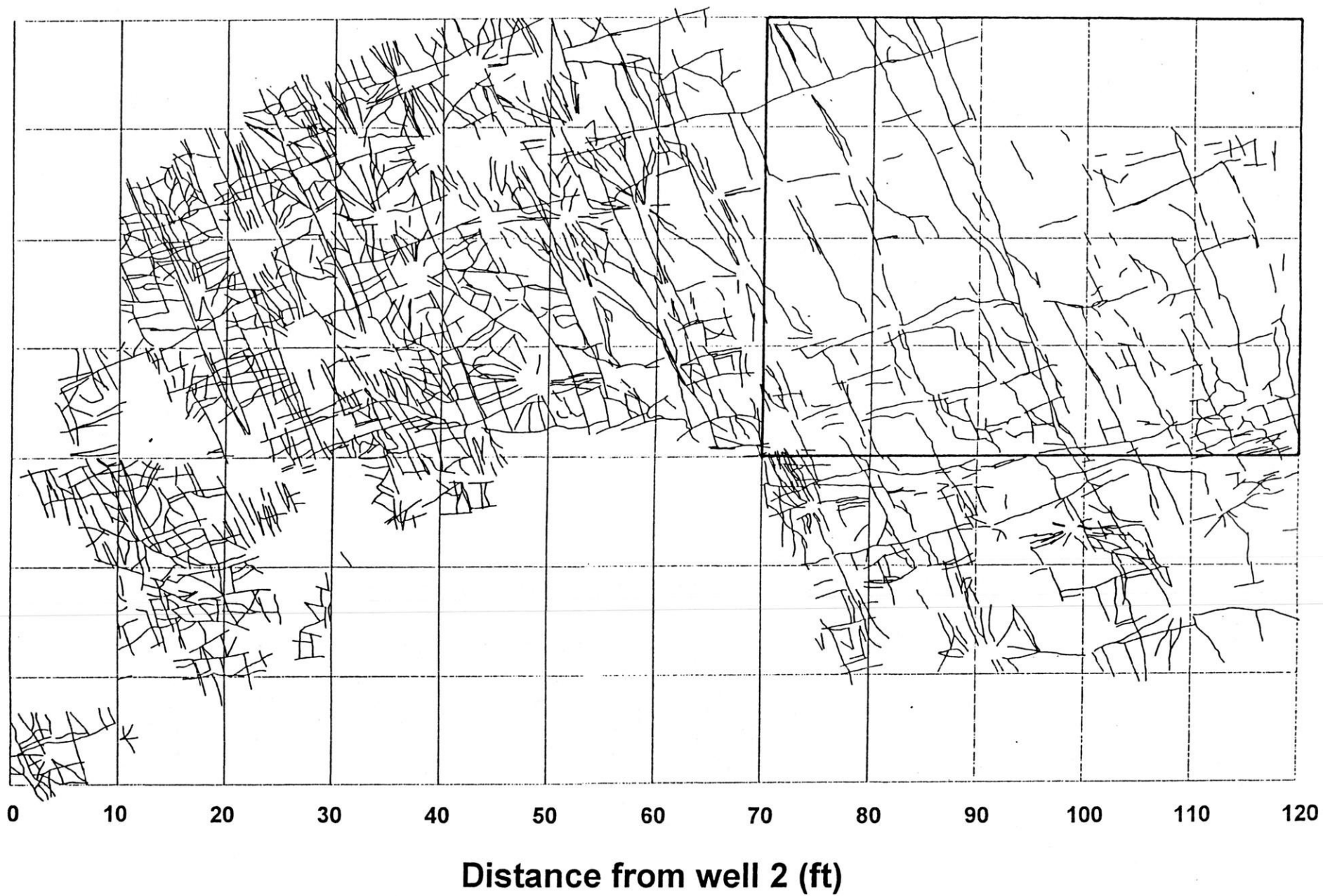


Figure 10. Map of quarry floor showing all fractures greater than 1 ft length. The dominant fracture sets as well as fractures caused by blasting during the quarrying operation can be seen.

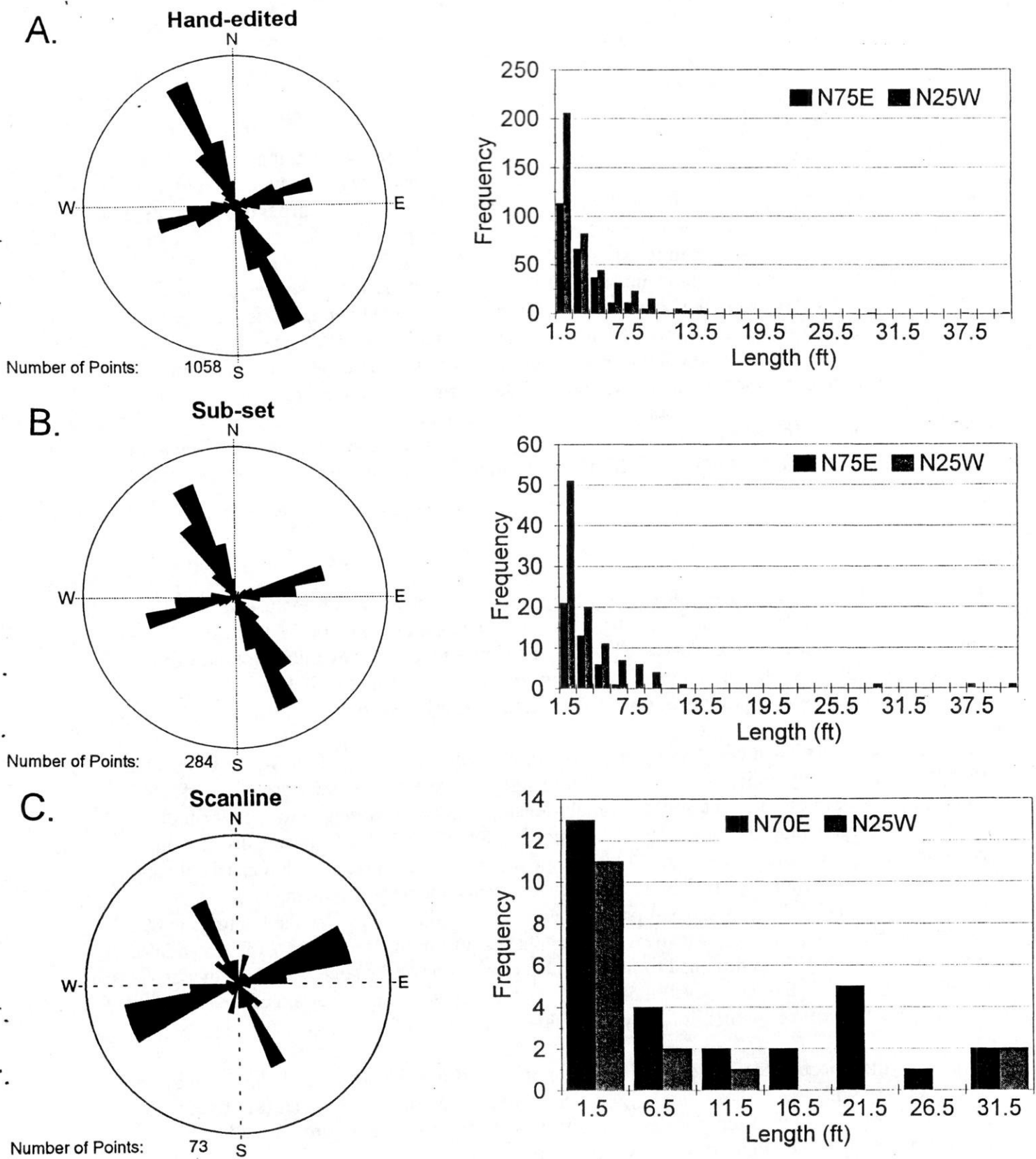


Figure 11. Rose diagrams of orientations (left column) and histograms of lengths (right column) of vertical fractures. Data were compiled using a variety of methods in order to minimize data from blast-influenced fractures. **A)** data from hand-edited map of quarry floor, **B)** subset of data from NE corner of study site, **C)** data from scanline surveys on bench above quarry floor. All methods provide consistent orientations of 075° and 155° for the vertical fracture sets.

Horizontal Fractures

Borehole logs (described above) from all holes indicate that at least six horizontal fractures are present in the subsurface at Bissen quarry. Fracture elevations vary slightly between holes and not all fractures are present in all holes. Fractures occur at elevations of approximately 92, 89.3, 85.5, 82.3, 78.5, and 75.5. The logs provide indications of the presence of fractures, however, the data cannot be used to develop the statistical characterization of fracture length and orientation needed for fracture-flow models. While there are differences in sedimentology between the rocks exposed in the quarry walls and those encountered in boreholes, the general lithofacies and depositional cycles were similar enough that we felt we could use outcrop characterizations of the horizontal fracture set, combined with borehole data, to develop the necessary input data for the fracture-flow models. Measurements of the characteristics of the bed-parallel discontinuities were obtained from vertical scanline surveys of the quarry walls; also completed in June 1994 by the UW-Madison Hydrogeology Field Class. Two vertical scanlines were measured along the north and west walls of the quarry. Scanlines were 9.7 and 13.4 ft in length.

Monitoring System

Recent work (*e.g.* Hsieh and Shapiro, 1993) suggests that identification of fracture locations is insufficient to characterize groundwater flow since only a limited number of fractures are "hydraulically" active. We identified the hydraulically important fractures and dissolution zones with a variety of tests, including borehole flow-meter, fluid temperature and electrical conductivity logs, as well as short-interval packer tests (described below).

Multi-level samplers, each with five to six ports, were installed in eleven of the 3-inch holes. The samplers, marketed by Solinst™ as the "Waterloo system", have a minimum port length of 0.5 ft and a packer length of 3 ft. The system of multi-level samplers was designed to monitor four horizontal fractures (approximate relative elevation 92, 82, 78, and 75 ft) and two dissolution zones (relative elevations 86 to 87 and 72 ft); some ports were also placed within matrix blocks. Fracture elevations vary slightly from hole to hole and given the design constraints of the Waterloo system (0.5-ft ports and 3-ft packers) we were not able to monitor the fractures at 89.3 and 85.5 ft elevation, nor were we always able to place a port in the fracture at 78 ft. In addition, the sampler in hole 17 was designed to monitor deeper portions of the site. Table 3 provides construction data for the multi-level samplers. Figure 15 is a schematic diagram of the site illustrating which zones are monitored by the multi-levels.

Two 1-1/4-inch piezometers were installed in one of the six-inch diameter boreholes (hole 6), the other two large-diameter holes (7 and 8) were cased to 2 ft and open below that (see figure 6 for locations). Table 4 summarizes the details of piezometer construction; figure 16 is a block diagram illustrating the monitoring intervals in each borehole.

Table 3. Construction data for multi-level sampling systems at Bissen Quarry

| ID | Port | | | | Open Interval | | | |
|------|----------------------|------------------------|-----------------------|--------------------|-------------------|----------------------|---------------|------------------|
| | Meas Point Elev (ft) | Midpoint from TOC (ft) | Midpoint from GS (ft) | Midpoint Elev (ft) | Top from TOC (ft) | Bottom from TOC (ft) | Elev Top (ft) | Elev Bottom (ft) |
| 1-1 | 100.423 | 7 | 4.1 | 92.495 | 6.75 | 7.75 | 92.745 | 91.745 |
| 1-2 | 100.423 | 12 | 9.1 | 87.495 | 10.75 | 13.25 | 88.745 | 86.245 |
| 1-3 | 100.423 | 17 | 14.1 | 82.495 | 16.25 | 17.25 | 83.245 | 82.245 |
| 1-4 | 100.423 | 20.5 | 17.6 | 78.995 | 20.25 | 20.75 | 79.245 | 78.745 |
| 1-5 | 100.423 | 24 | 21.1 | 75.495 | 23.75 | 24.25 | 75.745 | 75.245 |
| 1-6 | 100.423 | 27.5 | 24.6 | 71.995 | 27.25 | 36.31 | 72.245 | 63.185 |
| 4-1 | 100.023 | 7.25 | 4.05 | 91.82 | 7 | 8 | 92.07 | 91.07 |
| 4-2 | 100.023 | 12.25 | 9.05 | 86.82 | 11 | 13.5 | 88.07 | 85.57 |
| 4-3 | 100.023 | 20.75 | 17.55 | 78.32 | 20.5 | 21 | 78.57 | 78.07 |
| 4-4 | 100.023 | 24.25 | 21.05 | 74.82 | 24 | 24.5 | 75.07 | 74.57 |
| 4-5 | 100.023 | 27.75 | 24.55 | 71.32 | 27.5 | 38.325 | 71.57 | 60.745 |
| 9-1 | 99.935 | 7 | 4.45 | 92.01 | 3.476 | 7.25 | 95.534 | 91.76 |
| 9-2 | 99.935 | 11.5 | 8.95 | 87.51 | 10.25 | 12.75 | 88.76 | 86.26 |
| 9-3 | 99.935 | 16.5 | 13.95 | 82.51 | 15.75 | 16.75 | 83.26 | 82.26 |
| 9-4 | 99.935 | 20 | 17.45 | 79.01 | 19.75 | 20.25 | 79.26 | 78.76 |
| 9-5 | 99.935 | 23.5 | 20.95 | 75.51 | 23.25 | 23.75 | 75.76 | 75.26 |
| 9-6 | 99.935 | 27 | 24.45 | 72.01 | 26.75 | 36.05 | 72.26 | 62.96 |
| 10-1 | 100.332 | 7 | 4.08 | 92.285 | 6.75 | 7.75 | 92.535 | 91.535 |
| 10-2 | 100.332 | 12 | 9.08 | 87.285 | 10.75 | 13.25 | 88.535 | 86.035 |
| 10-3 | 100.332 | 17 | 14.08 | 82.285 | 16.25 | 17.25 | 83.035 | 82.035 |
| 10-4 | 100.332 | 20.5 | 17.58 | 78.785 | 20.25 | 20.75 | 79.035 | 78.535 |
| 10-5 | 100.332 | 24 | 21.08 | 75.285 | 23.75 | 24.25 | 75.535 | 75.035 |
| 10-6 | 100.332 | 27.5 | 24.58 | 71.785 | 27.25 | 37.75 | 72.035 | 61.535 |
| 11-1 | 99.925 | 7 | 4.366 | 91.999 | 6.75 | 7.75 | 92.249 | 91.249 |
| 11-2 | 99.925 | 12 | 9.366 | 86.999 | 10.75 | 13.25 | 88.249 | 85.749 |
| 11-3 | 99.925 | 16.5 | 13.866 | 82.499 | 16.25 | 16.75 | 82.749 | 82.249 |
| 11-4 | 99.925 | 20 | 17.366 | 78.999 | 19.75 | 20.25 | 79.249 | 78.749 |
| 11-5 | 99.925 | 23.5 | 20.866 | 75.499 | 23.25 | 23.75 | 75.749 | 75.249 |
| 11-6 | 99.925 | 29.5 | 26.866 | 69.499 | 26.75 | 37.12 | 72.249 | 61.879 |

Table 3. Construction data for multi-level samplers (cont.)

| ID | Port | | | | Open Interval | | | |
|------|-----------------|-------------------|------------------|---------------|---------------|-----------------|----------|-------------|
| | Meas Point Elev | Midpoint from TOC | Midpoint from GS | Midpoint Elev | Top from TOC | Bottom from TOC | Elev Top | Elev Bottom |
| 12-1 | 99.696 | 7 | 4.427 | 91.778 | 6.75 | 7.75 | 92.028 | 91.028 |
| 12-2 | 99.696 | 12 | 9.427 | 86.778 | 10.75 | 13.25 | 88.028 | 85.528 |
| 12-3 | 99.696 | 16.5 | 13.927 | 82.278 | 16.25 | 16.75 | 82.528 | 82.028 |
| 12-4 | 99.696 | 23.5 | 20.927 | 75.278 | 23.25 | 23.75 | 75.528 | 75.028 |
| 12-5 | 99.696 | 27 | 24.427 | 71.778 | 26.75 | 37.8 | 72.028 | 60.978 |
| 14-1 | 99.845 | 7 | 4.348 | 91.847 | 6.75 | 8.75 | 92.097 | 90.097 |
| 14-2 | 99.845 | 12.5 | 9.848 | 86.347 | 11.75 | 13.25 | 87.097 | 85.597 |
| 14-3 | 99.845 | 16.5 | 13.848 | 82.347 | 16.25 | 16.75 | 82.597 | 82.097 |
| 14-4 | 99.845 | 23.5 | 20.848 | 75.347 | 23.25 | 23.75 | 75.597 | 75.097 |
| 14-5 | 99.845 | 27 | 24.348 | 71.847 | 26.75 | 37.35 | 72.097 | 61.497 |
| 15-1 | 99.607 | 7 | 4.342 | 91.653 | 5.75 | 7.75 | 92.903 | 90.903 |
| 15-2 | 99.607 | 12 | 9.342 | 86.653 | 10.75 | 13.25 | 87.903 | 85.403 |
| 15-3 | 99.607 | 16.5 | 13.842 | 82.153 | 16.25 | 16.75 | 82.403 | 81.903 |
| 15-4 | 99.607 | 20 | 17.342 | 78.653 | 19.75 | 20.25 | 78.903 | 78.403 |
| 15-5 | 99.607 | 23.5 | 20.842 | 75.153 | 23.25 | 23.75 | 75.403 | 74.903 |
| 15-6 | 99.607 | 27 | 24.342 | 71.653 | 26.75 | 36.75 | 71.903 | 61.903 |
| 16-1 | 99.629 | 7 | 4.248 | 91.667 | 6.25 | 7.75 | 92.417 | 90.917 |
| 16-2 | 99.629 | 12 | 9.248 | 86.667 | 10.75 | 13.25 | 87.917 | 85.417 |
| 16-3 | 99.629 | 16.5 | 13.748 | 82.167 | 16.25 | 16.75 | 82.417 | 81.917 |
| 16-4 | 99.629 | 23 | 20.248 | 75.667 | 22.75 | 23.25 | 75.917 | 75.417 |
| 16-5 | 99.629 | 26.5 | 23.748 | 72.167 | 26.25 | 37.5 | 72.417 | 61.167 |
| 17-1 | 99.875 | 12.25 | 9.686 | 86.659 | 11 | 13.5 | 87.909 | 85.409 |
| 17-2 | 99.875 | 16.75 | 14.186 | 82.159 | 16.5 | 17 | 82.409 | 81.909 |
| 17-3 | 99.875 | 23.25 | 20.686 | 75.659 | 23 | 23.5 | 75.909 | 75.409 |
| 17-4 | 99.875 | 30.25 | 27.686 | 68.659 | 26.5 | 30.5 | 72.409 | 68.409 |
| 17-5 | 99.875 | 33.75 | 31.186 | 65.159 | 33.5 | 37.68 | 65.409 | 61.229 |
| 18-1 | 99.805 | 6.75 | 4.155 | 92.09 | 6.5 | 8 | 92.34 | 90.84 |
| 18-2 | 99.805 | 12.25 | 9.655 | 86.59 | 11 | 13 | 87.84 | 85.84 |
| 18-3 | 99.805 | 16.75 | 14.155 | 82.09 | 16 | 17 | 82.84 | 81.84 |
| 18-4 | 99.805 | 23.25 | 20.655 | 75.59 | 23 | 23.5 | 75.84 | 75.34 |
| 18-5 | 99.805 | 26.75 | 24.155 | 72.09 | 26.5 | 30.5 | 72.34 | 68.34 |
| 18-6 | 99.805 | 33.75 | 31.155 | 65.09 | 33.5 | 37.58 | 65.34 | 61.26 |

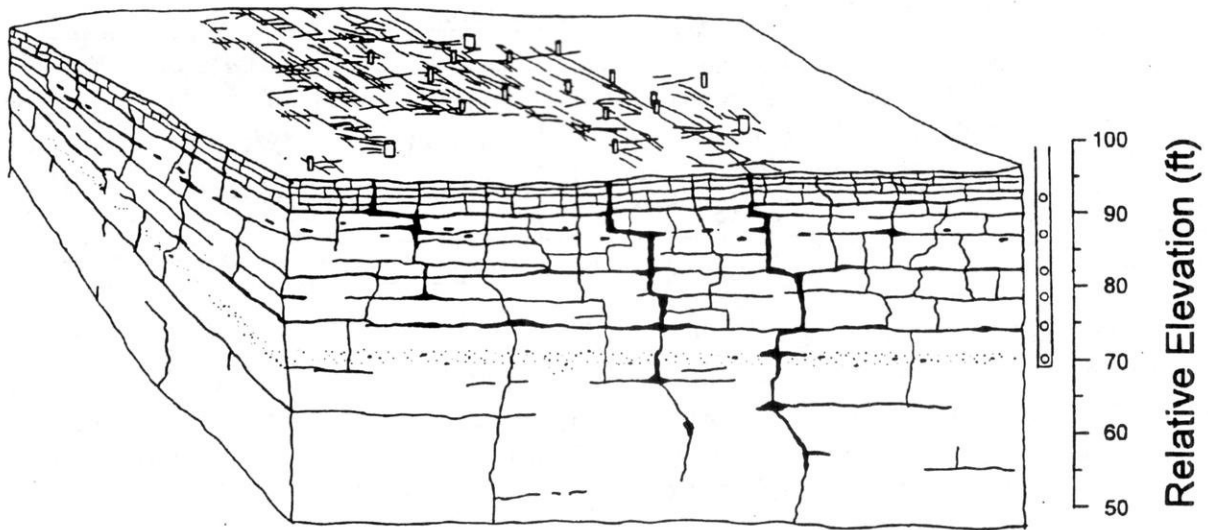


Figure 12. Schematic block diagram of site. Relative elevations are shown on the right along with a schematic multi-port sampler. Ports have been installed in four horizontal fractures (92 ft, 82.5 ft, 79 ft, and 75.5 ft elevation) and two dissolution zones (87.5 and 72 ft elevation). The horizontal fractures appear to be laterally continuous across the site. The upper dissolution zones is characterized by sparse but large vugs; the lower zone is characterized by abundant small vugs.

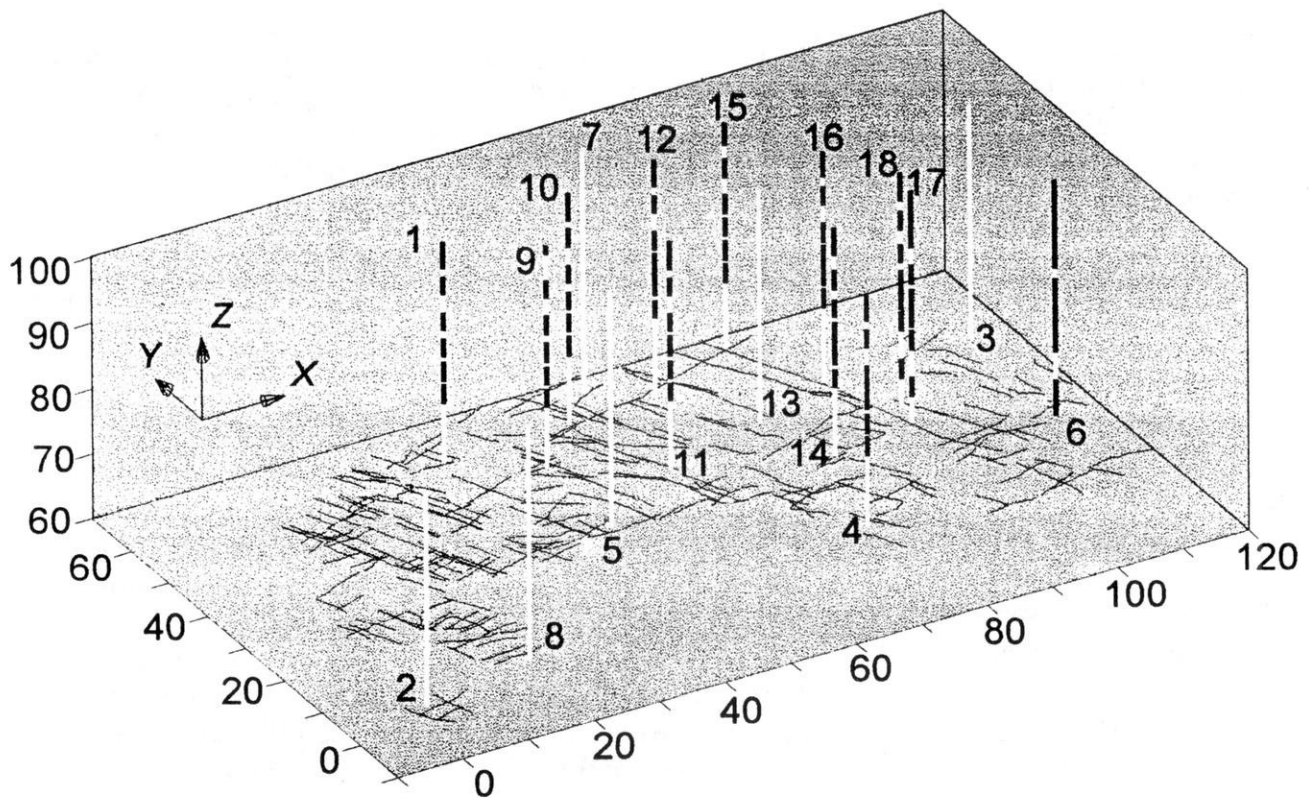


Figure 13. Block diagram of site showing the open intervals of the monitoring system; white zones are open intervals. Site coordinates and relative elevation (ft) are shown on the axes.

Table 4. Construction data for piezometers at Bissen Quarry

| Piez | Screen Interval | | | | | Gravel Pack | | |
|------|----------------------|-------------------|----------------------|------------------------|-------------------------|-------------------|----------------------|-------------------------|
| | Meas Point Elev (ft) | Top from TOC (ft) | Bottom from TOC (ft) | Midpoint from TOC (ft) | Elevation Midpoint (ft) | Top from TOC (ft) | Bottom from TOC (ft) | Elevation Midpoint (ft) |
| 6-1 | 98.431 | 28.55 | 29.55 | 29.05 | 69.381 | 27.9 | 31.85 | 69.203 |
| 6-2 | 98.42 | 15.15 | 16.15 | 15.65 | 82.77 | 15.05 | 16.7 | 82.545 |

Hydraulic Conductivity Testing

Data on the hydraulic conductivity of the fracture network at Bissen Quarry have been obtained from a variety of tests including a multi-well pumping test conducted with eight 35-ft open boreholes, a second pumping test conducted with multi-level samplers containing ports open over short intervals, and packer tests conducted with a 0.75-ft straddle interval. Each of these methods is described below.

Open-hole Pumping Test

Pumping tests, the standard method for determining the transmissivity and storativity of an aquifer, can be difficult to design and analyze in fractured-rock settings. We performed two pumping tests at the site -- an open-hole test, designed to measure the bulk conductivity of the dolomite; and a second test, after the installation of the multi-level samplers.

The open-hole test was conducted for 24 hours at pumping rate of approximately 0.12 ft³/s (55 gpm). Drawdowns were recorded in the pumping well and seven monitoring wells. Figure 14 shows the locations of the pumping well and monitoring wells, and the drawdown cone at the completion of the test. The elliptical shape of the drawdown cone suggests that the bulk horizontal conductivity is anisotropic, with the major axes of the hydraulic conductivity ellipse aligning approximately with the dominant vertical fracture sets mapped at the site.

Data were analyzed using a variety of solutions for flow in unconfined aquifers including Neuman (1975), Moench (1984), and Cooper-Jacob (1946). Pumping test analyses using the Neuman (1975) method provided the best match to the measured drawdowns. Calculated transmissivities range from 7.0×10^{-3} to 2.5×10^{-2} ft²/sec with a geometric mean of 1.5×10^{-2} ft²/sec. To convert transmissivities to hydraulic conductivities, we used an aquifer thickness of 40 ft. The dolomite at the site is approximately 300 ft thick, however, we believe the pumping stress was limited to shallow depths. Regional correlation of high-permeability features suggests that there is a large fracture at 40 ft depth (Muldoon and others, in prep). Heat-pulse logging of many holes in the Sturgeon Bay area suggests that these regional fractures can supply enough yield that the aquifer below them is essentially "unstressed" at pumping rates on the order of 10's of gpm (Gianniny and others, 1996). Essentially the large fracture at 40 ft. depth functions as the base of the shallow aquifer at the site. Calculated hydraulic conductivities range from 1.8×10^{-5} to 6.3×10^{-4} ft/s with a geometric mean of 3.9×10^{-4} ft/s; these values reflect the bulk conductivity of dolomite as averaged over the entire open length of the boreholes. Table 5 summarizes the transmissivity and storage values determined from the open-hole pumping test.

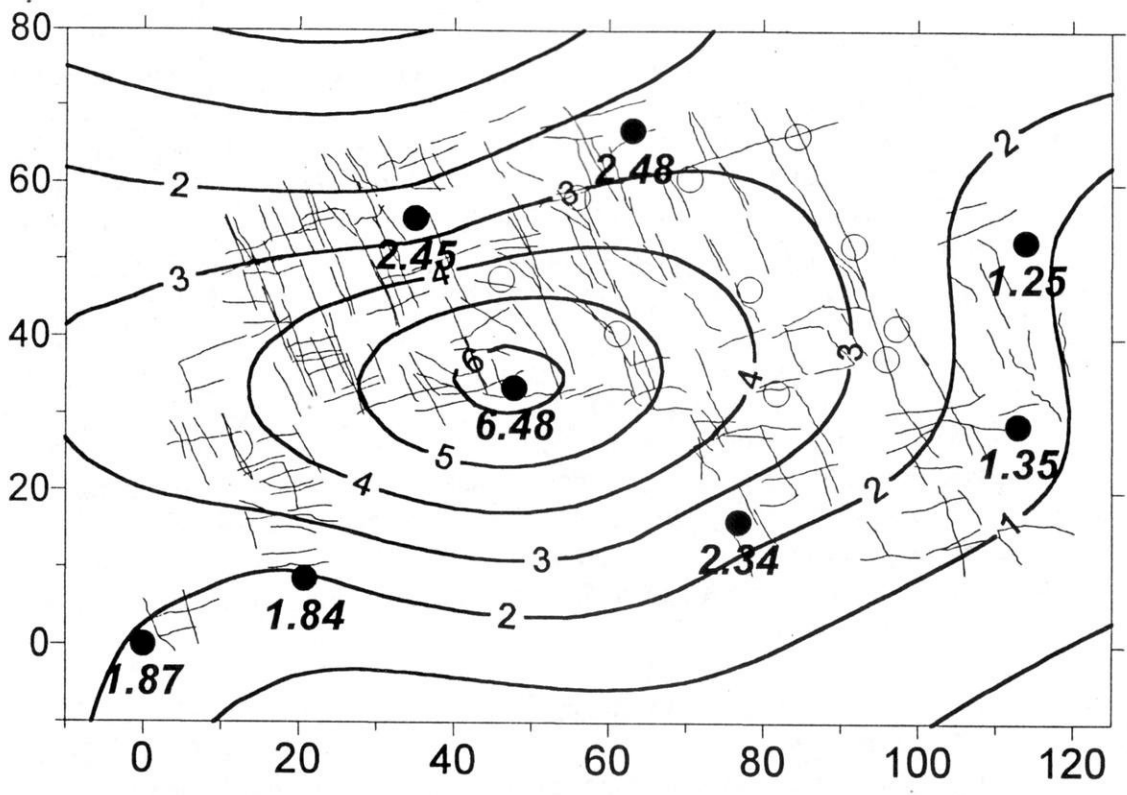


Figure 14. Map of drawdown at the end of a 24-hour pumping test completed in May 1993. Black dots indicate monitoring points, measured drawdowns are shown in italics, open circles indicate the locations of boreholes 9 to 18 which were installed at a later date.

Table 5. Results from open-hole pumping test.

| Well | T (ft ² /sec) | K (ft/sec) | S | Sy | β |
|------|--------------------------|----------------------|--------|-------|-------|
| 1 | 1.6x10 ⁻² | 4.0x10 ⁻⁴ | 0.0003 | 0.041 | 0.001 |
| 2 | 1.6x10 ⁻² | 4.0x10 ⁻⁴ | 0.0002 | 0.047 | 0.01 |
| 3 | 2.4x10 ⁻² | 5.9x10 ⁻⁴ | 0.0003 | 0.042 | 0.01 |
| 4 | 1.6x10 ⁻² | 4.0x10 ⁻⁴ | 0.0003 | 0.054 | 0.004 |
| 6-1 | 7.0x10 ⁻³ | 1.8x10 ⁻⁵ | 0.003 | 0.28 | 0.1 |
| 6-2 | 1.4x10 ⁻² | 3.5x10 ⁻⁴ | 0.0004 | 0.13 | 0.03 |
| 7 | 1.3x10 ⁻² | 3.3x10 ⁻⁴ | 0.0002 | 0.082 | 0.004 |
| 8 | 2.5x10 ⁻² | 6.3x10 ⁻⁴ | 0.0003 | 0.020 | 0.001 |

Multi-level Pumping Test

In order to test more discrete intervals in the dolomite, we conducted a 48-hr pumping test after the installation of the multi-level samplers. Water levels were monitored at the pumping well which was open from the water table to 35 ft depth and at 61 monitoring ports which were open over short intervals (see tables 3 and 4); the pumping rate was 0.036 ft³/s (16 gpm). Response to pumping was quite rapid; most ports appear to reach steady-state conditions within the first 300 minutes of the test. Figure 15a shows the locations of the pumping well, the multi-level samplers, and open boreholes; figure 15b is a plot of time-drawdown data for the ports in hole 4.

Data were analyzed using a variety of solutions for flow in unconfined aquifers including Neuman (1975), Moench (1984), and Cooper-Jacob (1946). All of these standard analysis methods make various assumptions in order to solve the equations for flow to a well and none of them are really appropriate for analyzing this test. If we assume a conceptual model in which the horizontal fractures function as "aquifers" while the matrix blocks function as confining units that are somewhat leaky due to the presence of the vertical fractures, then the Cooper-Jacob method may be the most appropriate to analyze the drawdown data from the multi-level ports completed in high-permeability zones.

The early-time data (first 10 minutes) are not well matched by any method, however, these data are sparse. As a result, we analyzed later-time data (10 to 300 minutes) with the Cooper-Jacob method in order to determine transmissivities. Since the ports are only open over short intervals, we corrected for partial penetration of observation points. This method requires a vertical anisotropy ratio. We have no direct measure of the anisotropy ratio at the site. Assuming that hydraulic gradient is somewhat correlated to the hydraulic conductivity distribution, we used the inverse of the ratio of vertical to horizontal hydraulic conductivity to estimate an anisotropy ratio of 0.025. Calculated transmissivities range from 6.5×10^{-1} to $14.1 \text{ ft}^2/\text{sec}$ with a geometric mean of $1.6 \text{ ft}^2/\text{sec}$. Table 6 summarizes the transmissivity and storage values determined from the open-hole pumping test. Assuming an aquifer thickness of 40 ft, calculated hydraulic conductivities range from 1.6×10^{-2} to $3.5 \times 10^{-1} \text{ ft/s}$ with a geometric mean of $4.1 \times 10^{-2} \text{ ft/s}$. This narrow range of hydraulic conductivities is similar to the range measured in the open-hole pumping test, however, the values are approximately three orders of magnitude higher, as the second test measures the hydraulic conductivity of individual fractures whereas the open-hole test measured a bulk hydraulic conductivity.

Packer Tests

A straddle-packer device, with an open interval of 0.90 ft was used to perform slug tests at vertical intervals of 0.75 ft in 11 of the small-diameter boreholes at the site. The short measurement interval was chosen to minimize the averaging inherent with most packer tests and to isolate and test individual fractures. Tests were analyzed using the Hvorslev method and the geometry of the packer interval was taken into account (Hvorslev, 1951). The hydraulic conductivity is quite variable with depth, ranging over five orders of magnitude in each hole. Figure 16, a block diagram, shows detailed profiles of hydraulic conductivity for ten of these holes. Laterally continuous zones of high hydraulic conductivity appear to develop along some

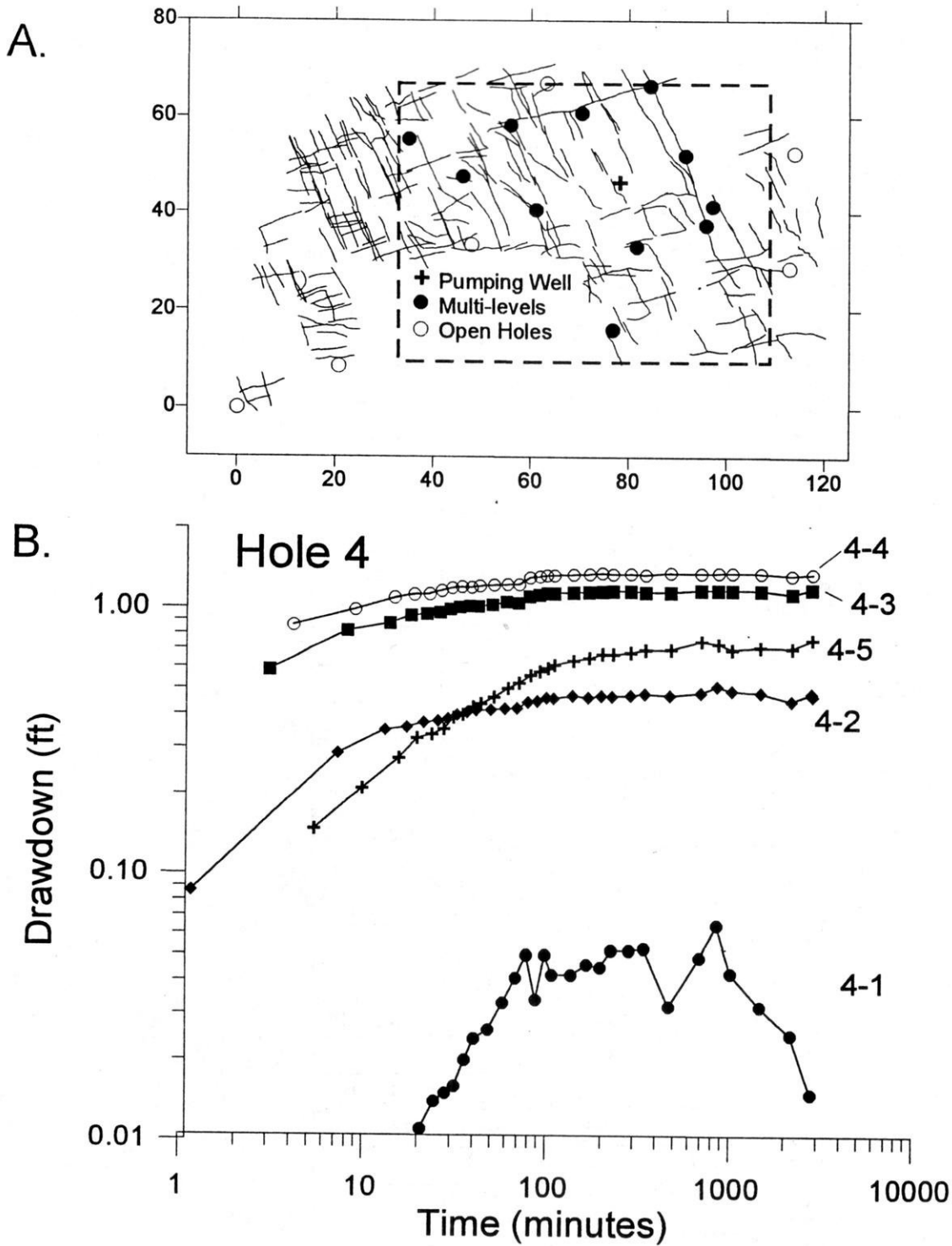


Figure 15. Pumping test monitored with multi-level samplers. **A)** Locations of pumping well, multi-level samplers (each with 5 to 6 ports), and open boreholes. **B)** Plot of time-drawdown for five monitoring ports in borehole 4.

Table 6. Results from pumping test monitored with multilevel samplers.

| Port | T(ft ² /s) | K(ft/s) | Port | T(ft ² /s) | K(ft/s) |
|------|-----------------------|-------------------------|------|-----------------------|-------------------------|
| 1-1 | 9.51 | 2.38 x 10 ⁻¹ | 12-1 | 1.42 | 3.54 x 10 ⁻² |
| 1-2 | 1.18 | 2.95 x 10 ⁻² | 12-2 | 1.23 | 3.07 x 10 ⁻² |
| 1-3 | 1.05 | 2.64 x 10 ⁻² | 12-3 | 2.95 | 7.37 x 10 ⁻² |
| 1-4 | 1.04 | 2.59 x 10 ⁻² | 12-4 | 1.23 | 3.09 x 10 ⁻² |
| 1-5 | 1.04 | 2.60 x 10 ⁻² | 12-5 | 1.57 | 3.93 x 10 ⁻² |
| 1-6 | 1.08 | 2.69 x 10 ⁻² | | | |
| | | | 14-2 | 4.46 | 1.12 x 10 ⁻¹ |
| 4-1 | 11.81 | 2.95 x 10 ⁻¹ | 14-3 | 0.65 | 1.62 x 10 ⁻² |
| 4-2 | 2.67 | 6.68 x 10 ⁻² | 14-4 | 0.84 | 2.11 x 10 ⁻² |
| 4-3 | 1.15 | 2.86 x 10 ⁻² | 14-5 | 1.16 | 2.90 x 10 ⁻² |
| 4-4 | 1.09 | 2.73 x 10 ⁻² | | | |
| 4-5 | 1.33 | 3.31 x 10 ⁻² | 15-1 | 1.57 | 3.92 x 10 ⁻² |
| | | | 15-2 | 2.36 | 5.90 x 10 ⁻² |
| 9-1 | 9.20 | 2.30 x 10 ⁻¹ | 15-3 | 1.31 | 3.28 x 10 ⁻² |
| 9-2 | 1.71 | 4.26 x 10 ⁻² | 15-4 | 1.12 | 2.79 x 10 ⁻² |
| 9-3 | 1.43 | 3.59 x 10 ⁻² | 15-5 | 1.27 | 3.18 x 10 ⁻² |
| 9-4 | 1.36 | 3.41 x 10 ⁻² | 15-6 | 1.30 | 3.24 x 10 ⁻² |
| 9-5 | 1.35 | 3.39 x 10 ⁻² | | | |
| 9-6 | 1.38 | 3.45 x 10 ⁻² | 16-1 | 2.01 | 5.03 x 10 ⁻² |
| | | | 16-2 | 1.69 | 4.23 x 10 ⁻² |
| 10-1 | 4.62 | 1.15 x 10 ⁻¹ | 16-3 | 1.21 | 3.02 x 10 ⁻² |
| 10-2 | 1.91 | 4.79 x 10 ⁻² | 16-4 | 1.36 | 3.40 x 10 ⁻² |
| 10-3 | 1.43 | 3.57 x 10 ⁻² | 16-5 | 1.65 | 4.12 x 10 ⁻² |
| 10-4 | 1.08 | 2.71 x 10 ⁻² | | | |
| 10-5 | 1.20 | 3.01 x 10 ⁻² | 17-1 | 1.95 | 4.87 x 10 ⁻² |
| 10-6 | 0.97 | 2.41 x 10 ⁻² | 17-2 | 1.99 | 4.98 x 10 ⁻² |
| | | | 17-3 | 1.41 | 3.53 x 10 ⁻² |
| 11-1 | 14.09 | 3.52 x 10 ⁻¹ | 17-4 | 1.35 | 3.37 x 10 ⁻² |
| 11-2 | 1.19 | 2.97 x 10 ⁻² | 17-5 | 1.54 | 3.85 x 10 ⁻² |
| 11-3 | 1.55 | 3.87 x 10 ⁻² | | | |
| 11-4 | 1.53 | 3.81 x 10 ⁻² | 18-2 | 1.55 | 3.88 x 10 ⁻² |
| 11-5 | 1.51 | 3.77 x 10 ⁻² | 18-3 | 1.34 | 3.35 x 10 ⁻² |
| 11-6 | 1.20 | 3.00 x 10 ⁻² | 18-4 | 1.27 | 3.17 x 10 ⁻² |
| | | | 18-5 | 0.88 | 2.20 x 10 ⁻² |
| | | | 18-6 | 1.36 | 3.39 x 10 ⁻² |

bedding planes (relative elevations 85.5, 82.3, and 75.5) and within the vuggy zones (approximately 86 and between 68 and 70 ft elevation). Vertical fractures appear to intersect the bottom portions of hole 13 and hole 17 as both of these holes exhibit high hydraulic conductivity from 60 to 70 ft elevation. Measured hydraulic conductivities range from 2.3×10^{-8} to 1.4×10^{-2} ft/s; the geometric mean of all tests is 9.9×10^{-6} ft/s. The results of 372 packer tests indicate a bimodal distribution of fracture and matrix hydraulic conductivities (figure 17). The bimodal distribution of packer-test hydraulic conductivity values is expected in fractured-carbonate settings (Bradbury and others, 1991) as some packer intervals test matrix conductivity while other intervals are intersected by high-conductivity fractures or dissolution zones.

Correlation Between Hydraulic Conductivity Distribution and Geologic Data

Comparison of the stratigraphic log and hydraulic conductivity profile for hole 5 (figure 18) suggests that horizontal discontinuity surfaces such as cycle boundaries and bedding planes separating major lithofacies are commonly enhanced by dissolution to form high-permeability features. Heat-pulse flowmeter and fluid temperature logs suggest that the primary flowpath at the site is the fracture at approximately 75 ft elevation which is an especially well-developed cycle boundary. High-permeability features between 75 and 80 ft elevation appear to be due to a combination of vuggy porosity within the crystalline dolomite and discrete fractures. Contacts between the restricted marine lithofacies and the open marine crystalline dolomite (primarily the fenestral mudstones and thinly and crinkly laminated facies) appear to develop into significant high-permeability features (77.5, 79, and 82.5 ft elevation).

Head Distribution

The distribution of hydraulic head in fractured-rock aquifers can be difficult to characterize as these aquifers commonly exhibit significant spatial and temporal variations in head as well as complex responses to recharge events. In addition, detailed measurements of head in northern Door County (Bradbury and Muldoon, 1992) suggest that hydraulic head within an open borehole may be controlled by a limited number of high-permeability fractures. Given that the head distributions in fractures may be very different than the head distribution in matrix blocks, it is clear that choice of monitoring method will significantly influence measured head distributions. We have monitored head in both open boreholes that provide head measurements integrated over approximately a 30-ft saturated section as well as in the discrete intervals of the multi-level samplers. The significant differences in the results of these two monitoring techniques shows the necessity of discrete zone monitoring to describe the head distribution in fractured carbonate aquifers. All head measurements are included in WOFR 98-3 (Muldoon, 1998).

Open Boreholes

Water-levels in the open boreholes were measured 17 times during the period August 1993 to June 1994; these data suggest a very dynamic flow system with water-level variations in individual wells of approximately 1 ft. Data from the original eight open-boreholes suggest that local groundwater flow was originally to the west (figure 19a). A drainage ditch, constructed as part of the quarrying operation, was installed in mid-1993. After ditch installation, the gradient became

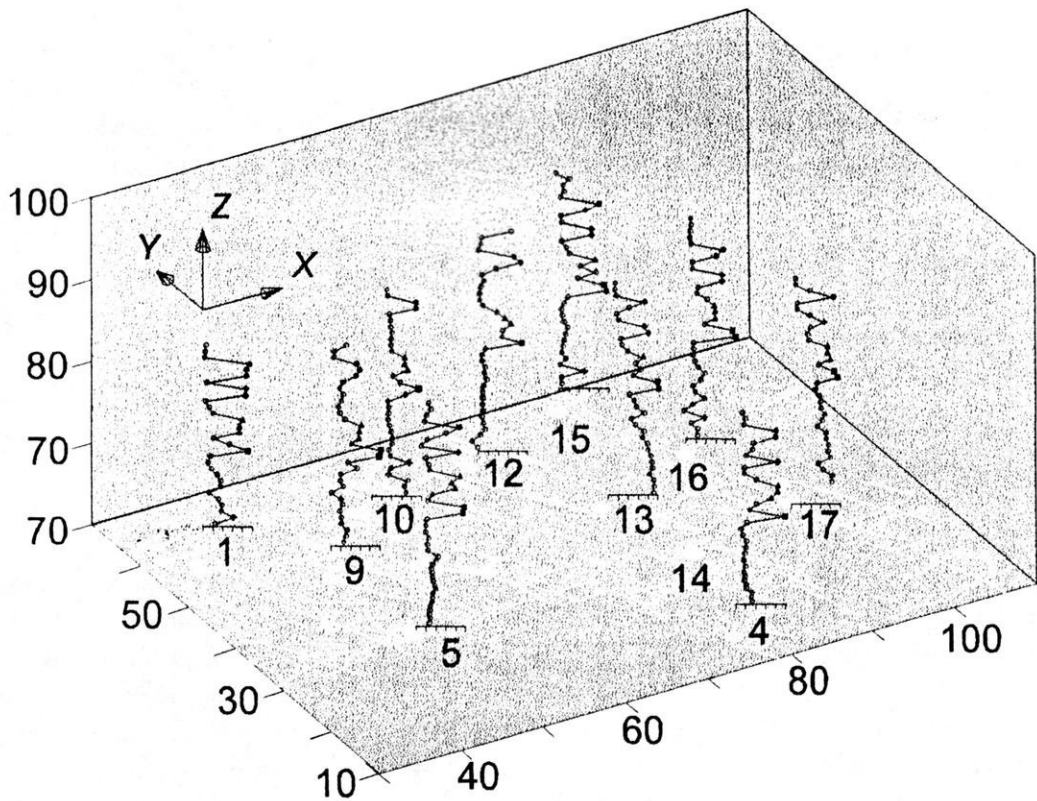


Figure 16. Block-diagram of hydraulic conductivity profiles for ten holes. Profiles are plotted at well location. X-axis of each profile is logarithmic and ranges from 10^{-2} to 10^{-7} ft/sec .

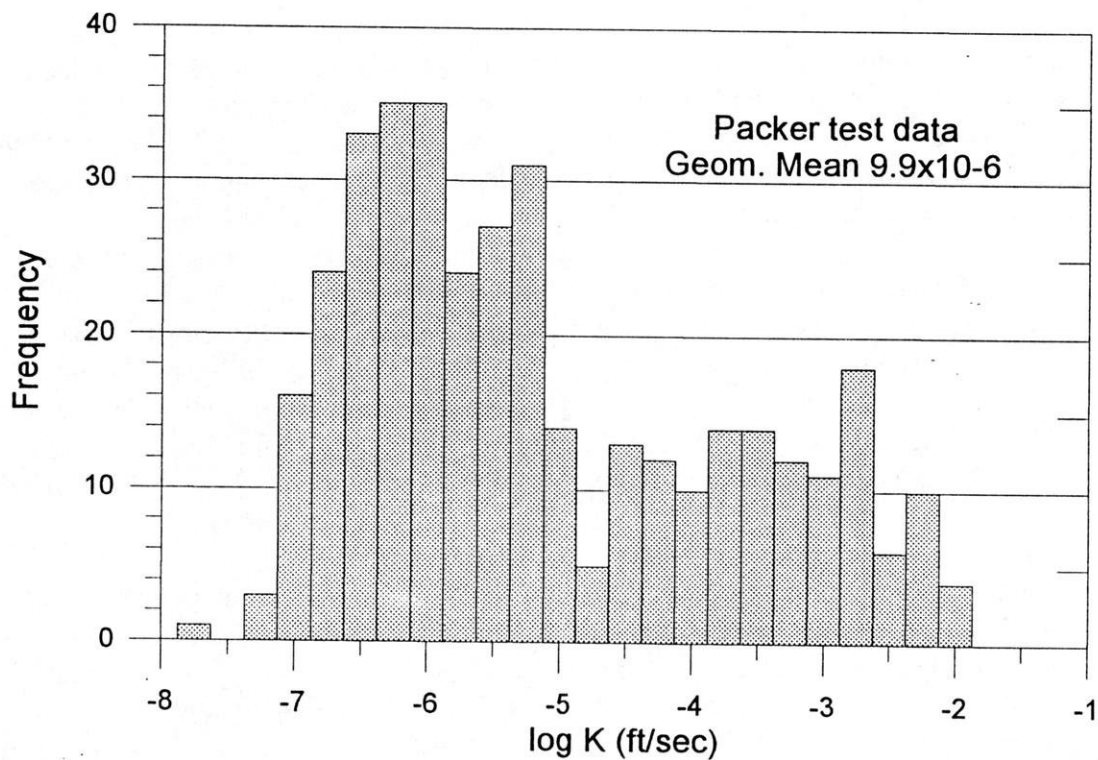


Figure 17. Histogram of 372 hydraulic conductivity values measured with short-interval packer tests. The bimodal distribution clearly shows the distribution of both low-conductivity matrix blocks and high-conductivity fracture and dissolution zones.

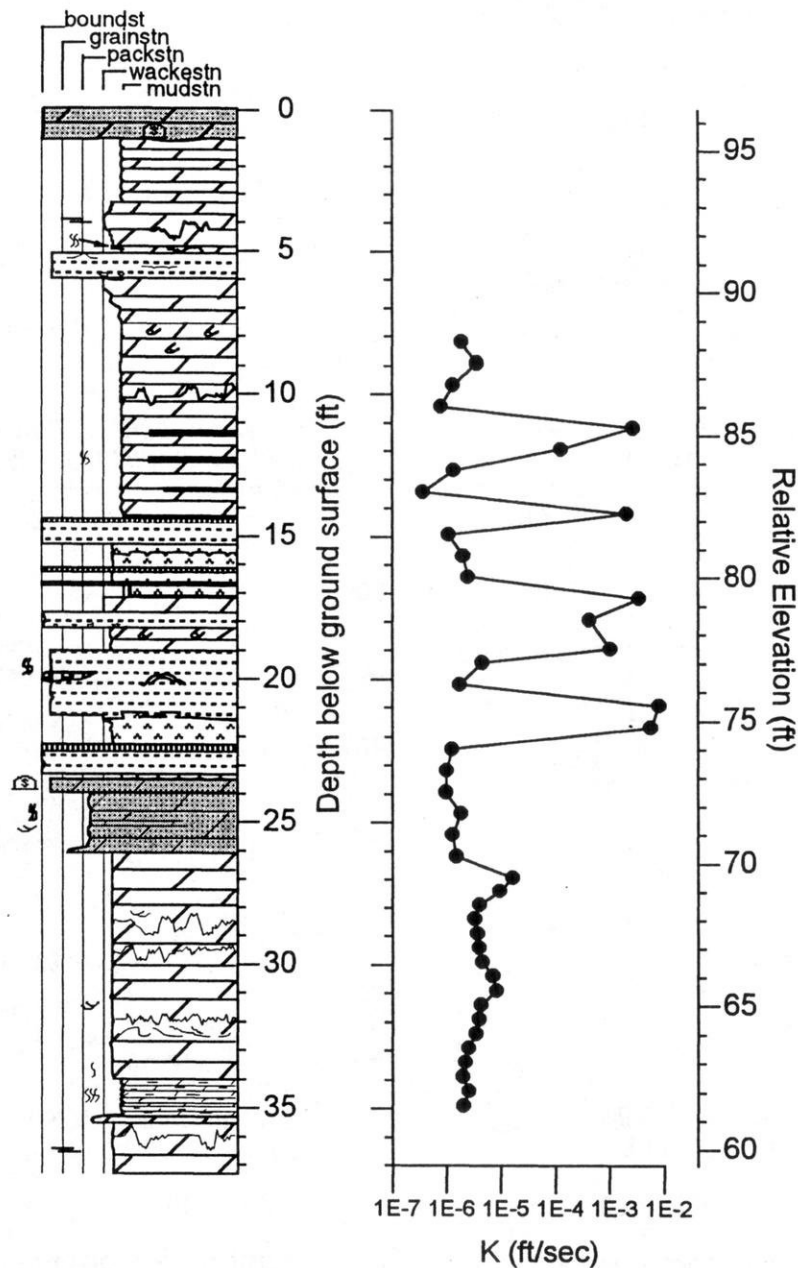


Figure 18. Correlation between stratigraphic features and hydraulic conductivity profile from hole 5. The fracture at approximately 75 ft elevation is an especially well-developed cycle boundary. High-permeability features between 75 and 80 ft elevation appear to be due to a combination of vuggy porosity within the crystalline dolomite and discrete fractures. Contacts between the restricted marine lithofacies and the open marine crystalline dolomite (primarily the fenestral mudstones and thinly and crinkly laminated facies) also form significant high-permeability features (77.5, 79, and 82.5 ft elevation).

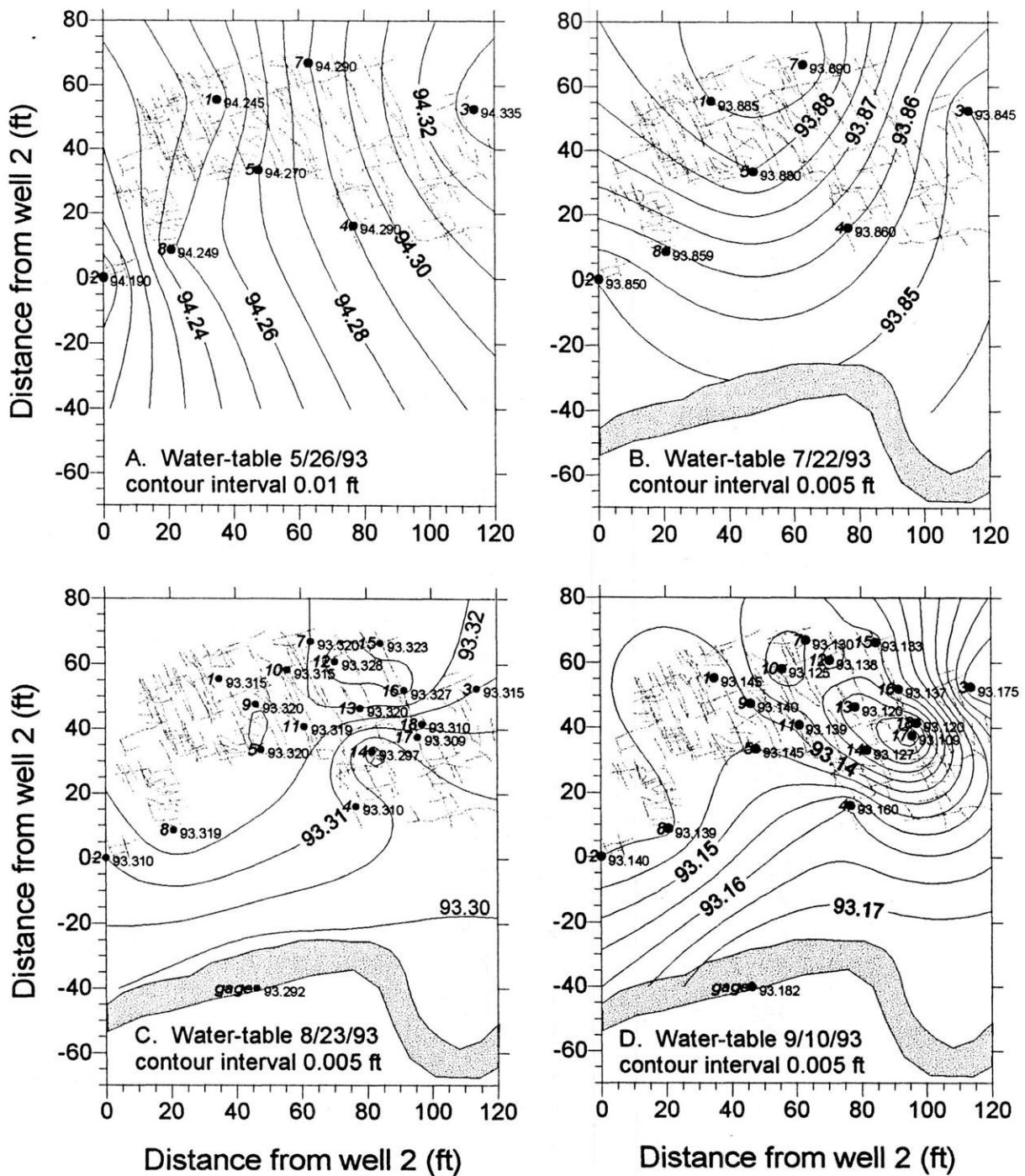


Figure 19. Hydraulic head distribution at Bissen Quarry in open boreholes. Head values (to the right of the symbol) and measuring points (in italics to the left of symbol) are shown on each map. Note that the contour interval varies for the different plots. **A)** Water-table elevation on 5/26/93, prior to installation of the drainage ditch. **B)** Water-table elevation on 7/22/93 after installation of drainage ditch. **C)** Water-table elevation on 8/23/93. **D)** Water-table elevation after rain the previous day, 9/10/93.

less steep and switched to the south-southeast (figure 8b). Water levels from 10 additional boreholes, drilled in August 1993, provide a more detailed picture of the local water-table response to recharge. At the site scale, local ridges and drain points develop due to the distribution of transmissive fractures. Figure 19c shows the water-table configuration after a week without rain. Flow is still generally towards the ditch, however a ridge of higher heads has developed in the northeast of the site. After rain on September 9, the gradient reverses and water flows out of the ditch, forming a ridge of higher heads from the southeast to the northwest corner of the site (figure 19d).

Multi-level Samplers

Installation of the multi-level samplers in June 1994 allowed us to determine the head distribution in discrete transmissive zones as well as to assess the vertical components of the hydraulic gradient. Head data were collected on 16 days from June to August 1994 for a total of over 1500 discrete head values.

Figure 20 shows water levels versus time for piezometers in hole 6 and multi-level ports in hole 14. The piezometers in hole 6 show an annual head variation of approximately 1.5 ft from spring to fall (figure 20a) while the multi-level ports varied approximately 0.5 ft over the summer (figure 20b). Data from piezometers in hole 6 indicate an upward vertical gradient in April 1994 suggesting that there may be transient reversals of head during recharge events (figure 20a). The multi-levels had not yet been installed in April 1994 and so the limited data from hole 6 are the only indication of upward vertical gradients during the time-frame of this project. Subsequent data collected during 1995 and 1996 indicate that the reversal of vertical gradients is an annual event (Muldoon, 1998). During the summer, vertical gradients were generally downward at the site; the average gradient between the top (14-1) and bottom (14-5) port in hole 14 was 0.01 (figure 20b). Similar to hole 14, the other holes with multi-level samplers exhibited a relatively steep gradient between the shallowest fracture at approximately 92 ft elevation and the dissolution zone at 87 ft elevation and moderate downward gradients between ports at 87, 78, and 75 ft elevation.

The magnitude and direction of the horizontal gradient varies across the site and from one discrete zone to the next; in general, horizontal gradients are quite low within large fractures because the high transmissivities allow head to dissipate. The head distributions for discrete high-permeability zones, illustrated in figure 21, are rather complex. The shallowest two monitoring zones both exhibit "drain points" -- lows in hydraulic head where water appears to move downward through vertical fractures. In the fracture at 92 ft elevation (figure 21a), water enters from the southwest and northeast corners of the site and drains have developed around holes 12 and 18. The drain within the vuggy zone at 87 ft elevation (figure 21b) is centered around holes 9, 10, and 11. The fractures at 82, 78, and 75 ft elevation (figures 21c, d, and e) all exhibit small gradients and no drain features. Flow is primarily to the west in zone 3 (82 ft elevation); in zones 4 (78 ft elevation) and 5 (75 ft elevation) a north-south ridge of higher head is present near the center of the site and flow is away from the ridge to east and west. The vuggy zone at 72 ft elevation exhibits a relative strong gradient to the south. The head configurations shown in figure

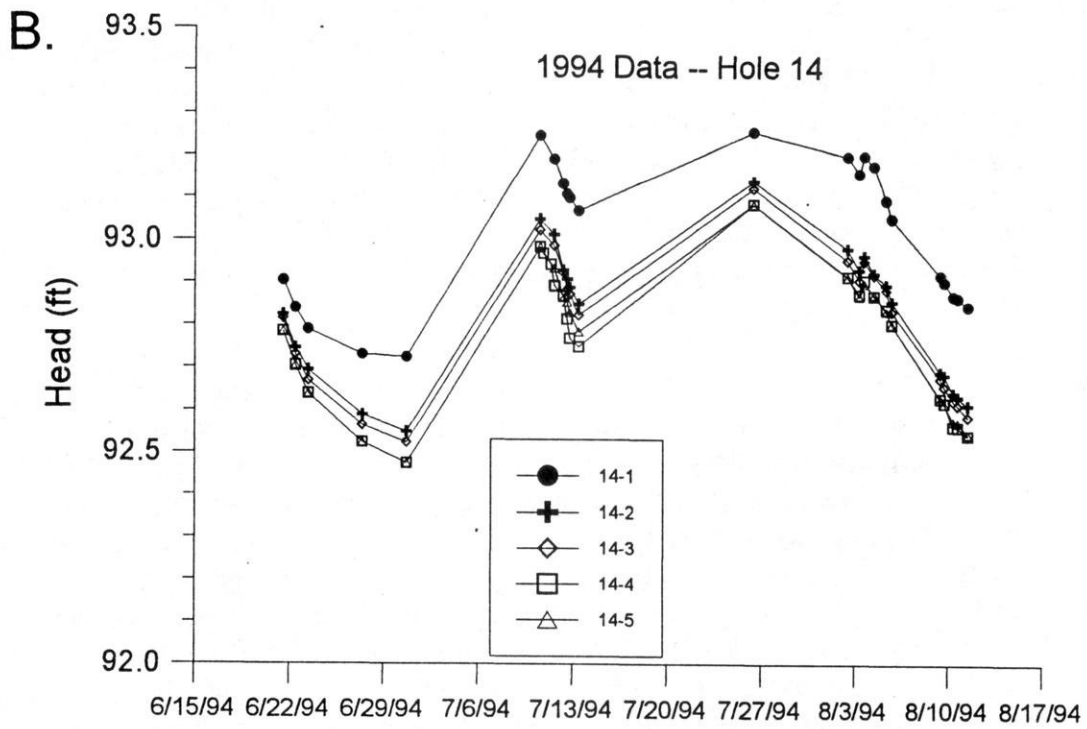
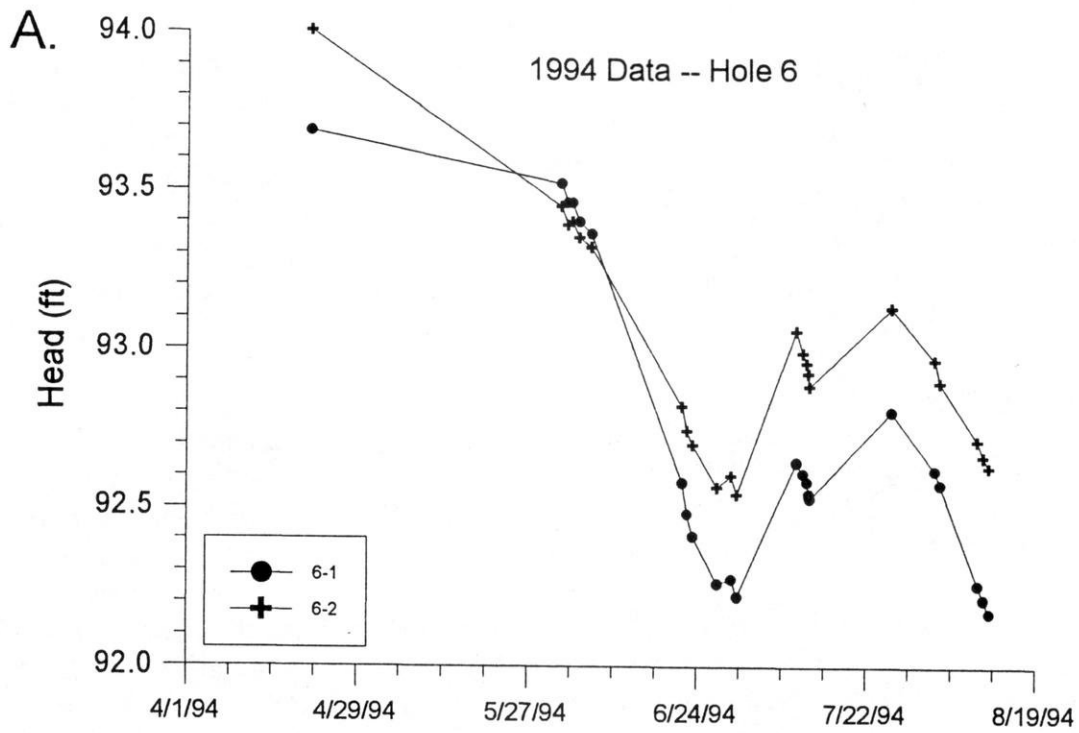


Figure 20. Water-levels versus time for **A)** piezometers in hole 6 and **B)** multi-level ports in hole 14.

21 were measured on July 7, 1994; plots for other dates suggest that the head configuration for the various monitoring zones remained relatively stable through the summer of 1994.

There could be many causes for the complex head distribution described above. These include lack of hydraulic continuity within the discrete zones, hydraulic conductivity variations within the discrete zones, instrumentation error (the multi-level sample port might not have been installed in the most transmissive part of a fracture or dissolution zone), and measurement error. It is difficult to separate these potential effects from each other.

The presence of open boreholes may also complicate the distribution of head within individual fractures. These boreholes provide direct pathways for water to flow from an upper fracture, into the borehole and out a lower fracture. In future work, we will seal off the open boreholes, either with removable packers or by abandoning the holes, so as to minimize the effect of vertical connection on the flow system.

Implications for Monitoring

The hydrogeologic site characterization completed at the Bissen Quarry was designed to determine both "continuum" aquifer properties, determined by standard monitoring techniques (*i.e.* "open-hole" pumping tests), as well as the properties of discrete fractures. Comparison of distributions of hydraulic head and hydraulic conductivity determined by these two approaches suggests that standard hydrogeologic field techniques, including long-interval monitoring wells, are of limited use in providing information on the flow characteristics of fractured-carbonate aquifers at a site-specific scale.

A simple comparison of hydraulic conductivity values measured at Bissen Quarry illustrates this point quite well. If we assume that the head distribution measured 7/22/93 in the open boreholes (see figure 19b) provides a reasonable estimate of the gradients at the site and we estimate an effective porosity of 1%, we can then calculate groundwater travel time for a 80-ft long flow path. Figure 22 shows the hydraulic gradient and flow-line for which travel times were calculated; table 7 summarizes the results. The variation in calculated travel times is a graphic illustration of the difference in the "continuum" versus the "discrete" approach to aquifer characterization. Tracer test results (described in the following chapter) indicate that hydraulic conductivity values determined by standard monitoring techniques such as the open-hole pumping test or the geometric mean value of packer test results provide unrealistic estimates of travel time. The maximum hydraulic conductivity measured by packer tests provided realistic estimates of travel time.

The above calculations assume a relatively simple distribution of hydraulic head, data from the multi-level samplers (figures 20 and 21) reveal that the head distribution at the site is much more complex. Accurate determination of head distribution is essential to determining flow directions, designing a monitoring system, or designing an effective remediation plan. Wisconsin monitoring well code (NR141) specifies that water-table wells have a 3- to 10-ft screen and that open

Table 7. Comparison of measured hydraulic conductivity values and calculated travel times

| Test Method | Hydraulic Conductivity (ft/s) | Calculated Travel Time* (units vary) |
|----------------------|----------------------------------|---|
| Pumping tests | | |
| <i>Open Holes</i> | Maximum | 6.3×10^{-4} |
| | Minimum | 1.8×10^{-5} |
| | Geometric Mean | 3.9×10^{-5} |
| <i>Multi-levels</i> | Maximum | 3.5×10^{-1} |
| | Minimum | 1.6×10^{-2} |
| | Geometric Mean | 4.1×10^{-2} |
| Packer Tests | | |
| | Maximum | 1.4×10^{-2} |
| | Minimum | 2.3×10^{-8} |
| | Geometric Mean | 9.9×10^{-6} |

* Calculations use a horizontal hydraulic gradient of .04/80 and assume an effective porosity of 1%

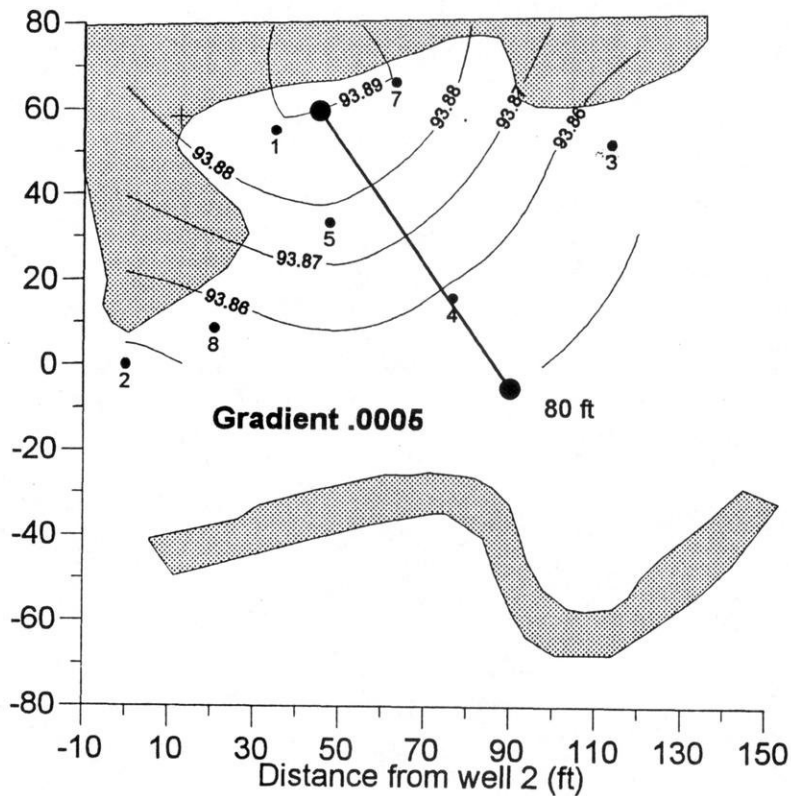


Figure 22. Head distribution, hydraulic gradient, and flow path used in calculating travel times.

bedrock wells (without screen) must be cased to a minimum depth of 2 feet and open below that. Neither of these standard monitoring well designs would be capable of providing the detailed head information required for determination of groundwater flowpaths at site-specific scales in settings similar to Bissen Quarry.

CHAPTER 3

TRACER TESTS

Tracer tests are an especially valuable tool for characterization of fractured-rock aquifers in that flow velocities, hydraulic connectivity of the fracture network, transport properties, and chemical reaction parameters can be directly observed. Davis and others (1985) report that the earliest tracer tests may have been performed up to 2000 years ago. Quantitative tracer experiments in porous media have long been used as a tool for understanding groundwater movement (Slichter, 1905). Recently, detailed tracer studies in relatively homogeneous granular aquifers (*e.g.*, LeBlanc and others, 1991; Moltyaner and others, 1993; Mackay and others, 1986; Sudicky, 1986) have contributed to a better understanding of the important role that heterogeneities play in both groundwater flow and transport processes.

Test Design and Methodology

As with any aquifer test, a successful tracer test needs to be well-designed in order to yield appropriate information. The first step is to establish the purpose of the test -- whether it is to determine the hydraulic characteristics (*i.e.* flow velocities and connectivity of the fracture network) or the transport parameters (*i.e.* dispersivity, role of matrix diffusion, chemical reaction parameters) of the groundwater flow system. Once the purpose of the test has been established, design parameters that should be considered include the following: test configuration, tracer injection method, choice of tracer, and sample analysis method. Davis and others (1985) provide a general guide to the practical application of groundwater tracers. The National Research Council Committee on Fracture Characterization and Fluid Flow (1996) discusses some special considerations of designing tracer tests in fractured-rock settings while Alexander and Quinlan (1992) outline procedures for tracer tests in karst environments.

Test Configuration

Tracer test configurations can be categorized into two main types: natural-gradient tests (including borehole-dilution tests) and controlled-gradient tests which include divergent, convergent, and two-well tests. The methodology, advantages, and disadvantages of each of these test configurations are briefly described below.

Natural-gradient Tests

Borehole-dilution tests provide an estimate of groundwater flux through a packed-off section of a borehole. A pulse of tracer is injected into the isolated interval and continually mixed. The natural groundwater flux through the borehole removes the tracer over time. By monitoring concentration over time, one can obtain the groundwater flow rate.

Natural-gradient tests are conducted by injecting one or more tracer pulses that are then transported by the natural, undisturbed groundwater flow system. These tests can be designed to

measure both the hydraulic and transport properties of the aquifer depending on the choice of tracer(s) used. Natural-gradient tests are difficult to conduct in fractured-rock settings and few tests are reported in the literature. The most well-known of these tests are costly, complex, three-dimensional tracer experiments conducted as part of radioactive waste disposal site characterization efforts such as the Stripa mine in Sweden (Abelin and others, 1991 a,b) and the Fanay-Augères project in France (Billaux and others, 1989).

Natural-gradient tests require monitoring tracer movement in three-dimensions over longer times than controlled-gradient tests. Both injection and sample recovery must be designed to minimize disturbance to the flow system; this usually requires relatively slow injection of tracer so as to not create an injection mound and recovery of small sample volumes so as to not induce large gradients towards the sample recovery points. Fractured-rocks are especially challenging settings for performing natural-gradient tracer tests for the following reasons:

- 1) designing a monitoring system is difficult since the majority of flow is within discrete, high-permeability fractures and the connectivity of these features is difficult to characterize without running tracer tests;
- 2) the tracer may bypass the monitoring system due to preferential or channelized flowpaths within discrete fractures;
- 3) there is often uncertainty in determining flow directions based on hydraulic measurements alone;
- 4) installing a dense, three-dimensional network of monitoring points in rock is expensive;
- 5) calculation of tracer mass in the subsurface is usually not possible due to limited monitoring points.

Controlled-gradient tests

Controlled-gradient tests provide flexibility in terms of input and monitoring locations as these are not dependant on the natural configuration of the flow system. Additional advantages of such tests are that 1) tests can be run for shorter periods of time, and 2) tests are run within a steady-state flow field, thus simplifying numerical modeling. Typical configurations for controlled-gradient tests include converging, diverging, and two-well tests. Tests can be run with both conservative as well as reactive tracers in order to characterize transport parameters.

In converging tests, a well is pumped to establish a steady-state flow field. Tracer is then injected into one or more wells some distance from the pumping well and tracer concentrations are monitored at the pumped well. The advantages of this type of test are that sampling is simplified, the amount of tracer recovered can be determined, and ideally the bulk of the tracer has been removed by the end of the test. The disadvantage of this configuration is that it only tests the portion of the aquifer between the injection well(s) and withdraw well. In addition, hydraulic properties of a fracture network (such as connectivity) determined under one pumping scenario are probably not representative for other flow-field configurations. Multi-well converging tests have been performed in the fractured dolomite at the WIPP site using tracers with differing molecular diffusivities in order to evaluate the role of matrix-diffusion in transport (McKenna and Meigs, 1997).

In divergent tests, water is injected to a recharge well at a constant rate in order to establish a steady-state flow field. Tracer is then injected -- as a pulse, a step increase, or continuously -- and concentrations are monitored at observation wells in the vicinity of the recharge well. Sampling concerns for this test are similar to the those of natural-gradient tests -- tracer may bypass the monitoring system and sample volumes need to be small so as not to disturb the flow field. The advantage of a divergent test is that it samples a larger volume of aquifer material than a simple two-well convergent test. A variation of the divergent test is the "push-pull" test where tracer is injected into the aquifer, injection is stopped and the aquifer "rests" for some time interval, and then pumping is resumed and the tracer is pulled back out of the formation. This type of test is used primarily to assess diffusion rates of the tracer.

Two-well tests involve pumping one well while recharging a second well, ideally at the same rate. Once a steady-state flow doublet has been established, tracer is injected to the recharging well and samples are collected from the pumping well. Tracer injection can be as a pulse, or the pumped water can be recharged. Recirculating tests are more difficult to analyze than either divergent or convergent tests because the tracer concentration varies over time. The main advantage of the recirculating test is logistical -- reinjecting the pumped water minimizes the volume of water necessary for injection and disposal of the pumped water is not a concern. Several two-well tests, conducted in an isolated fracture, have been reported for fractured-carbonate aquifers (Shapiro, 1988; Shapiro and Nicholas, 1989; Leap, 1992; Cady and others, 1993; Dronfield and Silliman, 1993).

Tracer tests completed at Bissen Quarry during the summer of 1994 include two convergent tracer tests and one natural-gradient test; detailed descriptions of each test are included in a later section.

Choice of Tracer

A wide variety of tracers, including radioactive substances, fluorescent dyes, soluble salts, fluorocarbons, inert gases, latex microspheres, and a wide variety of organic compounds, have been used in groundwater investigations. Choice of tracer primarily depends on 1) purpose of test, and 2) available sampling and analytical procedures. Conservative tracers are well-suited for tracer tests designed to evaluate hydraulic properties; determination of transport properties usually requires both conservative and reactive tracers. Some tracers, such as gases, require special sampling procedures. No one reference provides an all-inclusive list of tracers, Alexander and Quinlan (1992) provide a general summary of natural and introduced tracers. The following list, modified from ASTM D-5717-95 (1995), summarizes some of the properties of an ideal tracer. It is:

1. non-toxic to people and the ecosystem;
2. either not naturally present in the system or present at very low, near-constant levels;
3. in the case of chemical substances, soluble in water with the resulting solution having approximately the same density as water;
4. in the case of particulate tracers, neutral in buoyancy and of known (presumably constant) size distribution;

5. unambiguously detectable over a wide range of concentrations;
6. in the case of conservative tracers, resistant to adsorptive loss and/or to chemical, physical, or biological degradation, while reactive tracers should have known molecular diffusivities;
7. capable of being analyzed quickly, economically, and quantitatively;
8. easy to introduce to the flow system;
9. inexpensive and readily available.

In addition, it does not modify the hydraulic conductivity or other properties of the aquifer under investigation (Davis and others, 1985).

Commonly used tracers, available for this study and having many of the above properties, include inorganic halogen ions (bromide, Br⁻; chloride, Cl⁻; and iodide, I⁻) and fluorescent dyes (for example, rhodamine WT and fluorescein). Fluorescent dyes have the advantage that qualitative tests can be monitored passively, using cotton "bugs" (Alexander and Quinlan, 1992) that are lowered into piezometers and later scanned with a long-wave UV lamp or fluorometer to test for the presence of the dye. Since these tracers are detectable in the parts per billion range using a standard fluorometer, input concentrations can be kept in the range of 1 to 10 ppm thus avoiding density problems while providing a detectability range of four to five orders of magnitude.

Tracer tests using inorganic halogen ions require active monitoring, and the resulting water samples are typically analyzed using ion-selective electrodes or ion chromatography. Electrodes have detection capabilities to the parts per million range while ion chromatography is typically accurate to the tenths of ppm. For input concentrations in the range of 500 to 1000 mg/l, these tracers have a detectability range of 3 1/2 to four orders of magnitude. Input concentrations greater than 1000 mg/l appear sufficient to induce density-driven flow. At the Cape Cod tracer test site, LeBlanc and others (1991) noted minor density-induced sinking of the plume with an input concentration of 890 mg/l of dissolved solids.

The Private Water Supply Section of the Wisconsin Department of Natural Resources granted a variance of section NR 112.05 to Ivan Bissen so that we could perform tracer tests at Bissen Quarry. The variance allowed the use of inorganic halogen ions (Cl⁻, Br⁻, I⁻) as well as the use of a fluorescent dye (rhodamine WT) for the period October 20, 1993 to October 20, 1994. While we believe rhodamine WT to be a safe and effective tracer, we have not used it at the site due to safety issues raised by the Wisconsin Department of Health and Social Services.

Tracer Injection

When designing tracer injection, the factors to be considered include: 1) rate and duration of injection, and 2) volume and concentration of tracer. Tracers can be injected as discrete, small-volume pulses or continuously over the length of the test. Each method has advantages and disadvantages and choosing the duration of injection and the concentration of tracer depends on a variety of factors including 1) the types of aquifer parameters the test is designed to measure, 2) the number of tests to be run at the site and 3) estimates of the amount of dilution that is likely to be encountered over the travel distances of interest.

Continuous injection tests yield cumulative breakthrough curves and are usually conducted over a time frame such that the concentration in the monitoring well(s) eventually reaches the input concentrations. These tests are frequently run with both conservative as well as reactive tracers and are especially useful for characterizing retardation rates for solute transport modeling. Additional advantages of continuous-injection tests are that 1) it is less likely that the pulse will be "lost" due to dilution or dispersion, 2) input concentrations do not need to be as high, thus minimizing density effects, and 3) the continuous injection tends to damp out variations in transport that are due to injection conditions. The primary disadvantages of such a test are the logistic problems generated by 1) longer injection times, 2) large volumes of tracer, and 3) the resulting large tracer mass in the groundwater. Typically one mixes tracers with groundwater from the site and tries to maintain ambient temperature until the resulting tracer is injected into the groundwater system. Maintaining uniform concentration and ambient temperature for a large volume of tracer over a long time frame is logistically complicated.

Pulse tracer tests use small volumes of tracer injected over a relatively short time interval compared to the length of the test. Logistically, short-term, small-volume injections are easier, however, dilution and dispersion of tracer results in low concentrations at monitoring locations and it is not uncommon for a pulse to be "lost" prior to recovery at monitoring points. Despite these problems, we chose to perform pulse tracer tests because we were most interested in determining hydraulic connectivity of the fracture network and were thus interested in performing several tests within the summer field season. Small tracer volumes and rapid dilution means the site quickly recovers to background concentrations thus allowing more tests to be performed.

Monitoring Method and Frequency

Monitoring method will be determined by 1) the purpose of the test, 2) configuration of the test, and 3) the choice of tracer. Tests designed to evaluate hydraulic connectivity can sometimes be monitored passively to determine presence or absence of tracer; an example would be the use of cotton "bugs" that adsorb fluorescent dyes (Alexander and Quinlan, 1992). Other passive monitoring strategies include thermal-couples wired to a datalogger and passive gas collectors. Most tracers, however, require collection of water samples throughout the duration of the test. Sample volumes from non-pumping sampling points need to be minimized so as not to induce large gradients. An appropriate sampling frequency is chosen given the estimated travel time for the tracer.

Multi-well tracer tests generate numerous samples. Length and scale of tests will determine how many samples are collected; but even short-term small tests can generate hundreds of samples. The number of samples can be minimized by collecting samples from only selective monitoring points during the test. Selective sampling is most effective for tracer tests with relatively predictable tracer movement and was used successfully in the Cape Cod tracer experiment (LeBlanc and others, 1991). Tracer tests in fractured-rock aquifers tend to be less predictable and thus we sampled all ports for the duration of each test.

At Bissen Quarry, the gradients within the horizontal fractures are quite small and travel times are rapid; as a result we designed a monitoring method that minimized the sample volume collected and allowed rapid sample recovery from many ports simultaneously. While small sample volumes are advantageous in terms of minimizing disturbance to the flow field, one needs to insure that an adequate volume has been purged from the sample line so the sample is being drawn from the groundwater system at the time of sample collection, rather than from groundwater that has been sitting in the sampling tube since the previous sample collection. Figure 23 shows the sampler developed for tracer tests at Bissen Quarry. A vacuum placed on the glass flask pulled samples from 5 to 6 ports simultaneously. Small-diameter (0.058-in ID) nylon tubing was placed down the larger diameter multi-level tubes (3/8-in ID) to the base of each sampling port. Tubing from each port was connected to two 20-ml sampling vials. The tubing within the vials was placed so that the first 20-ml of water filled the first vial from the bottom up (figure 23). Once the first vial was full, the water exited from the top of the vial and spilled over to the second vial. Thus the first 20-ml constitute purge water and the second 20 ml constitute the sample volume which was then capped and saved for later analysis. After sample collection, the sample tubing was clamped off so that the water stayed in the tubing rather than flowing back down the hole. This helped minimize disturbances to the flow field and facilitated more rapid sample collection during subsequent sampling rounds. The volume of a 30-ft length of the small-diameter tubing is approximately 16 ml; so the above sampling method ensured that at least one purge volume was removed from the deeper ports while the shallower ports had two or more purge volumes removed prior to sample collection.

The purpose of the tracer tests at Bissen Quarry was to define the connectivity of the fracture network and thus we were testing the rapid-flow component of the flow system. Sampling frequencies were typically on the order of every 15 minutes for the first few hours of a test and gradually increased to one to six hours in the later portions of the controlled-gradient tests. The natural gradient test was run for 12 days; initial sampling frequency was similar to the controlled-gradient tests; samples were collected approximately every 2 to 3 hours the second day; approximately every 6 hours the third day, and then daily until the completion of the test.

Sample Analysis

Sample analysis forms a significant cost both in terms of time and expense for any tracer test. In order to be effective, the analytical method needs to be rapid, inexpensive, and have the necessary degree of accuracy. All samples collected in the 1994 tracer tests at Bissen Quarry were analyzed using ion-selective electrodes. Evaluation of the ion-selective electrode analyses from the natural-gradient test, which involved injection of both chloride and bromide, suggested that the electrodes were erroneously detecting the other ion. In addition, high background levels of sulfate in some samples would sometimes form on the electrode tip interfering with the analyses. As a result, selected samples from the controlled-gradient chloride test and the natural-gradient test were also analyzed by ion chromatography. Insufficient sample volumes remained from the first controlled-gradient bromide test to allow reanalysis by ion chromatography.

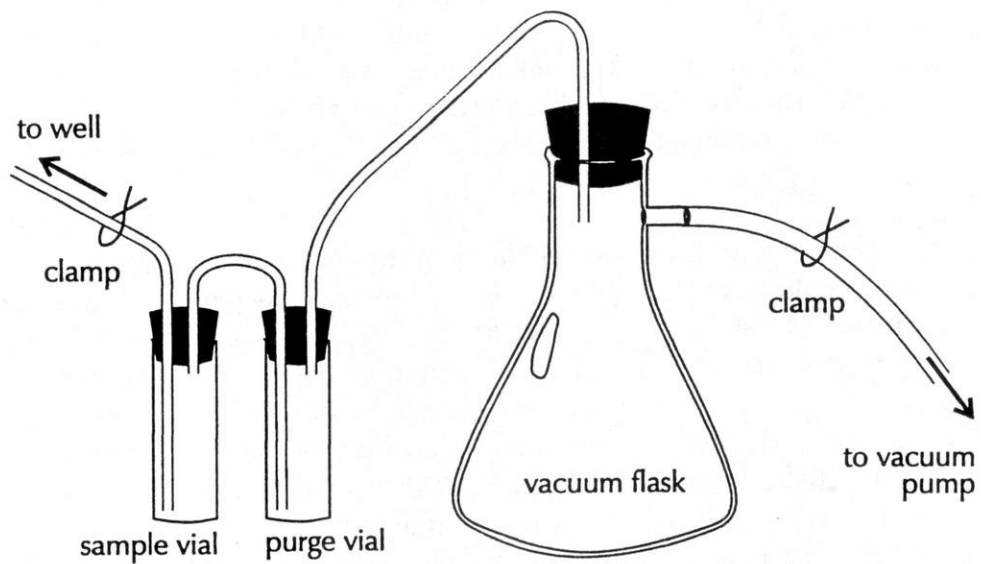
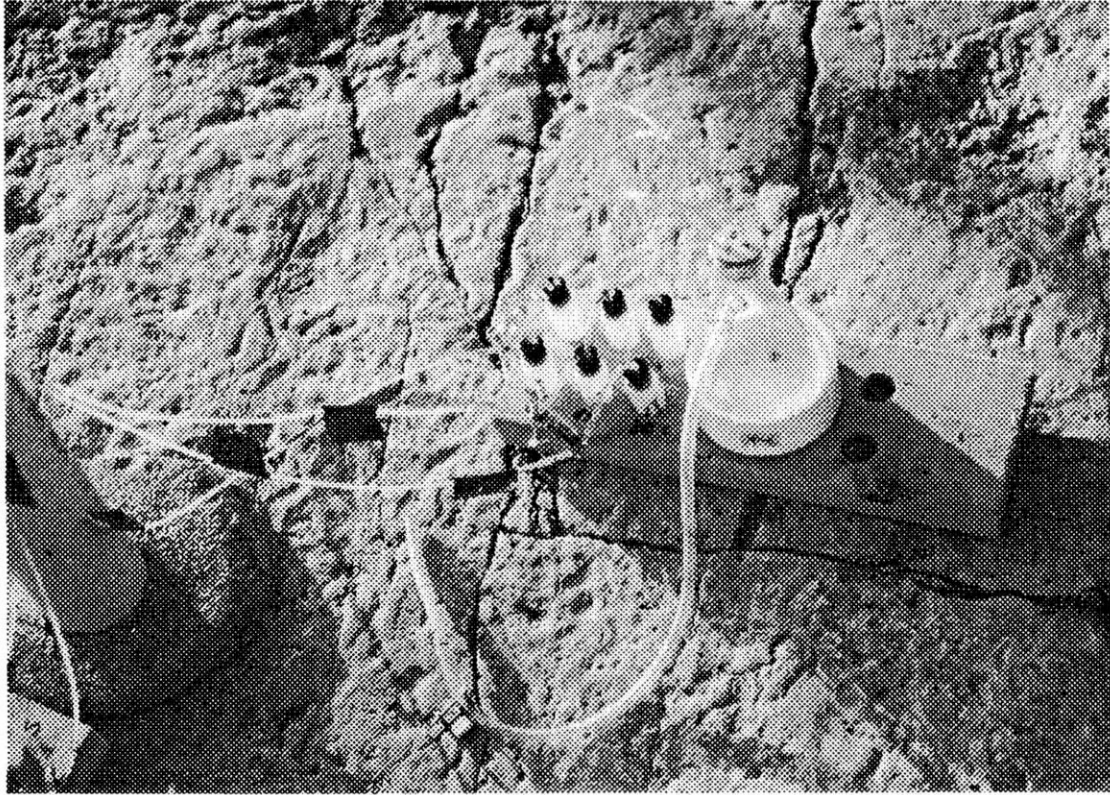


Figure 23. Sampler used in tracer tests at Bissen Quarry. Sampler was designed to rapidly collect multiple samples while minimizing the sample volume.

Ion-selective electrode analyses:

The ion-selective electrodes used in this study are relatively accurate over a range of 1-1000 ppm (Orion™ Research, Inc, 1991). For the analyses, we prepared standard solutions of the following concentrations: 1, 2, 5, 10, 25, 50, 100, 250, 500, and 1000 mg/l of bromide, chloride, and iodide. The electrodes yield a millivolt response that is inversely and logarithmically related to concentration. We would determine a calibration curve by measuring the standards, plotting millivolts versus standard concentrations on a semi-log plot, fitting a best-fit straight line to the calibration data and then using the calibration curves to calculate concentrations for the unknown samples. Typically 15 to 20 unknown samples would be measured and then the calibration samples would be measured. If the readings were consistent, more unknown samples would be analyzed, otherwise the electrode tip would be cleaned, and a new calibration curve would be determined before analyzing additional samples.

During several of the tests, we performed preliminary field analyses on selective samples. Ion-selective electrode analyses are very temperature dependant and it was difficult to maintain the standards and samples at a constant temperature under field conditions. As a result, all samples were subsequently analyzed under more controlled conditions. The first test was analyzed by the first author, while in the field, so that results could be used to design future tests. Samples from subsequent tests were analyzed by student technicians at the UW Soils Department Laboratory and the WGNHS.

Ion-chromatography analyses:

Selected samples from the 1994 tracer tests were also analyzed using Prof. Jim Bockheim's Dionex 2000i ion chromatograph (IC) in the UW Soils Department. An AS4A column was used with a conductivity detector to analyze the following inorganic anions: Cl^- , Br^- , NO_3^- , SO_4^{2-} . Calibration standards were set up to look the linearity of response of bromide while background concentrations of the other anions remained constant. Standards had the following concentrations: 15 mg/l Cl^- , 1 mg/l NO_3^- , 30 mg/l SO_4^{2-} and variable Br^- concentration (10 mg/l, 6 mg/l, 3 mg/l, 0.5 mg/l, 0.25 mg/l).

An auto-sampler allowed analysis of 72 samples (9 trays of 8 samples) in each day's run. Analytical procedure consisted of a complete set of calibration standards at the start of each run to check for linearity of response, a 10 mg/l calibration standard at the start of each tray, and the last sample of each tray alternated between a random replicate sample and a low-concentration standard.

Background Chemistry

A round of background samples was collected from all sampling ports in late June, 1994. All samples were analyzed for Cl^- and Br^- using ion-selective electrodes. We attempted to analyze the background sample for I^- as well, unfortunately an unknown interference caused instability in the I^- readings. Davis and others (1985) note that bacteriological activity can create interferences with iodide-selective electrodes. We noted extensive algae growth in the open boreholes prior to

the installation of the multi-levels and believe that this may be causing the interference. In addition to the ion-selective analyses, selected samples from the June sampling round were submitted to the UW Soil and Plant Analysis Laboratory for more complete cation/anion analysis. Table 8 summarizes background values of Cl^- and Br^- prior to any tracer injection. Chloride values determined from ion-selective electrode analysis range from 2.78 to 21.98 mg/l, most values agree reasonably well with values from the Soil and Plant Analysis Lab. Bromide concentrations for all but one sample are less than 1 mg/l.

Since water chemistry in the Silurian aquifer exhibits significant spatial and temporal variability (Bradbury and Muldoon, 1992), one to three samples were collected within the 24 hours prior to the initiation of each tracer test. These samples provided measures of background Cl^- and Br^- concentrations for specific tests. Measured background Cl^- concentrations were subtracted from Cl^- concentrations plotted in the breakthrough curves; the background Br^- concentrations were typically less than 1 mg/l and so this correction was not performed on the Br^- data

Description of Tracer Tests and Results

Several controlled-gradient tracer tests have been completed at the site as well as one natural-gradient test. The set-up of each test, injection conditions, monitoring schemes, and results are described below. Each test generated from over 300 to over 1000 samples; the sample results are briefly summarized in this report. WGNHS Open File Report 98-3 (Muldoon, 1998) includes a complete listing of all sample results from each test.

Controlled-gradient Bromide Test

The set-up for this test, performed July 12-13, 1994 is shown in figure 24. This test was designed to test the fracture at 75 ft elevation. Injection and withdrawal pumps were started three hours prior to the initiation of tracer injection in order to establish a steady-state flow field. One liter of 500 mg/l Br^- tracer was injected into port 9-5 for 9.5 minutes at a rate of approximately 105 ml/min. Two liters of ambient groundwater, also injected at 105 ml/min, were used to flush tracer from the injection port; injection was stopped following the flushing. Water was continuously withdrawn from port 14-4 at a rate of 67 ml/min; the small-diameter of the sampling tube was the rate-limiting factor for withdrawal.

Tracer concentrations were monitored at one upgradient location (hole 1), the injection location (hole 9), and two downgradient locations (holes 11 and 14). At each monitoring location we sampled three ports: the port open to the injection fracture zone (75 ft elev), the port above the injection fracture (78 ft elevation), and the port below the injection fracture (71 ft elev). Samples were collected at approximately 15-minute intervals for first 2 hours and 30-minute intervals from 2-11 hours.

Tracer was detected at only three ports; table 9 summarizes tracer detection data and figure 25 shows the breakthrough curves for the ports in holes 9 (left) and 14 (right). Tracer was detectable in the injection port (9-5) until approximately 100 minutes into the test. Tracer moved

Table 8. Background Cl⁻ and Br⁻ values from Bissen Quarry. All units are mg/l.

| | | Ion-selective Electrodes | | Soil & Plant Lab | | | | Ion-selective Electrodes | | Soil & Plant Lab | |
|------|-----------------|--------------------------|-----------------|------------------|------|-----------------|-----------------|--------------------------|-------|------------------|--|
| Port | Cl ⁻ | Br ⁻ | Cl ⁻ | diff | Port | Cl ⁻ | Br ⁻ | Cl ⁻ | diff | | |
| 1-2 | 9.89 | 1.69 | 10.00 | 0.11 | 14-1 | 10.69 | 0.35 | | | | |
| 1-3 | 6.90 | 0.22 | 8.00 | 1.10 | 14-2 | 11.99 | 0.40 | | | | |
| 1-4 | 6.02 | 0.22 | 6.50 | 0.48 | 14-3 | 11.74 | 0.42 | | | | |
| 1-5 | 12.49 | 0.34 | 14.00 | 1.51 | 14-4 | 8.64 | 0.33 | | | | |
| 1-6 | 16.11 | 0.43 | 17.50 | 1.39 | 14-5 | 8.90 | 0.49 | | | | |
| | | | | | | | | | | | |
| 4-1 | 12.6 | 0.23 | 14.00 | 1.40 | 15-1 | 4.11 | 0.83 | 3.00 | -1.11 | | |
| 4-2 | 12.23 | 0.22 | 14.00 | 1.77 | 15-2 | 8.46 | 0.30 | 10.50 | 2.04 | | |
| 4-3 | 9.28 | 0.19 | 9.00 | -0.28 | 15-3 | 8.11 | 0.29 | 10.50 | 2.39 | | |
| 4-4 | 11.09 | 0.22 | 11.50 | 0.41 | 15-4 | 8.29 | 0.32 | 9.50 | 1.21 | | |
| 4-5 | 21.86 | 0.39 | 22.50 | 0.64 | 15-5 | 7.29 | 0.28 | 11.50 | 4.21 | | |
| | | | | | 15-6 | 7.77 | 0.36 | 11.00 | 3.23 | | |
| 9-1 | 4.75 | 0.13 | | | | | | | | | |
| 9-2 | 7.90 | 0.18 | | | 16-1 | 2.71 | 0.73 | | | | |
| 9-3 | 7.90 | 0.19 | | | 16-2 | 5.89 | 0.24 | | | | |
| 9-4 | 7.14 | 0.19 | | | 16-3 | 6.69 | 0.25 | | | | |
| 9-5 | 10.91 | 0.21 | | | 16-4 | 6.61 | 0.23 | | | | |
| 9-6 | 10.91 | 0.22 | | | 16-5 | 6.69 | 0.58 | | | | |
| | | | | | | | | | | | |
| 10-2 | 7.26 | 0.20 | 7.50 | 0.24 | 17-1 | 10.69 | 0.25 | 15.00 | 4.31 | | |
| 10-3 | 6.02 | 0.22 | 7.00 | 0.98 | 17-2 | 9.29 | 0.23 | 13.50 | 4.21 | | |
| 10-4 | 5.87 | 0.22 | 7.00 | 1.13 | 17-3 | 7.35 | 0.19 | 10.00 | 2.65 | | |
| 10-5 | 10.32 | 0.19 | 11.50 | 1.18 | 17-4 | 7.51 | 0.21 | 11.00 | 3.49 | | |
| 10-6 | 10.32 | 0.23 | 12.50 | 2.18 | 17-5 | 7.51 | 0.27 | 10.50 | 2.99 | | |
| | | | | | | | | | | | |
| 11-1 | 7.84 | 0.21 | 9.00 | 1.16 | 18-1 | 4.80 | 0.20 | | | | |
| 11-2 | 12.49 | 0.27 | 13.00 | 0.51 | 18-2 | 9.29 | 0.29 | | | | |
| 11-3 | 8.17 | 0.21 | 9.50 | 1.33 | 18-3 | 7.29 | 0.18 | | | | |
| 11-4 | 7.45 | 0.25 | 9.00 | 1.55 | 18-4 | 7.29 | 0.18 | | | | |
| 11-5 | 11.00 | 0.25 | 12.00 | 1.00 | 18-5 | 7.20 | 0.18 | | | | |
| 11-6 | 10.91 | 0.28 | 13.50 | 2.59 | 18-6 | 7.29 | 0.21 | | | | |
| | | | | | | | | | | | |
| 12-1 | 3.11 | 0.16 | | | | | | | | | |
| 12-2 | 6.69 | 0.19 | | | | | | | | | |
| 12-3 | 6.25 | 0.21 | | | | | | | | | |
| 12-4 | 8.07 | 0.20 | | | | | | | | | |
| 12-5 | 8.90 | 0.23 | | | | | | | | | |

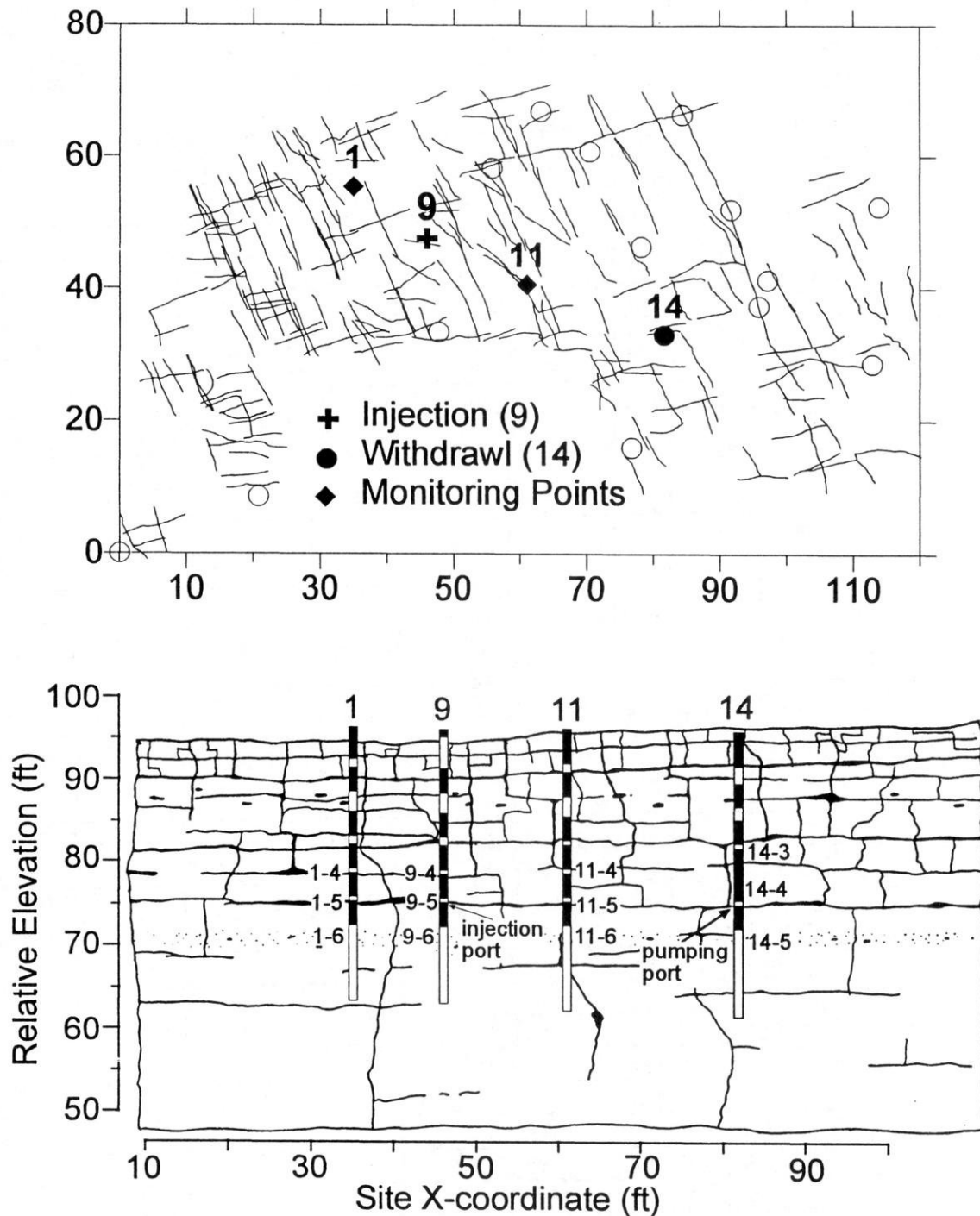


Figure 24. Set up for the controlled-gradient Br^- tracer test conducted in the fracture at 75 ft elevation. Map shows location of wells. Cross section is projected onto X-axis of site; white zones indicate multi-level ports. Tracer was injected at port 9-5 and water was withdrawn from port 14-4; monitoring ports are labeled.

Table 9. Summary of results from the controlled-gradient bromide tracer test

| Port | Detection | Peak Conc. (mg/l) | Peak Arrival (min)* | Distance from Injection (ft) | Velocity (ft/day) |
|------|-----------|-------------------|---------------------|------------------------------|-------------------|
| 1-4 | no | 1.29 | -- | 13.98 | -- |
| 1-5 | no | 0.72 | -- | 13.54 | -- |
| 1-6 | no | 0.78 | -- | 13.99 | -- |
| 9-4 | no | 1.45 | -- | 3.5 | -- |
| 9-5 | injection | 3.83 | -- | 0.0 | -- |
| 9-6 | yes | 13.24 | 150 | 3.5 | 33.6 |
| 11-4 | no | 1.10 | -- | 16.87 | -- |
| 11-5 | no | 0.74 | -- | 16.5 | -- |
| 11-6 | no | 1.45 | -- | 17.56 | -- |
| 14-3 | no | 1.12 | -- | 39.06 | -- |
| 14-4 | no | 0.70 | -- | 38.46 | -- |
| 14-5 | yes | 30.07 | 162 | 38.63 | 343.4 |

both downward to port 9-6 and horizontally to port 14-5; travel distances and average velocities are summarized in Table 9. Tracer moved rapidly in the horizontal direction, reaching 14-5 within the first 11 minutes of the test; the tracer peak reached 14-5 at 162 minutes (figure 25 and table 9). No tracer was detected at 14-4, the withdrawal port. It may be that the bulk of the tracer moved downward, under the influence of the vertical gradient, and so reached 14-5 rather than 14-4, or it may be that pumping, which induces radial flow to the port, may have diluted the tracer signal. Downward tracer movement to port 9-6, 3.5 feet below the injection port, was not as rapid as the horizontal transport to port 14-5. The tracer first reached port 9-6 at 75 minutes and the peak concentration was measured 150 minutes into the test (figure 25 and table 9).

Controlled-gradient Temperature Tests

Samples from the first tracer tests were analyzed in the week following the test; analysis, data entry, and generation of breakthrough curves took approximately five days. Given the time-intensive nature of that test, we decided to explore whether we could use temperature as a tracer. Such a test could be monitored using downhole thermocouples wired to a continuously-recording datalogger, thus eliminating the need to collect samples throughout the test and simplifying the analysis of tracer movement. During the week of 7/25/94 we obtained a thermocouple that would

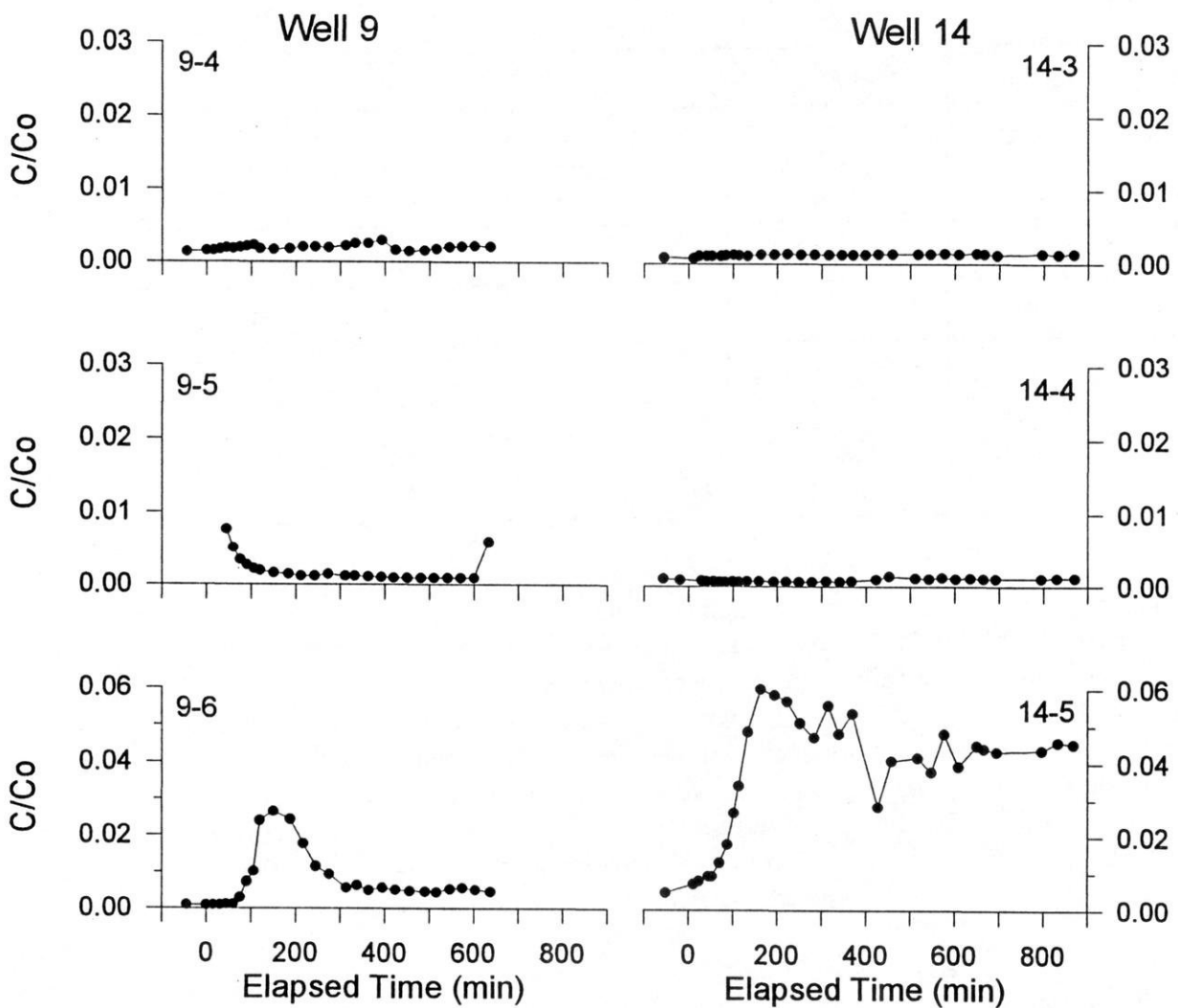


Figure 25. Breakthrough curves for the monitoring ports in holes 9 (left) and 14 (right). Note vertical axes for bottom ports are twice the scale of the shallower ports.

Table 10. Summary of controlled-gradient temperature tracer tests

| Date | Injection Volume* | Injection Temp C° | Injection Time | Pumping Port | Monitoring Port |
|-------------|--------------------------|--------------------------|-----------------------|---------------------|------------------------|
| 7/26/94 | 5.75 liters | 29.3 | 13:25-14:37 | 12-4 | 12-4 |
| 7/26/94 | 7.25 liters | 29.3-31.1 | 17:15-18:46 | 12-4 | 12-5 |
| 7/27-29/94 | 12.5 liters | 34.1 | 15:49-16:56 | 12-5 | 12-4 |

*All injections were to port 15-5.

fit down the 3/8-in diameter multi-level tubing and performed three controlled-gradient temperature tracer tests. These tests were conducted between holes 12 and 15. Tracer was always injected into port 15-5 (fracture at 75 ft elevation), however, the withdrawal port and the monitoring port varied for different tests. A packer was installed in hole 13 to seal off the fracture at 75 ft elevation so as to minimize any effects of having an open hole nearby.

Background temperature variations at port 12-4 (fracture at 75 ft elevation) were measured every minute and recorded every 5 minutes for approximately 21 hours prior to any tracer injection. Figure 26 shows that temperature ranged from 10.75 to 12.0 C°; several events may have influenced temperature fluctuations including a brief rain shower and the pumping of port 14-4 to obtain injection water for the tracer tests to be conducted the following day.

Table 10 summarizes the injection data and monitoring configuration for the three temperature tracer tests. The first test, conducted with the injection port (15-5) and the withdrawal and monitoring port (12-4) in the fracture at 75 ft elevation, was inconclusive. Temperature was recorded every minute; the maximum temperature was 12.5°; figure 27 shows the results of this test. It is not clear if the temperature fluctuations are due to the tracer injection.

Believing that the tracer had probably moved downward, rather than laterally, we chose to monitor temperature one port down (12-5) while maintaining the same injection/pumping configuration as the first test. Figure 28 shows the results from this second test. Both injection and withdrawal were stopped after 135 minutes. We continued to monitor temperature through the night and it appears that a tracer pulse may have moved through between 20:00 and 23:00 or the change in temperature may have been natural variation.

In order to better determine whether the temperature variations we were seeing were caused by injection, we completed a third test during which we injected hot water with a concentration of 500 mg/l Br⁻. Since pumping seemed to mask the temperature signal, we changed the configuration of this test; injection was again into the fracture at 75 ft (port 15-5) temperature was monitored in the same fracture at port 12-4; however, we pumped from one port down at 12-5. The results of this test are shown in figure 29. There are two clear temperature pulses at port

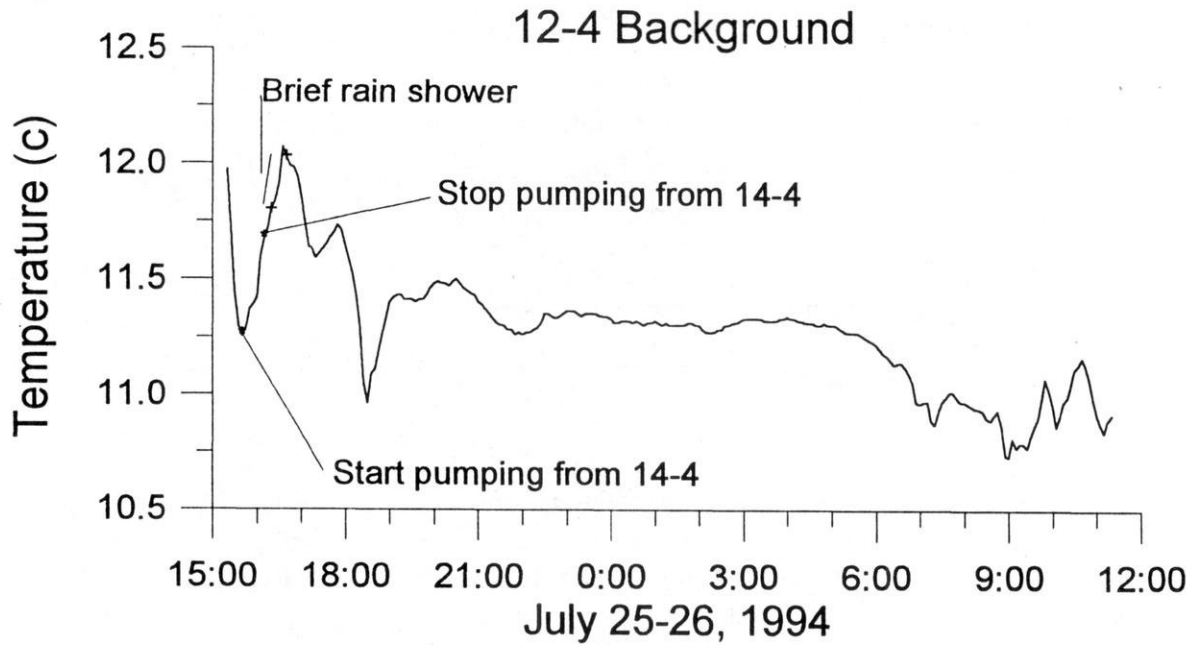


Figure 26. Background temperature fluctuations at port 12-4.

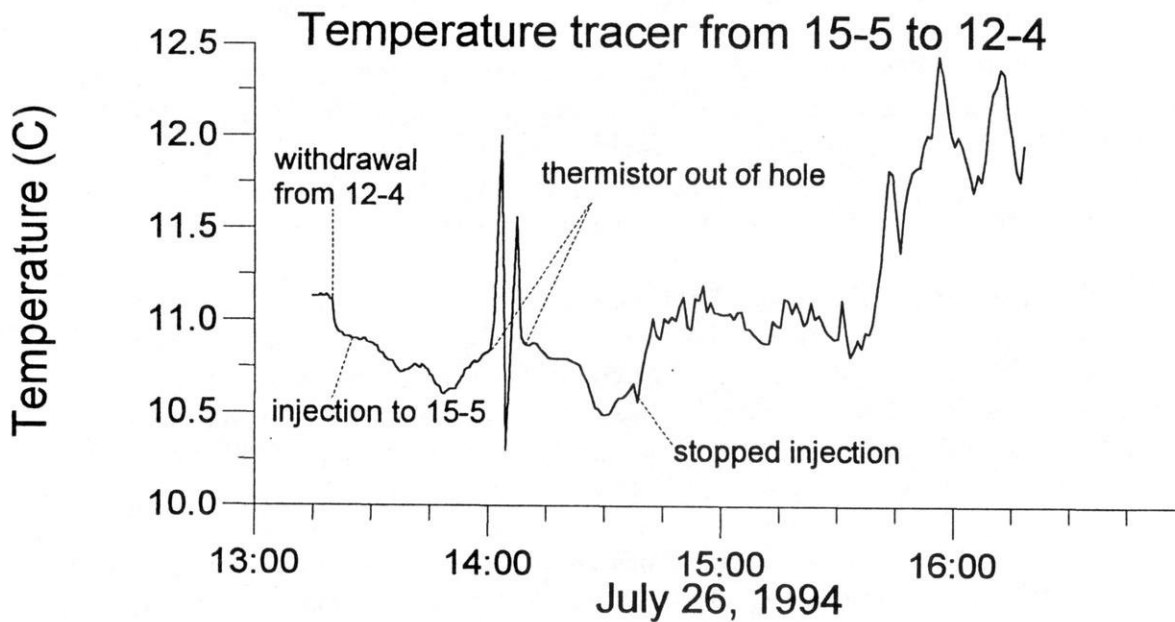


Figure 27 Results of first temperature tracer test. Test was conducted in fracture at 75 ft elevation; injecting to port 15-5, pumping and monitoring port 12-4.

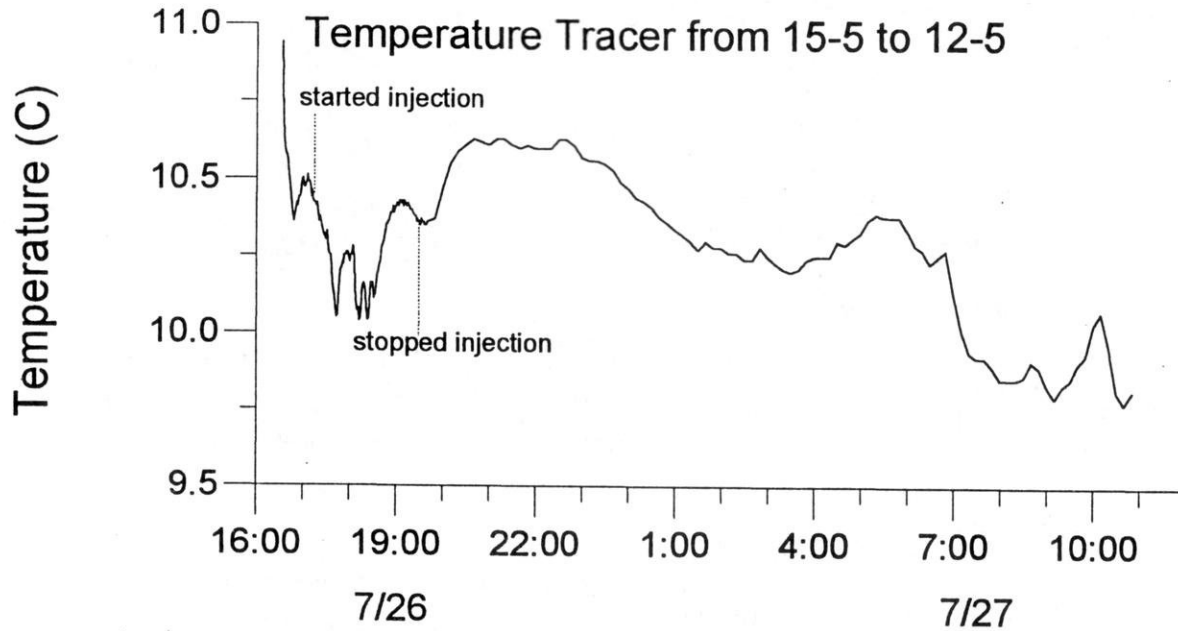


Figure 28. Results from second temperature tracer test. Hot water was injected into the fracture at 75 ft elevation at port 15-5; withdrawal was from same fracture at 12-4; monitoring temperature one port down at 12-5.

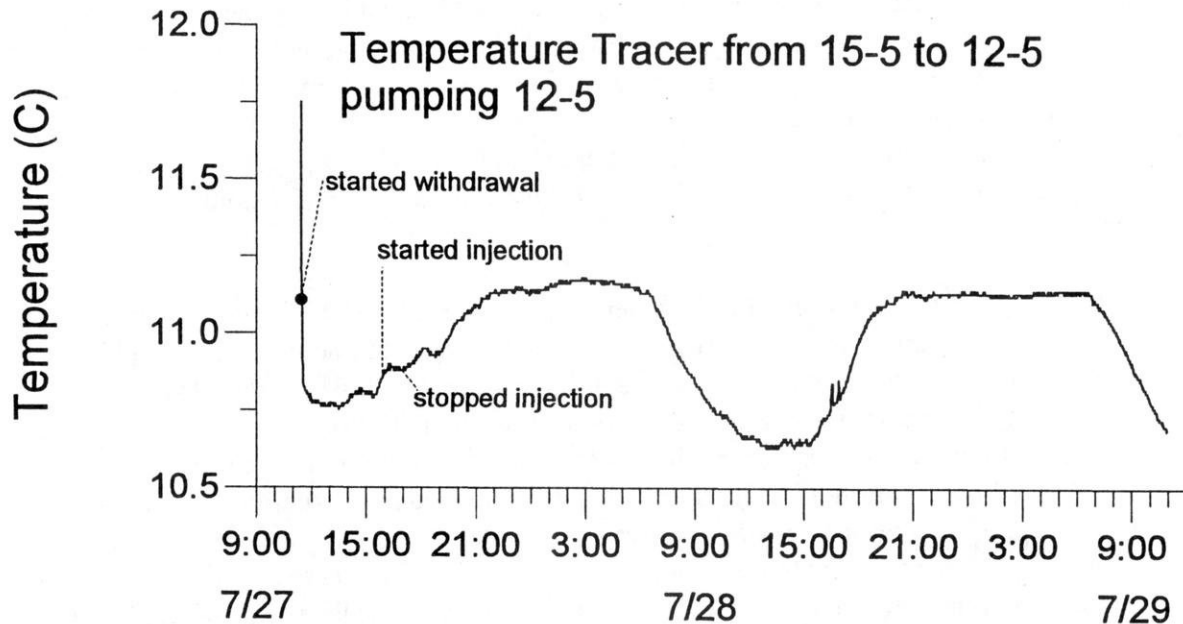


Figure 29. Results from tracer test using both temperature and bromide between holes 15 and 12. Injection and temperature monitoring were conducted in the fracture at 75 ft, water was withdrawn one port below the monitoring port. The temperature pulses are due to diurnal fluctuations and are not related to the tracer injection.

12-4, however, these appear to be diurnal and not related to the tracer injection. Field analysis for Br⁻ confirmed these results. Bromide was not detected in the port 12-4 (the temperature monitoring port), however, it was detected at 15-6, the port below the injection port; at hole 16 in ports 16-4 (elev 75 ft) and 16-5 (elev 71 ft); and in hole 10 at an elevation of 71 ft (port 10-6). The tracer moved downward and to the south and never reached the port where temperature was being monitored. These strong diurnal fluctuations, coupled with the fact that pumping seemed to strongly effect the temperature signal; lead us to discontinue trying to use temperature as a tracer.

Controlled-gradient Iodide Test

A controlled-gradient iodide tracer test was conducted 8/3-8/4/94 on holes 1, 10, 12, and 15. Some constituent in the site water caused interference with the ion-selective electrode and made it impossible to analyze the samples. At the conclusion of the test, hole 13 was pumped at 15 gpm for 4 hours.

Controlled-gradient Chloride Test

This test was designed to monitor tracer movement along a vertical fracture. All the previous tests indicated significant downward movement of tracer pulses and thus we chose to inject into the fracture at 82 ft elevation in order to have a greater vertical distance for monitoring. Several multi-levels had been placed along vertical fractures (see figure 6) and two test configurations were possible; one using holes 10, 12 and 15 and the other using holes 15, 16, 17 and 18. Since we had just run an unsuccessful iodide tracer test from hole 15 to 1 and were concerned about interferences, we chose to run the chloride test between holes 15 and 17. A general southerly direction of flow had been suggested by the open-borehole head data and by the last temperature tracer test, however, head data from the fracture at 82 ft elevation (see figure 21) suggested that flow was to the west. Given our uncertainty in flow direction, we chose to conduct the test at higher injection/withdraw rates so as to induce a steeper gradient. We also used a larger volume (5 liters) of higher concentration tracer (1000 mg/l) so that the tracer signal would not be diluted below detectable levels.

Figure 30 diagrams the set-up and monitoring scheme for this test. Port 15-3 was chosen as the injection port and 17-2 as the withdrawal port. The packer remained in hole 13 to seal off the fracture at 75 ft elevation and minimize any effects of having an open hole nearby. Withdrawal, at a rate of 500 ml/min, started approximately 24 hours prior to the initiation of the test. The next day, five liters of 1000 mg/l Cl⁻ tracer were injected at a rate of 250 ml/min; tracer injection was immediately followed by injection of 5 liters of ambient groundwater. Tracer concentrations were monitored at the ports at or below 82 ft elevation in holes 15, 16, 17, and 18. Sampling frequency was every 15 minutes for the first two hours of the test, and decreased to every 30 minutes from 2 to 6 hours into the test. After 6 hours, samples were collected intermittently at 8, 12, and 20 hours. Selected samples were analyzed with an ion-selective electrode in the field and all samples were subsequently analyzed by student technicians at the UW Soils Department Laboratory. Selected samples were also analyzed by ion chromatography. Results from all analyses can be found in WOFR 98-3 (Muldoon, 1998).

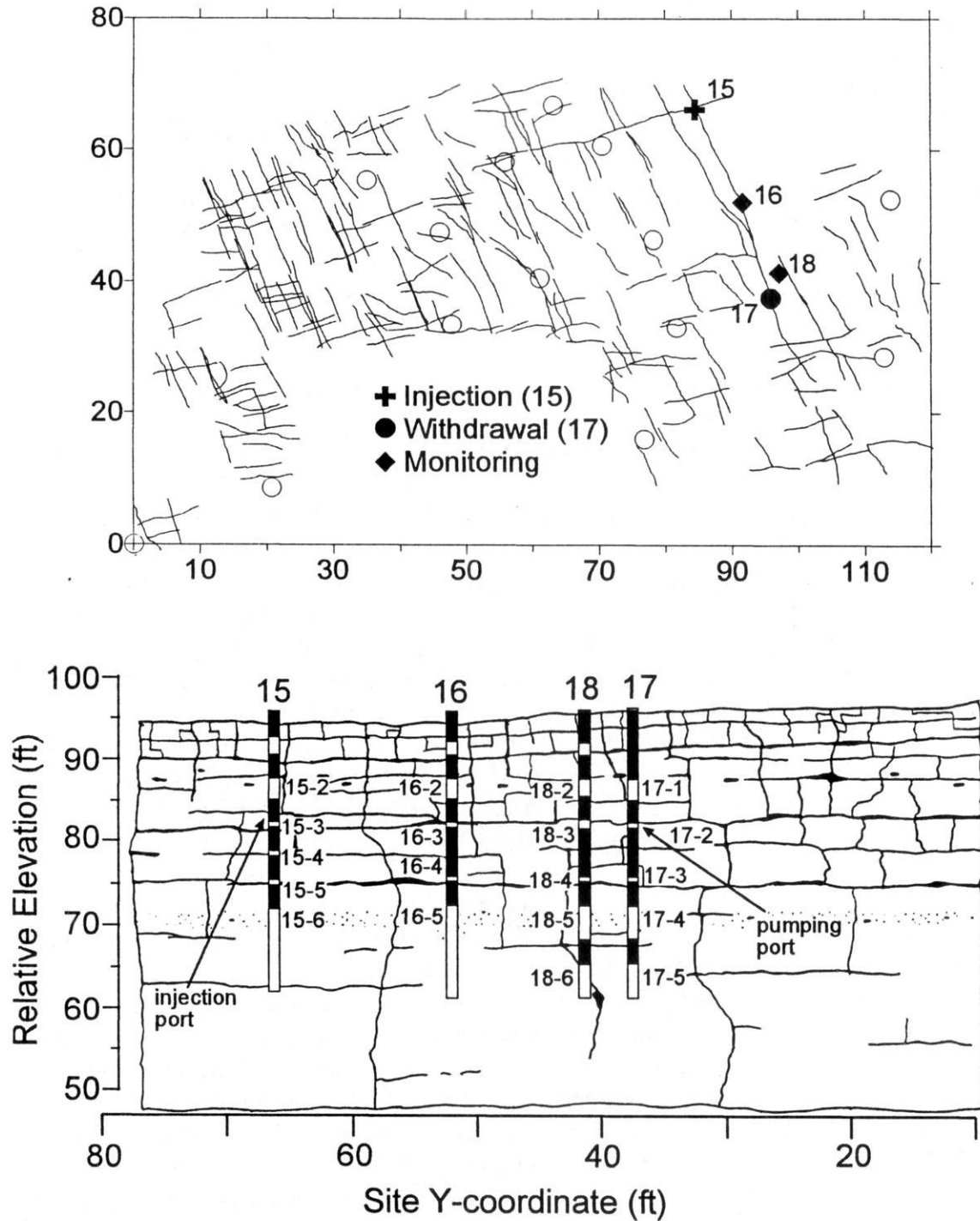


Figure 30. Set up for controlled-gradient chloride tracer test conducted in the fracture at 82 ft elevation. Map shows location of wells. Cross section is projected onto the east axis of the site (y-direction); white intervals indicate multi-level ports. Tracer was injected at port 15-3 and water was withdrawn from port 17-2; monitoring ports are labeled.

Two sets of background samples were collected prior to tracer injection. Background chloride concentrations were relatively high, ranging from approximately 10 to 40 mg/l. One exception was anomalously high values from the ion-selective electrode analyses of samples from port 15-6 (field analysis 61.4 mg/l, lab analysis 69.6 mg/l). As the ion chromatography analysis indicated a lower concentration (17.0 mg/l), the high values appear to be due to interference from the Br⁻ and I⁻ tracers that had been used the previous week and which may have remained near port 15-6. Given the high background concentrations of chloride, it was necessary to correct measured tracer concentrations prior plotting breakthrough curves. C/Co was calculated by subtracting the background concentration from the measured tracer concentration and then dividing by the input concentration. All tracer concentrations noted in the following discussion have been corrected for background concentration.

Tracer results are summarized in table 11 and breakthrough curves are shown in figures 31 and 32. These results indicate unambiguous tracer detections in hole 15. For holes 16, 17, and 18, measured tracer concentrations (above background) range from 2.89 to 11.6 mg/l. It is not clear if these concentrations represent true tracer pulses given 1) the high background chloride concentrations, 2) the inherent natural variability of water-quality in fractured-rock settings, and 3) the accuracy of the analytical methods. Even though absolute values are not equal, the parallel trends from different analytical techniques suggests that trace amounts of tracer reached hole 16 and the upper ports of hole 17. In evaluating the breakthrough curves, the field ion-selective electrode and ion chromatograph results were believed to be somewhat more reliable than the lab ion-selective electrode results because of the order in which samples were analyzed. Samples from each port were kept in time-sequence order for the lab ion-selective analyses. Electrode drift, due to precipitate formation on the electrode tip, could result in gradually increasing measured chloride concentrations between electrode cleanings thus suggesting false positive tracer detections. Samples were randomized in terms of their time-sequence for both the field ion-selective electrode and ion chromatograph analyses.

The breakthrough curves for hole 15 (figure 31) indicate that the bulk of the tracer moved rapidly downward to the fracture at 75 ft elevation where it exited the hole. Much less tracer reached port 15-6. Peak concentrations at ports 15-5 and 15-6 were 542.1 mg/l and 34.9 mg/l, respectively. Breakthrough curves for ports 15-3 and 15-4 indicate that the tracer was not fully flushed from the injection port during injection. The injection phase lasted a total of 39 minutes, consisting of 18.5 minutes of tracer injection and 18.5 minutes of flushing. Tracer was detectable in the injection port (15-3) for the first 208 minutes of the test. We believe this "double pulse", seen most clearly at port 15-4, was caused by the injection procedure. The injection tubing was placed at the base of the port for tracer injection and presumably some tracer moved up into the multi-level tubing during injection as well as outward from the port. During the flushing stage, we did not retract the injection tube and hence we did not fully flush the tracer. The effects of the second pulse seem to dissipate with distance as the curve for port 15-5 shows one pulse which arrived .97 hours (58 minutes) into the test. Calculated velocities for tracer movement in hole 15 are included in table 11.

Table 11. Summary of results from controlled-gradient chloride tracer test

| Port | Detection | Peak Conc.* (mg/l) | Peak Arrival (hr) | Distance from Injection (ft) | Velocity (ft/day) | Notes** |
|------|-----------|--------------------|-------------------|------------------------------|-------------------|-------------------------|
| 15-3 | injection | 148.1 | 1.45 | 0.0 | -- | |
| 15-4 | yes | 819.3 | 0.42 | 3.5 | 200.0 | |
| 15-5 | yes | 542.1 | 0.97 | 7.0 | 173.2 | |
| 15-6 | yes | 34.9 ⁺ | 5.48 | 10.5 | 46.0 | based on IC analyses |
| 16-3 | trace? | 11.6 | 12.48 | 16.0 | 30.8 | based on lab ISE & IC |
| 16-4 | trace? | 9.0 | 5.48 | 17.3 | 75.8 | based on lab ISE & IC |
| 16-5 | trace? | 7.3 | 7.0 | 18.9 | 64.8 | based on lab ISE & IC |
| 17-2 | trace? | 6.5 ⁺ | 7.0 | 31.0 | 106.3 | based on field ISE & IC |
| 17-3 | trace? | 7.1 | 12.58 | 31.6 | 60.3 | based on lab ISE & IC |
| 17-4 | trace? | 5.58 ⁺ | 20.38 | 33.8 | 39.8 | based on field ISE & IC |
| 17-5 | no | 3.89 ⁺ | -- | 35.3 | -- | based on IC analyses |
| 18-3 | no | 3.9 ⁺⁺ | -- | 27.9 | -- | |
| 18-4 | no | 2.89 ⁺ | -- | 28.7 | -- | |
| 18-5 | no | 5.55 ⁺ | -- | 29.7 | -- | |
| 18-6 | no | 3.81 ⁺ | -- | 32.7 | -- | |

* Unless noted, peak concentrations are from laboratory ion-selective electrode analysis

** ISE = ion-selective electrode, IC = ion chromatography

⁺ Reported peak concentrations are from ion chromatography analysis

⁺⁺ Reported peak concentrations are from field ion-selective electrode analysis

The curves for holes 16 and 17 do not show sharp breakthrough curves, but rather low-concentrations of tracer moving through over longer time frames. Calculated velocities range from 30.8 to 106.3 ft/day. The tracer pulse is diluted quite rapidly. Tracer, at a concentration of 542.1 mg/l leaves hole 15 at 75 ft elevation; at port 16-4, which is 16 feet downgradient, measured tracer concentrations were on the order of 11.6 mg/l. This much dilution suggests that the bulk of the tracer pulse was not moving south along the vertical fracture, but rather in another direction.

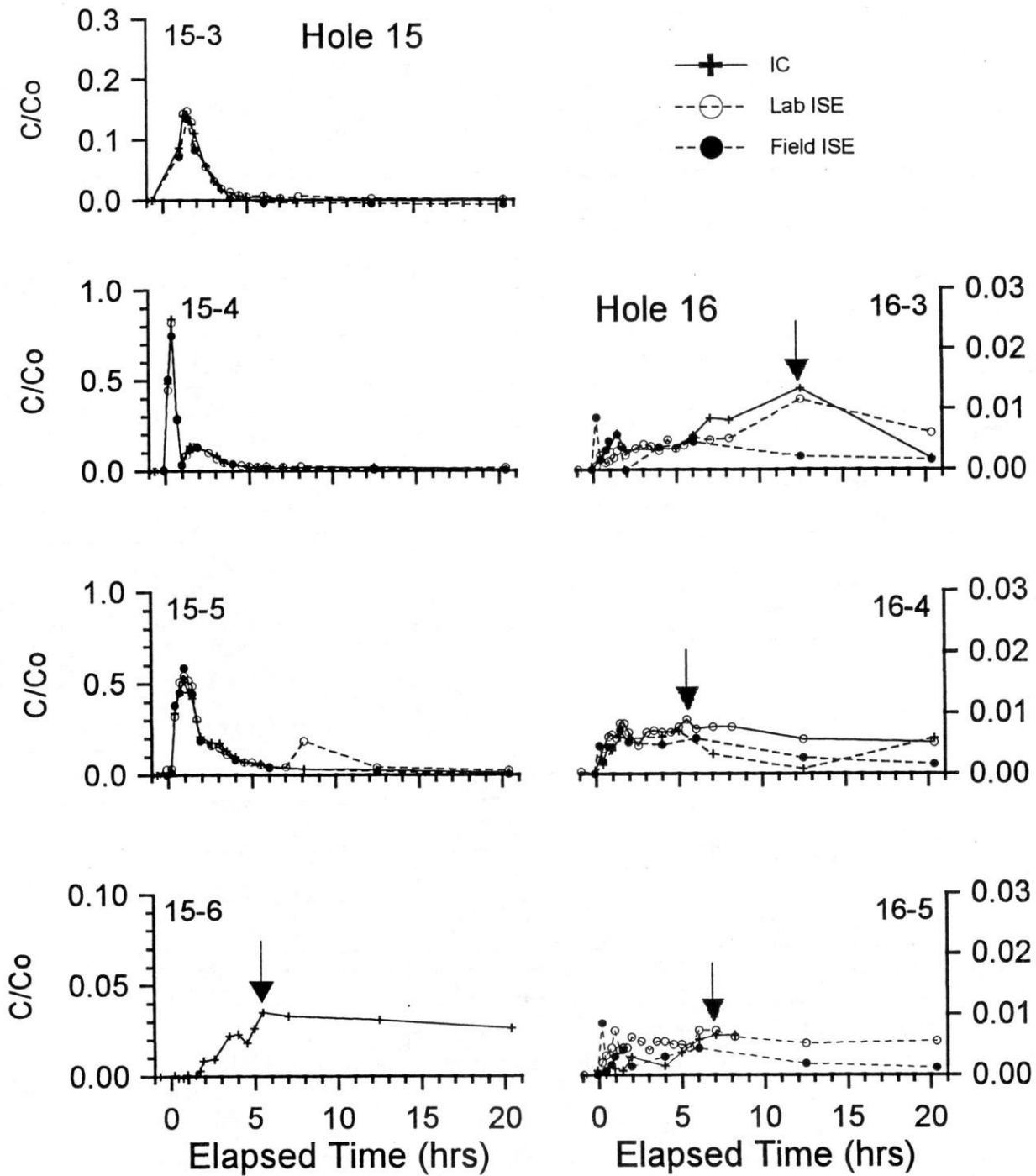


Figure 31. Breakthrough curves for monitoring ports in holes 15 (left) and 16 (right). Note that the Y-axis for ports in hole 15 is variable in scale while the Y-axis for all ports in hole 16 ranges from 0.0 to 0.03). The ion-selective electrode analyses are not shown for port 15-6 as these are believed to be unreliable due to interferences from other anions. Arrows indicate interpreted peak concentrations in hole 16 and port 15-6.

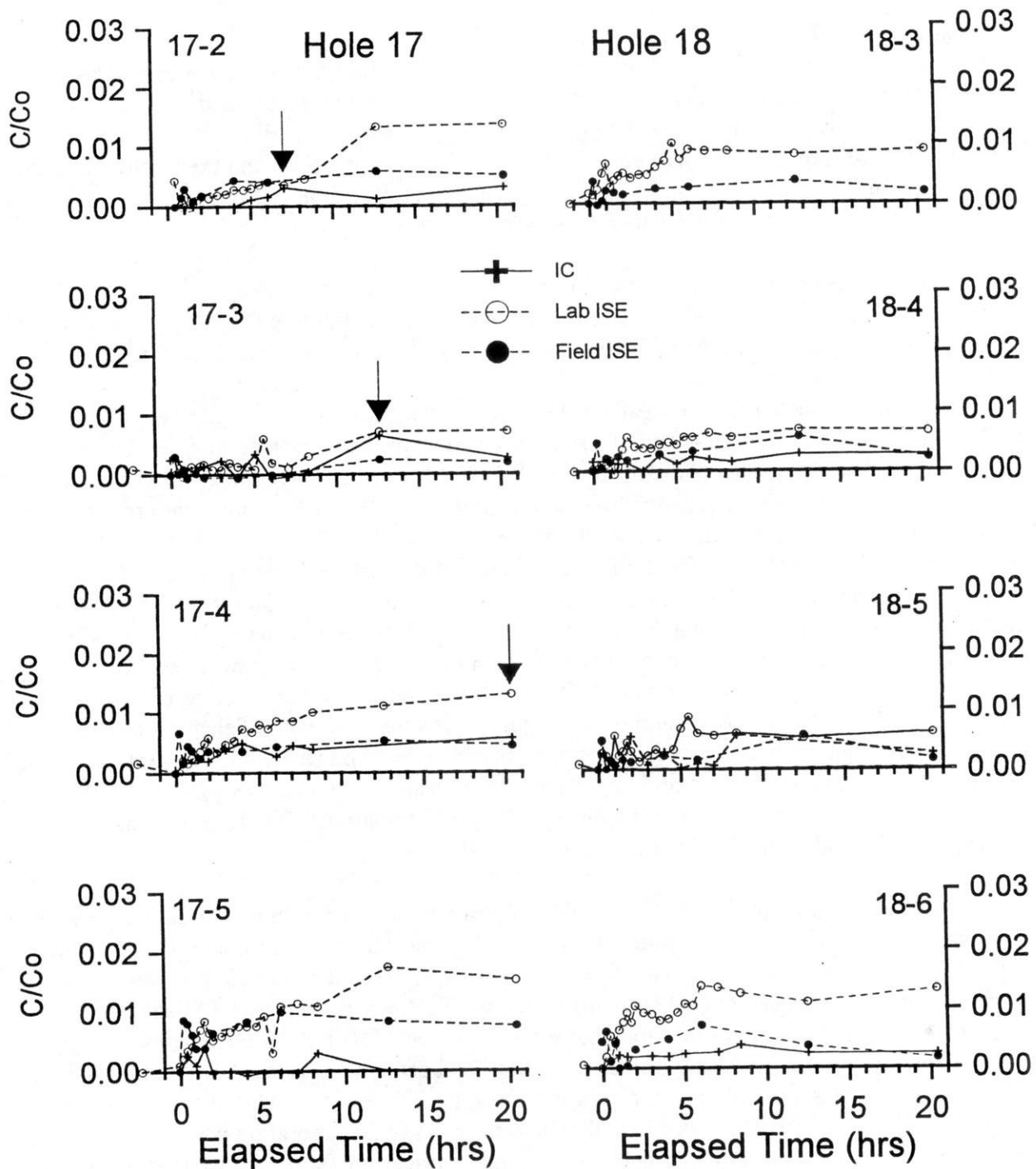


Figure 32. Breakthrough curves for monitoring ports in holes 17 (left) and 18 (right). Arrows indicate interpreted peak concentrations in hole 17.

At the conclusion of this test, hole 13 was pumped for approximately 16 hours in order to recover tracer from previous tests prior to initiation of the natural-gradient test.

Natural-gradient Chloride and Bromide Test

This test was designed to monitor tracer movement under natural gradient conditions. The previous tests indicated 1) significant downward movement of tracer pulses and 2) that the fracture at 75 ft elevation was the most significant flowpath at the site. We chose to use two tracers so as to investigate both the upper flow system (above 75 ft elev) and the fracture at 75 ft elevation. By injecting directly to the fracture at 75 ft elevation, we hoped to avoid the dilution problems we had seen in the controlled-gradient chloride test.

Figure 33 diagrams the set-up and monitoring scheme for this test, conducted from 8/9 to 8/20/94. Five rounds of water-level measurements were collected during the test. Figure 34 illustrates the configuration of hydraulic head just prior to the initiation of the tracer test.

We simultaneously injected five liters of 1000 mg/l Cl⁻ tracer into port 15-1 and five liters of 1000 mg/l Br⁻ tracer into port 15-5 at a rate of 250 ml/min. The packer remained in hole 13 to seal off the fracture at 75 ft elevation and minimize any effects of having an open hole nearby. Tracer injection to both ports was immediately followed by injection of 5 liters of ambient groundwater. Tracer concentrations were monitored at all ports in holes 11, 12, 14, 15 and 16. Sampling frequency was every 15 minutes for the first two hours of the test, and decreased to approximately every 30 minutes from 2 to 7.5 hours into the test. Throughout the first night, samples were collected approximately every three hours. On the second day of the test (8/10/94), samples were collected every two hours from 8:00 am to 6:00 pm and then every six hours through the night. By the third day (8/11/94), sample frequency had decreased to every six hours; for the remainder of the test (8/12-8/20/94), samples were collected daily. Selected samples were analyzed for chloride with an ion-selective electrode in the field and all samples were subsequently analyzed for both bromide and chloride by student technicians at the UW Soils Department Laboratory. Selected samples were also analyzed by ion chromatography. Results from all analyses can be found in WOFR 98-3 (Muldoon, 1998).

Tracer results are summarized in table 12 and breakthrough curves are shown in figures 35 to 39. This test was quite difficult to interpret for the following reasons: 1) the bromide- and chloride-selective electrodes would erroneously detect the other anion (see for example the breakthrough curve for port 15-3 in figure 35), 2) laboratory ion-specific electrode analyses frequently suggested elevated tracer concentrations that were not detected by ion chromatography, 3) some of ion-chromatography results suggest that samples had been concentrated by evaporation, and 4) the ion-chromatography sulfate concentrations inexplicably mimic the chloride concentrations, even in cases of clear chloride breakthrough which suggests that evaporation is not the cause. In evaluating the sometimes conflicting data, we assumed a tracer breakthrough was real if 1) the ion-selective electrode results were generally corroborated by the ion-chromatography results or if 2) the ion-chromatography results indicated unambiguous tracer breakthrough.

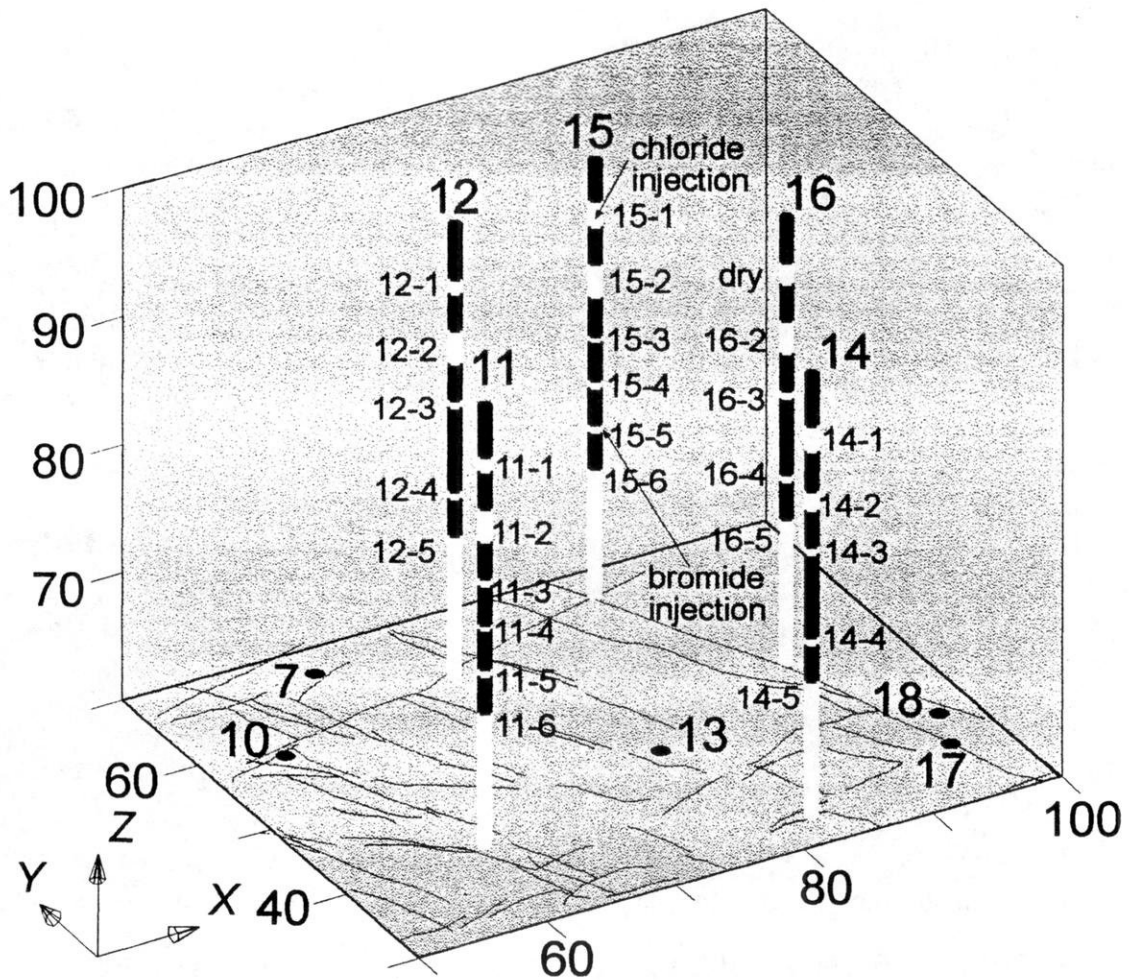


Figure 33. Set-up for natural-gradient tracer test; white zones indicate open intervals for the monitoring ports.

Chloride Results

Table 12 indicates that chloride was detectable in the upper three ports of hole 15, throughout hole 12, in port 16-2, and in port 14-5 (see figure 33 for port locations). Peak tracer concentrations, at all ports other than the injection port, are relatively low, ranging from 14.6 to 73.6 mg/l. The chloride breakthrough curves for hole 15 (figure 35) suggest that the tracer was greatly diluted in the injection fracture (approximately 92 ft elevation) before moving rapidly downward to ports 15-2 and 15-3. The fracture at approximately 82 ft elevation appears to have diluted the downward-moving tracer pulse to below detectable levels as chloride tracer was not detected at ports 15-4, 15-5, or 15-6. Detectable amounts of chloride tracer moved along the vertical fracture that connects holes 12 and 15; the chloride breakthrough curves for hole 12 are

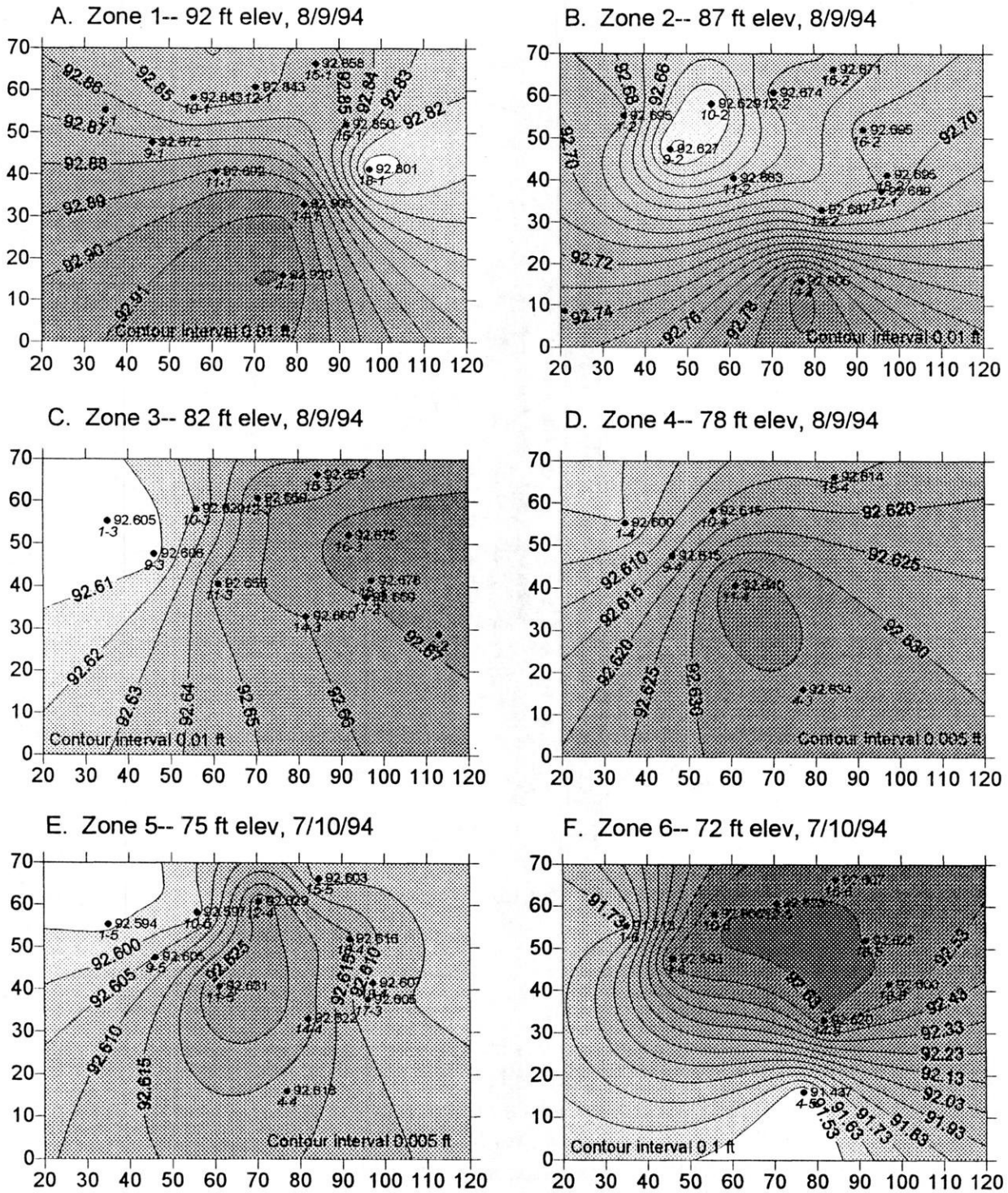


Figure 34. Hydraulic head distribution measured 8/9/94 prior to the initiation of the controlled-gradient tracer test. Shading grades from areas of higher head (dark gray) to areas of lower head (white). Note that the contour interval varies for the different plots.

Table 12. Summary of results from the natural-gradient tracer test

| Port | Peak Cl ⁻ Conc. (mg/l)* | Peak Cl ⁻ Arrival (hr) | Cl ⁻ Velocity (ft/day) | Peak Br ⁻ Conc. (mg/l)* | Peak Br ⁻ Arrival (hr) | Br ⁻ Velocity (ft/day) |
|------|------------------------------------|-----------------------------------|-----------------------------------|------------------------------------|-----------------------------------|-----------------------------------|
| 11-1 | -- | -- | -- | -- | -- | -- |
| 11-2 | -- | -- | -- | -- | -- | -- |
| 11-3 | -- | -- | -- | -- | -- | -- |
| 11-4 | -- | -- | -- | -- | -- | -- |
| 11-5 | -- | -- | -- | -- | -- | -- |
| 11-6 | -- | -- | -- | -- | -- | -- |
| 12-1 | 20.5 (ISE) | 36.27 | 10.0 | -- | -- | -- |
| 12-2 | 25.3 (ISE) | 22.07 | 17.2 | -- | -- | -- |
| 12-3 | 14.6 (ISE) | 36.15 | 11.8 | -- | -- | -- |
| 12-4 | 15.4 (ISE) | 36.15 | 14.8 | -- | -- | -- |
| 12-5 | 29.0 (ISE) | 103.82 | 5.8 | -- | -- | -- |
| 14-1 | -- | -- | -- | -- | -- | -- |
| 14-2 | -- | -- | -- | -- | -- | -- |
| 14-3 | -- | -- | -- | -- | -- | -- |
| 14-4 | -- | -- | -- | -- | -- | -- |
| 14-5 | 56.29 (IC) | 26.23 | 35.5 | -- | -- | -- |
| 15-1 | 428.1 (ISE) | 3.63 | -- | -- | -- | -- |
| 15-2 | 73.6 (ISE) | 6.67 | 18.0 | -- | -- | -- |
| 15-3 | 15.7 (ISE) | 5.72 | 39.9 | 10.8 (ISE) | 0.6 | 280.0 |
| 15-4 | -- | -- | -- | 120.5 (ISE) | 0.58 | 144.8 |
| 15-5 | -- | -- | -- | 138.7 (ISE) | 0.87 | -- |
| 15-6 | -- | -- | -- | 42.07 (IC) | 1.8 | 46.7 |
| 16-2 | 16.51 (IC) | 6.68 | 60.2 | -- | -- | -- |
| 16-3 | -- | -- | -- | -- | -- | -- |
| 16-4 | -- | -- | -- | -- | -- | -- |
| 16-5 | -- | -- | -- | 20.83 (IC) | 16.5 | 23.7 |

* Analytical method used to determine peak concentration is noted
 ISE = ion-selective electrode (lab analyses), IC=ion chromatography

presented in figures 36 and 37. The lateral tracer movement to hole 12 is slower than the downward movement seen in hole 15; peak arrival times in hole 12 range from 22.07 to 103.82 hours. Hole 16, similarly to hole 12, is located on a vertical fracture that is connected to hole 15. Peak tracer concentration at port 16-2 was detected just 6.68 hours into the test (figure 38) and tracer was not detected in any other port. Tracer also moved to port 14-5 and this breakthrough curve is shown in figure 38.

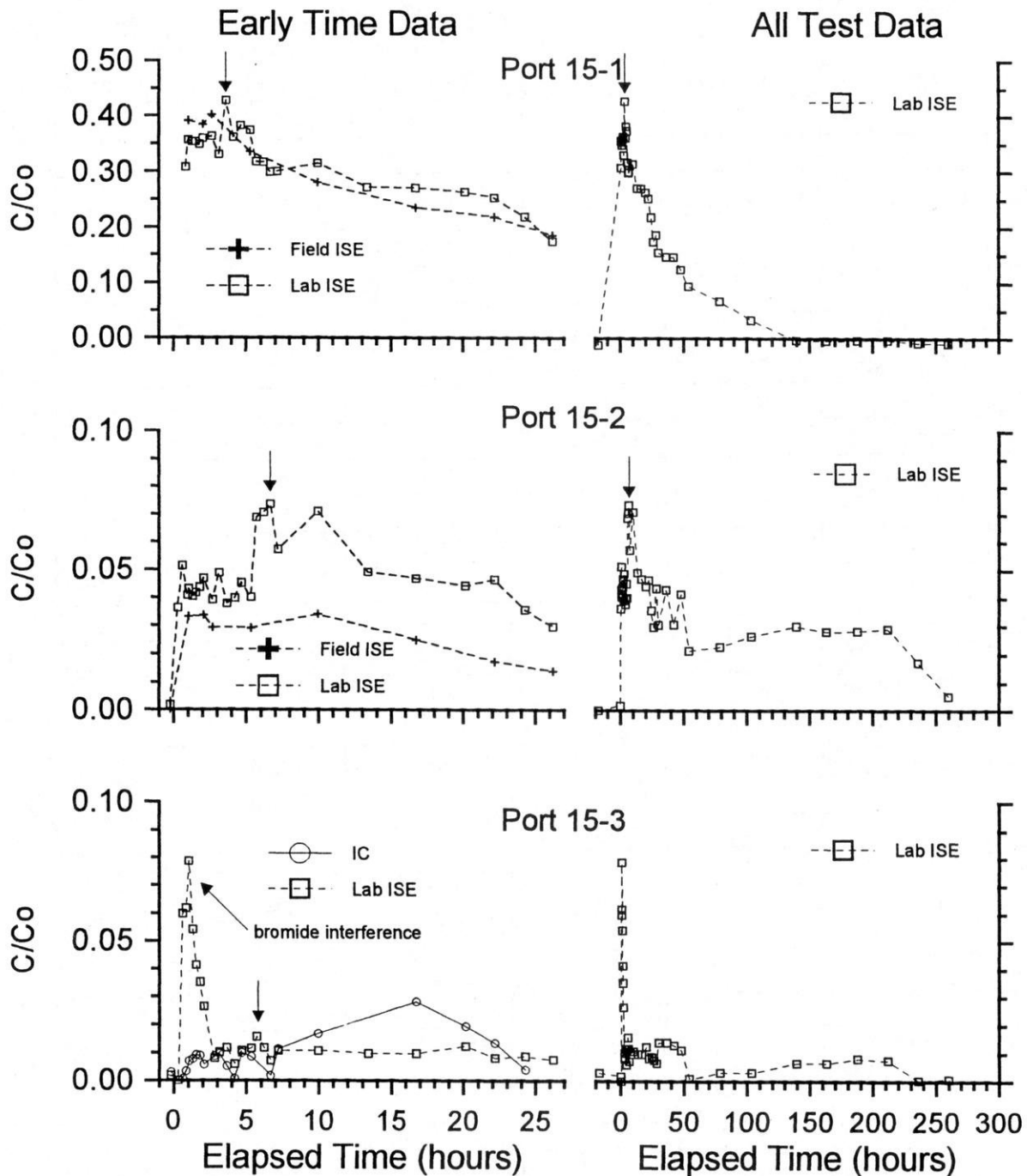


Figure 35. Chloride breakthrough curves for monitoring ports in holes 15. Early-time data are shown on the left and data for the entire test are shown on the right. Note that the Y-axis is variable in scale. Arrows indicate interpreted peak concentrations.

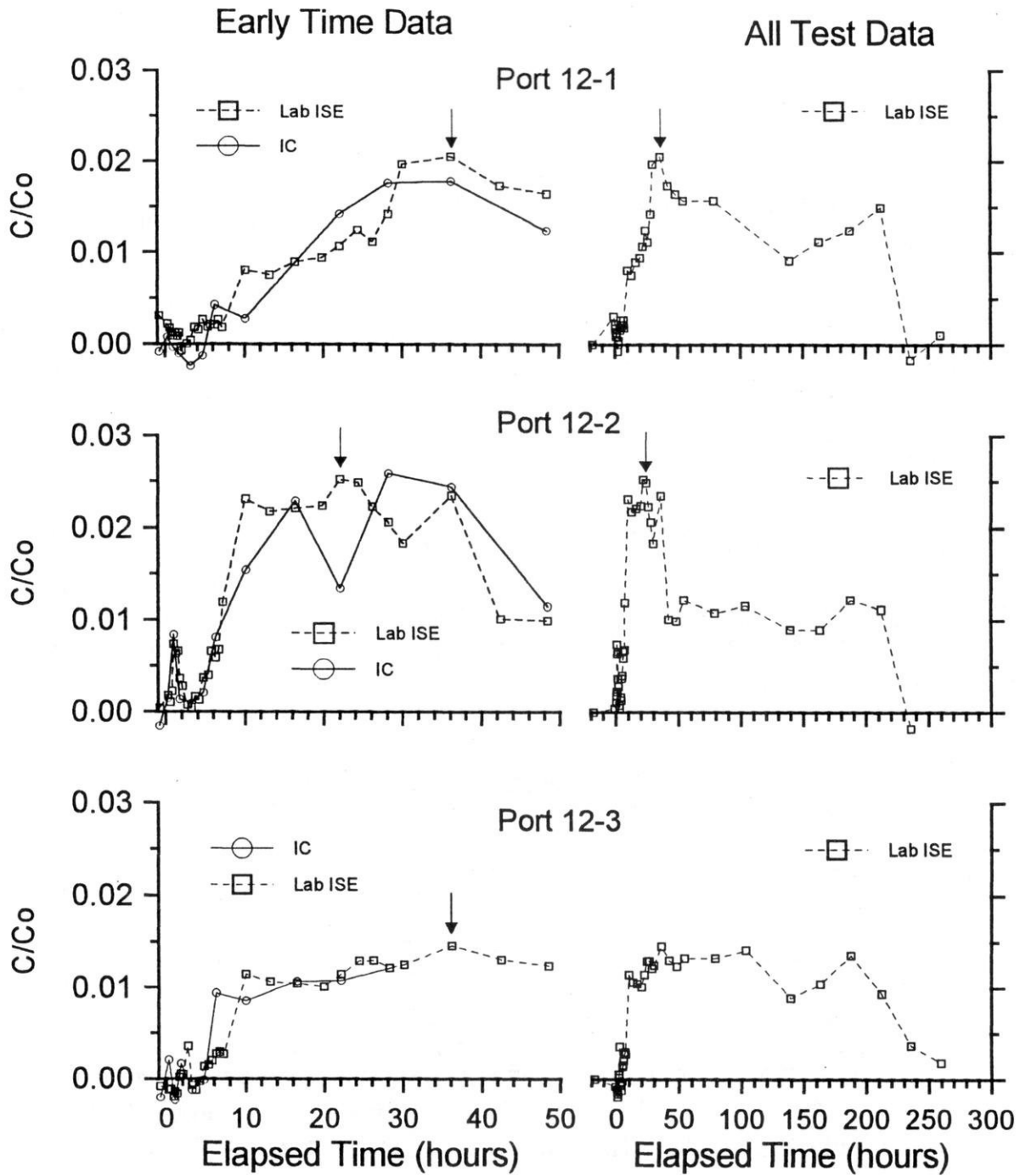


Figure 36. Chloride breakthrough curves for monitoring ports 12-1, 12-2, and 12-3. Early-time data are shown on the left and data for the entire test are shown on the right. Arrows indicate interpreted peak concentrations.

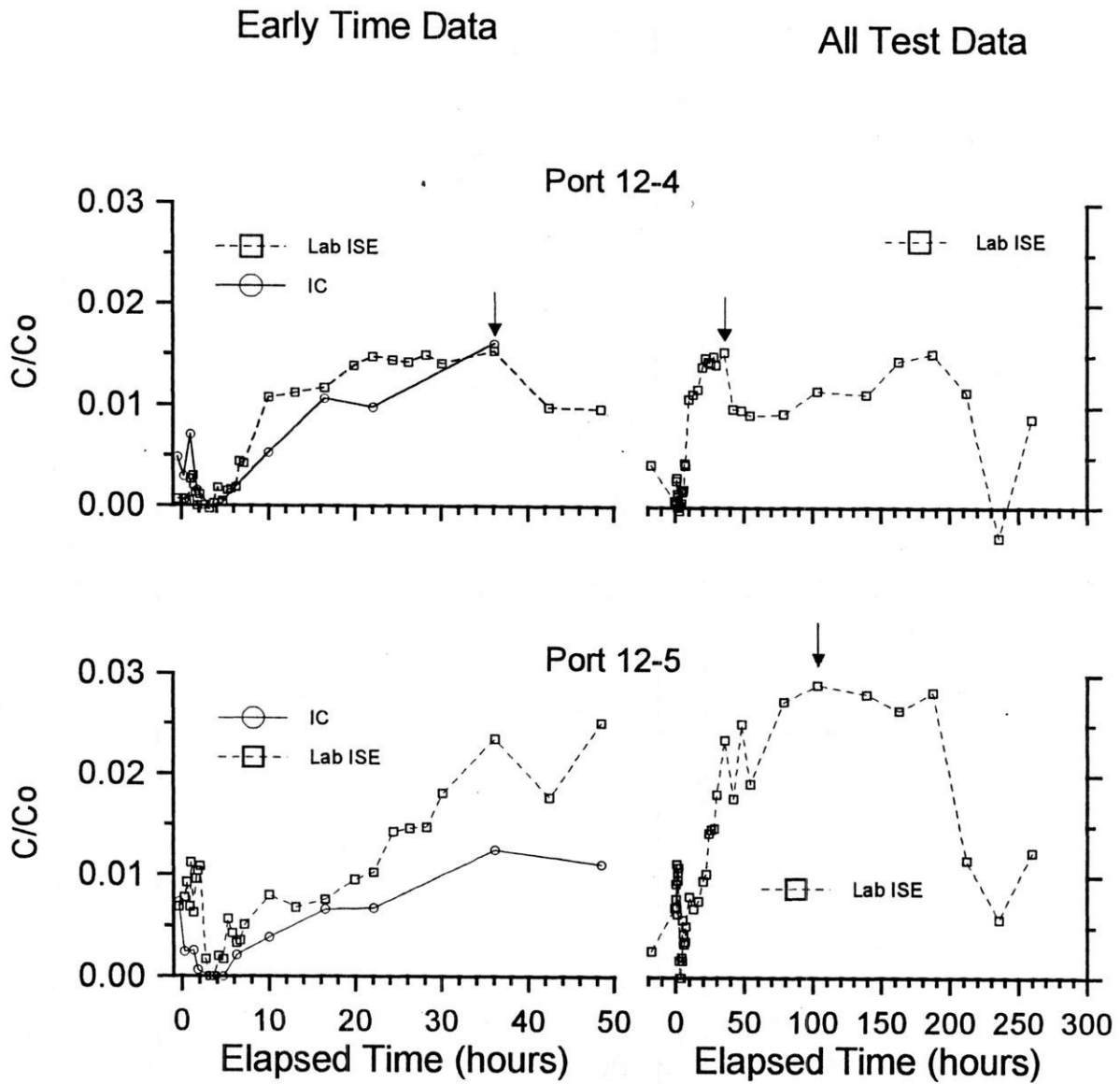


Figure 37. Chloride breakthrough curves for monitoring ports 12-4 and 12-5. Early-time data are shown on the left and data for the entire test are shown on the right. Arrows indicate interpreted peak concentrations.

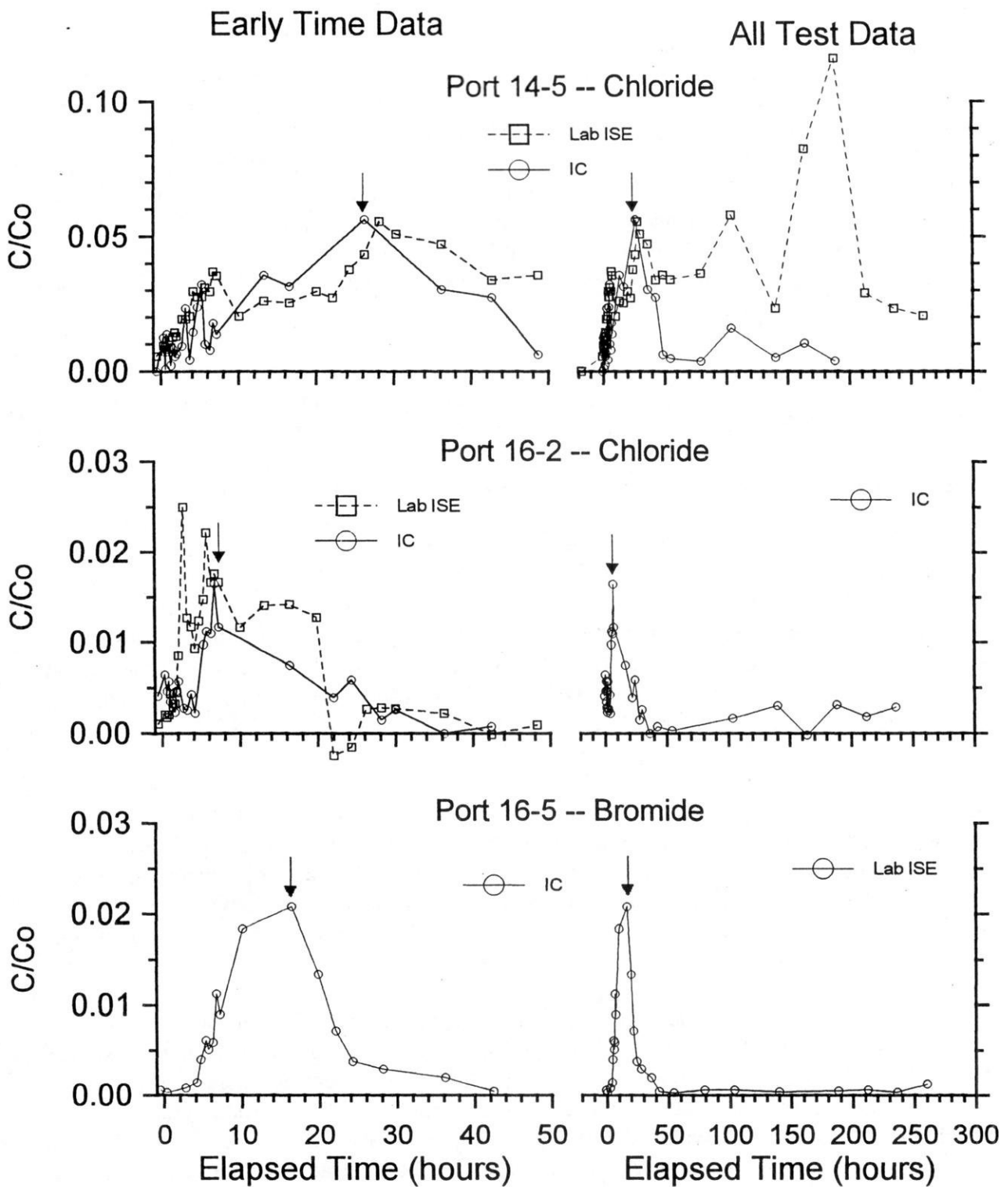


Figure 38. Both chloride and bromide breakthrough curves for monitoring ports in holes 14 and 16. Early-time data are shown on the left and data for the entire test are shown on the right. Arrows indicate interpreted peak concentrations.

The chloride tracer movement is not easily predicted by the measured head values (figure 34). The downward movement of tracer in hole 15 was expected as was the lateral movement to port 12-1 in zone 1 (figure 34a). In the other monitoring zones, head at hole 12 is typically higher than at hole 15. Head at port 16-2 (figure 34b) is also higher than 15-3, however, in zone 1 the reverse is true and it is likely that tracer moved towards hole 16 in zone 1 and then downward to port 16-2. We cannot confirm this idea with breakthrough data from port 16-1 as this port was dry for much of the test. It is also difficult to explain tracer movement to port 14-5 since in most monitoring zones, head in hole 14 is higher than at hole 15. If some tracer moved generally downward and southward from port 15-1 it would end up in the middle of the "head high" in zone 6 and then be able to move to port 14-5.

Bromide Results

Bromide was detected at ports 15-3, 15-4, 15-5, 15-6, and 16-5 (see figure 33 for port locations). The bromide breakthrough curves for hole 15 (figure 39) indicate that tracer moved both upward and downward from the injection port; apparently the injection rate of 250 ml/min was high enough to create a head mound and temporarily reverse the general downward gradient at hole 15. The tracer pulse dissipated within two hours in hole 15 and peak concentrations were relatively low, suggesting much dilution immediately upon injection. The bromide breakthrough curve for port 16-5 (figure 38) indicates slower movement, perhaps through matrix porosity.

The measured head data suggest that the bulk of the tracer injected into port 15-5 (figure 34e) may have moved to the north. It is not clear why tracer was detected at port 16-5 as the head at hole 16 is higher than at 15 in both zone 5 (figure 34e) and zone 6 (figure 34f). The "head mound" caused by injection may have been enough to move tracer to port 16-5.

Discussion

The tests conducted at Bissen Quarry during the summer of 1994 illustrate the complexities of designing, conducting, analyzing, and interpreting tracer tests in fractured carbonates. The goal of these tests were to 1) explore the hydraulic connectivity of the fracture network, 2) determine representative flow velocities at the site, and 3) establish a methodology for larger-scale tests to be conducted in the summer of 1995.

The fracture network at the site appears to be well-integrated both horizontally and vertically. The dominant horizontal flow paths are developed along bedding plane fractures at approximately 92, 82, and 75 ft elevation; in these large, open horizontal fractures, lateral tracer movement is quite rapid and the tracer pulses are greatly diluted. The controlled-gradient bromide test, in which tracer bypassed hole 11, suggests that flow within these horizontal fractures is within preferential pathways, or channels. In all tests, tracer also moved rapidly in the vertical direction.

The measured horizontal velocity for all tests are on the order of 10's to 100's of ft/day. The horizontal velocity measured in the controlled-gradient bromide test was 343.4 ft/day. Horizontal

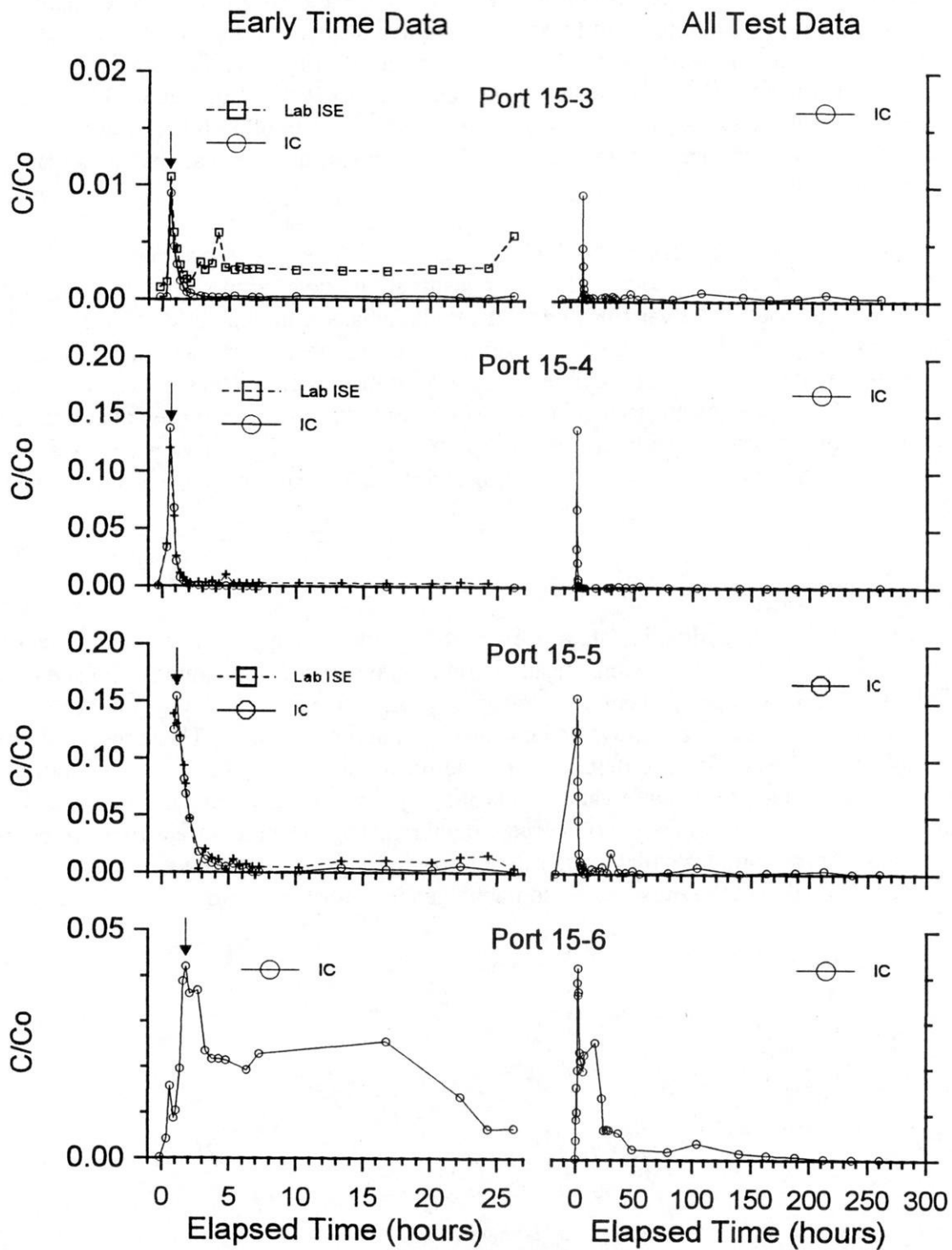


Figure 39. Bromide breakthrough curves for monitoring ports in hole 15; port 15-5 was the injection port. Early-time data are shown on the left and data for the entire test are shown on the right. Arrows indicate interpreted peak concentrations.

velocities are less certain for the controlled-gradient chloride test as tracer was only detected in trace quantities in surrounding holes but these range from 30.8 to 106.3 ft/day. As expected, horizontal velocities are somewhat slower for the natural-gradient test, ranging from 5.8 to 60.2 ft/day. Measured vertical velocities are also in the range of 10's to 100's of ft/day. Tracer injected into hole 9 (not on a vertical fracture) had a vertical velocity of 33.6 ft/day while tracers injected into hole 15 (at the intersection of two vertical fractures) had vertical velocities that ranged from 18 to 280 ft/day.

The limitations of using anionic tracers at this site became apparent over the summer. Iodide could not be used as a tracer due to an unknown constituent in the groundwater interfering with the ion-selective electrode. The variable and relatively high background chloride concentrations limited the usefulness of chloride as a tracer. Bromide was the most effective tracer. Another major limitation of anionic tracers is that injection concentrations need to be kept below approximately 1000 mg/l so as not to induce density-driven flow, however, these concentrations are easily diluted in the large, open fractures. In future tests, we will inject larger volumes of tracer with the goal of being able to trace over longer distances before the pulse is diluted below detectable levels.

Implications for Monitoring

Tracer results indicate that hydraulic data alone are poor predictors of transport at small scales. Even with the detailed, three-dimensional head distribution measured in the multi-level samplers, it was difficult to predict tracer movement. Transport at site-specific scales appears to be dominated by discrete fracture pathways and channels within the fractures. These results suggest that contaminants will be difficult to detect in these settings, especially with standard monitoring wells constructed with long open intervals. Monitoring systems designed to monitor the high-permeability pathways are more likely to intercept contaminants. The measured tracer velocities of 10's to 100's of ft/day suggests that standard monitoring frequencies, such as quarterly sampling, would not detect the presence of contaminants in a timely fashion.

CHAPTER 4

APPLICATION OF A FRACTURE FLOW MODEL

Purpose

Groundwater investigations in fractured-rock settings usually require predictions of flow rates, velocities, and contaminant concentrations. Commonly-used groundwater flow models (e.g. MODFLOW, McDonald and Harbaugh, 1988) solve flow equations based on the physics of flow through porous media, and the applicability of such models to fractured-rock settings is often unclear. Fracture-network models, such as FRACMAN/MAFIC (Dershowitz and others, 1993) and SDF (Rouleau, 1988) solve equations based on the physics of fracture-flow, and may be more appropriate for fractured-rock applications. Unfortunately, detailed field studies necessary to test such models are rare. The site characterization and tracer experiments at the Bissen Quarry, discussed in this report, offer an ideal opportunity to test such models against a complete set of field data.

Model Selection

As an application of fracture-network modeling to the Bissen Quarry site we applied the Stochastic Discrete Flow (SDF) code of Rouleau (1988). The SDF code generates statistically-similar sets of fractures in two-dimensional space and then moves groundwater through the resulting fracture network. The model requires statistical measures of fracture properties, including fracture density, length, orientation, and aperture. The code simulates fractures as openings between smooth parallel plates, with fracture transmissivity proportional to the cube of fracture aperture. Major assumptions incorporated into the model include (1) steady state, laminar flow, (2) two-dimensional flow of an incompressible viscous fluid, and (3) an impermeable rock matrix (no matrix storage). Bradbury and Muldoon (1993) previously applied this model to fractured dolomite in central Door County, and modified it to incorporate pumping and injection wells and particle tracking. They provide details of the code's theory and documentation.

Model Objectives

We applied the SDF code to the Bissen site in an attempt to simulate the controlled-gradient bromide experiment of July 12-14, 1994, described earlier in this report. In this experiment, a bromide tracer was injected into port 9-5 while port 14-4 was pumped. The tracer experiment was intended to follow a single flow line in the aquifer, and tracer breakthrough occurred at three monitoring points. This well-controlled test is ideal for SDF modeling because it is essentially two-dimensional, has known boundary heads, and produced measurable results. The fracture scanline and borehole data collected at the quarry are ideal inputs to the SDF code.

The goal of the SDF simulation was to reproduce the tracer test using a fairly simple set of model parameters in order to gain insight on the transport properties of the fractured dolomite. Specific

objectives were to reproduce the hydraulic heads, flow rates, and tracer concentrations observed in the field.

Model Configuration

Location of Section

The SDF model is configured as a two-dimensional section between wells 1 and 14 (fig 40). This section is 20 m long, 10 m high, and 1 m thick. Hydraulic head measurements made during the tracer tests show that a significant downward gradient and a slight horizontal gradient to the northeast (toward well 1) existed during the test. Figure 41 shows the distribution of hydraulic head in the section; for modeling purposes, heads were converted to metric units (meters).

Boundary Conditions

The SDF model requires simple rectangular boundary conditions consisting of either constant-heads or constant fluxes along various boundary segments. In addition, the code requires two bounding domains: an inner domain in which the model calculates head and flux, and outer domain in which non-active fractures occur. The outer domain is necessary to prevent the unrealistic truncation of fractures extending across the boundaries of the inner domain.

The boundaries of the model were set at constant heads based on the field measurements during the test. Heads are assigned at boundary segment ends; the model interpolates heads between boundary points. Two additional heads were assigned to the locations of the injection and withdrawal ports for the test. Figure 42 shows the model boundary conditions.

Input Parameters

The cross-sectional model includes two statistically different fracture sets: horizontal fractures and vertical fractures. Fracture densities (area of fractures per volume of rock) and lengths were estimated from scanline measurements in the Bissen Quarry. Fracture apertures were estimated from measurements on the quarry floor and from modeling simulations in central Door County (Bradbury and Muldoon, 1993). We assume log-normal distributions for fracture lengths and apertures. Table 13 summarizes the model input data for the two fracture sets.

Table 13. Fracture input data for the SDF model

| Fracture set | density, m ⁻¹ | length, mean, m | length, std dev | aperture, mean, m | aperture, std dev |
|----------------|--------------------------|-----------------|-----------------|-------------------|-------------------|
| 1 (horizontal) | 1.27 | 3.86 | 1.48 | 0.0003 | 0.5 |
| 2 (vertical) | 0.47 | 0.76 | 1.22 | 0.0001 | 0 |

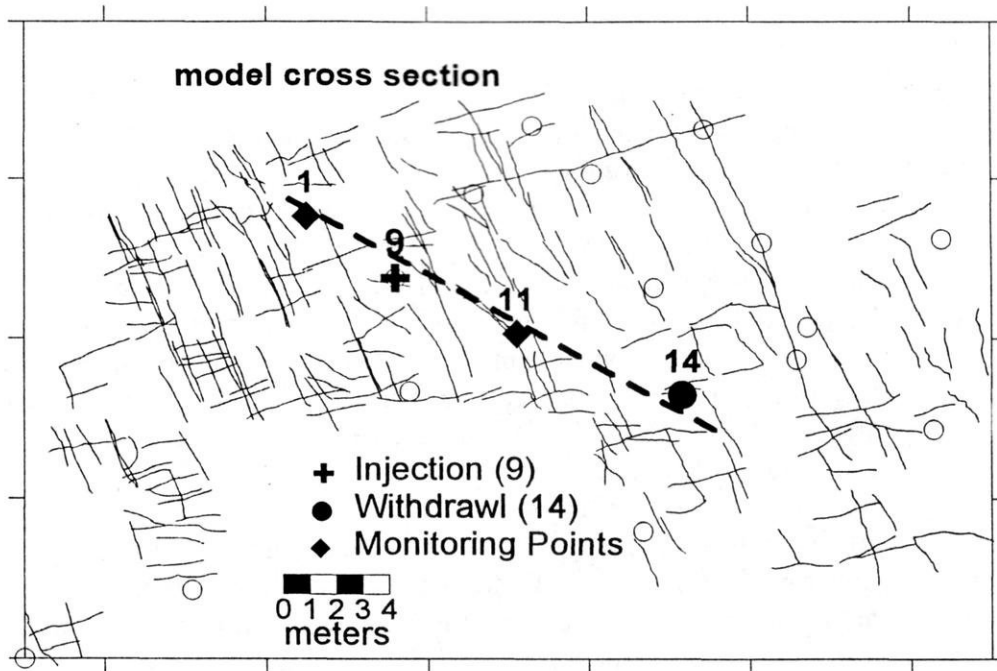


Figure 40. Location of model cross section for simulating the controlled-gradient tracer experiment of July 12-13, 1994.

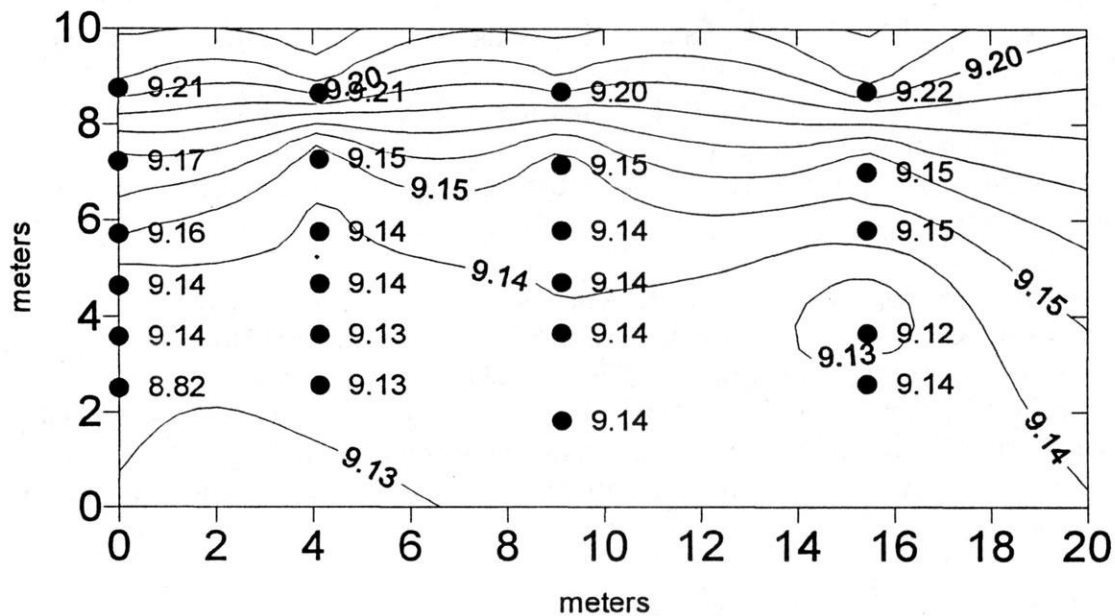


Figure 41. Field-measured hydraulic heads along the model cross section.

Modeling Procedure

The modeling procedure consisted of several steps. First, we generated several realizations of the fracture network, and examined the resulting synthetic networks to confirm that they realistically simulated field conditions. Second, we solved for flow through the fracture network, and again examined the results to confirm that they were realistic. Third, we simulated the tracer experiment by forward particle tracking. The SDF code, as modified by Bradbury and Muldoon (1993) uses the flow velocities generated by the flow solver to move particles advectively along connected fractures. At fracture junctions, the model assumes complete mixing, and the probability of a given particle following a particular fracture is proportional to the flux distribution in the divergent pathways. Particles were introduced into the flow field at the location of port 9-5. Each simulation included 100 particles.

The final tracer simulation consisted of a series of Monte Carlo runs, each run using identical but different random number seeds to initiate the fracture and particle generation. Each resulting realization of the fracture network was statistically identical even though the individual fractures were not. The entire Monte Carlo simulation contained 20 realizations, for a total of 2000 particle paths. Following the simulation we grouped all 2000 particle paths to determine the probability of a particle occupying any particular location in the fracture network. The resulting probability distribution is analogous to the distribution of tracer concentration in the aquifer.

Model Results

Synthetic Fracture Network

Figure 43 shows one model realization of a synthetic fracture network along the model cross section. The realization includes 82 horizontal fractures, ranging in length from 0.1 to 137 m, with an average length of 11.3 m. The realization includes 148 vertical fractures, ranging in length from 0.01 to 8.6 m, with average length 1.3 m. The simulated hydraulic head distribution (fig 43) is similar to the measured hydraulic head distribution (fig 41). The effective porosity of this network is 0.04 percent.

Verification of the SDF model is difficult because the model generated heads only at fracture intersections, while field heads are rarely measured at fracture intersections. However, the model-calculated flux at the pumping (withdrawal) well is 53.9 ml/min, in good agreement with the measured value of 67 ml/min. The simulated flux at the injection well is only 2.8 ml/min, while actual injection was 105 ml/min. However, injection was not continued throughout the 900 min test, and the simulated injection rate is probably appropriate for the steady-state average flux at the injection port.

Groundwater Velocities and Particle Pathways

The model simulated groundwater velocities in individual fractures ranging from zero to 862 m/day, with an average velocity of 44 m/day. For comparison, the field tracer data suggest that average velocities in excess of 90 m/day occurred during the test.

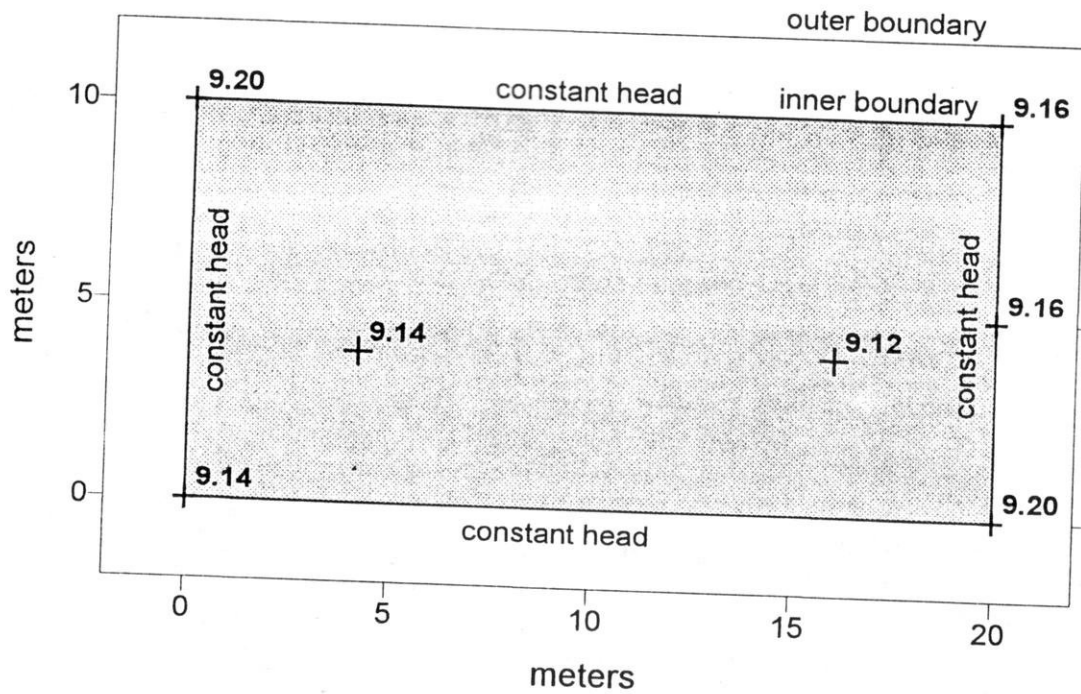


Figure 42. Boundary conditions for the SDF model.

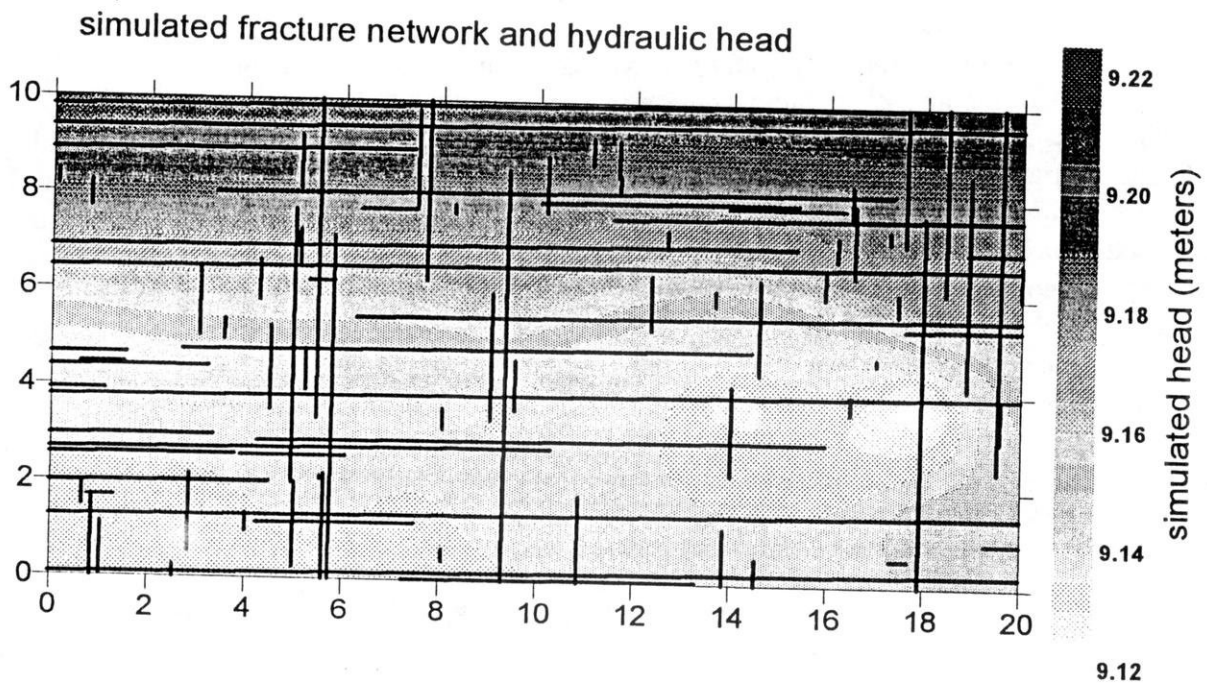


Figure 43. One realization of the simulated fracture network, showing the simulated distribution of hydraulic head.

Particle pathways differed for each realization, but only a limited number of pathways existed for each realization. Figure 44 shows particle traces for one realization. In this realization, 100 particles started at the injection well. Of these particles, 55 reached the withdrawal well and 45 reached the eastern boundary. The average travel time from injection to withdrawal was 28.8 hours. It is clear from figure 43 that a single horizontal fracture intersecting the pumping and injection wells is the dominant control on particle movement. Within this fracture, flow diverges, with some particles moving to the west and some moving east. Some particles also move downward to intersect other horizontal fractures before moving laterally.

Simulated tracer concentrations

The results of the 20 Monte Carlo simulations suggest that the tracer should spread laterally in both directions and also move downward from the injection well. Figure 45 shows relative simulated concentrations based on the distribution of particle positions from the 20 runs. As expected, the highest concentrations occur at the injection well. Significantly lower concentrations reach the pumping well. Much of the simulated tracer spreads to the east and downward, in response to the hydraulic gradient.

Figure 46 shows simulated breakthrough, or arrival, of tracer at the pumping well. The simulated concentrations are highest in the first 48 hours of the test, but arrivals continued for over 350 hours into the test.

Discussion

The SDF simulation fits the data from the July, 1994 bromide test remarkably well, and helps explain some of the field observations during that test. Although designed as a controlled-gradient test, the pumping stress was clearly not sufficient to overcome completely the existing regional hydraulic gradient to the northeast. Due to this regional gradient, some tracer moved to the east, and was never detected, leaving less tracer to move to the pumping well. As a result, concentrations in the withdrawal well were less than expected. Based on the shape of the tracer probability plot, it is easy to understand why tracer was not detected in intermediate monitoring points; particle probabilities there are low, and are probably overestimated by the SDF model because the model ignores three-dimensional effects. The model simulates the long breakthrough tails observed in the field test, and simulated and measured tracer velocities are quite similar.

Results of simulation of the July tracer test suggest that the SDF code is a useful tool for predicting contaminant movement in fractured-carbonate aquifers.

one realization of particle pathways

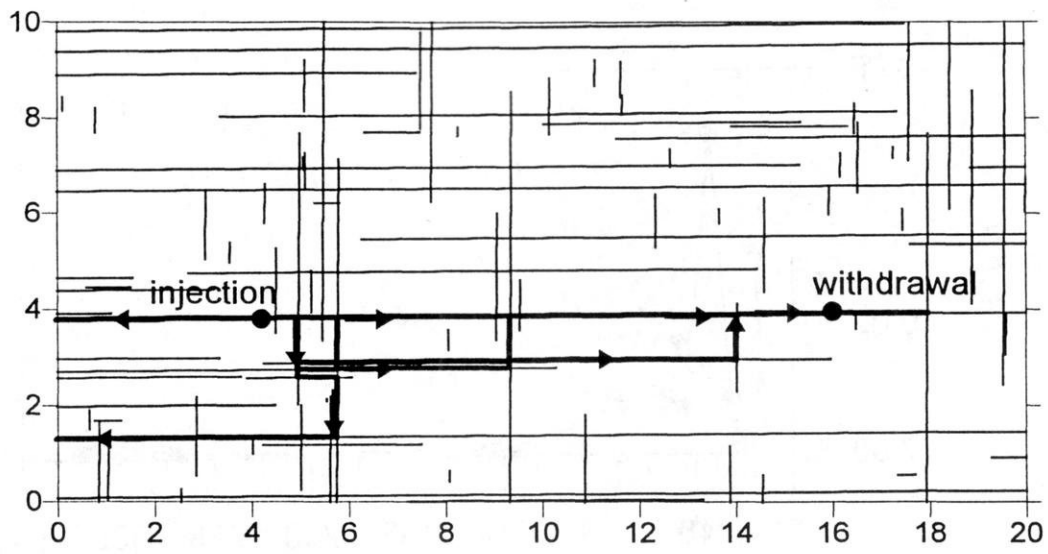


Figure 44. One realization of particle pathways generated by the SDF model.

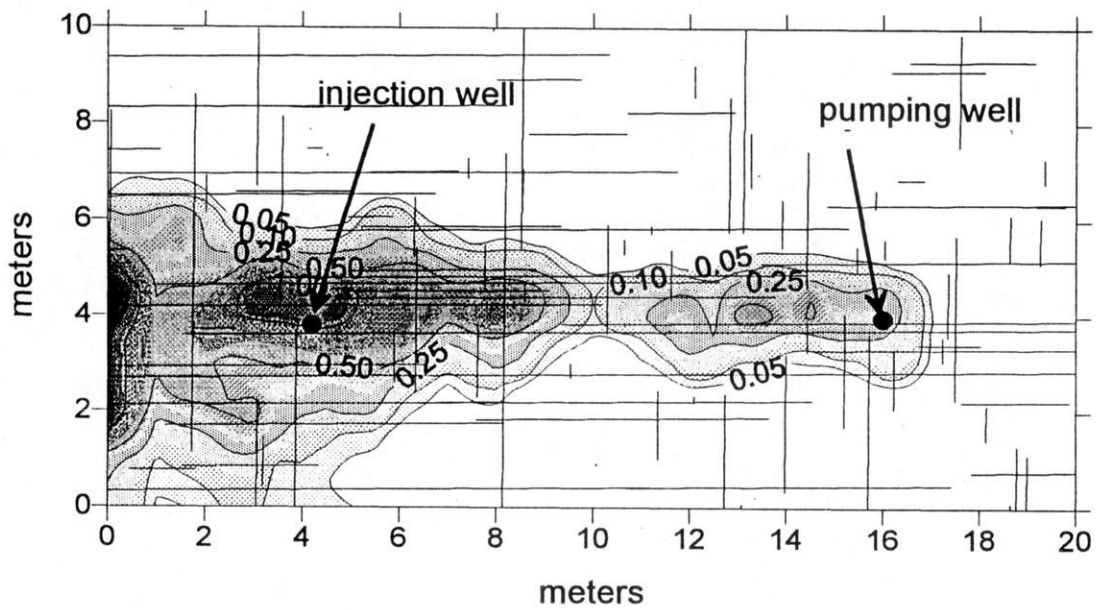


Figure 45. Concentration probabilities based on stochastic particle paths.

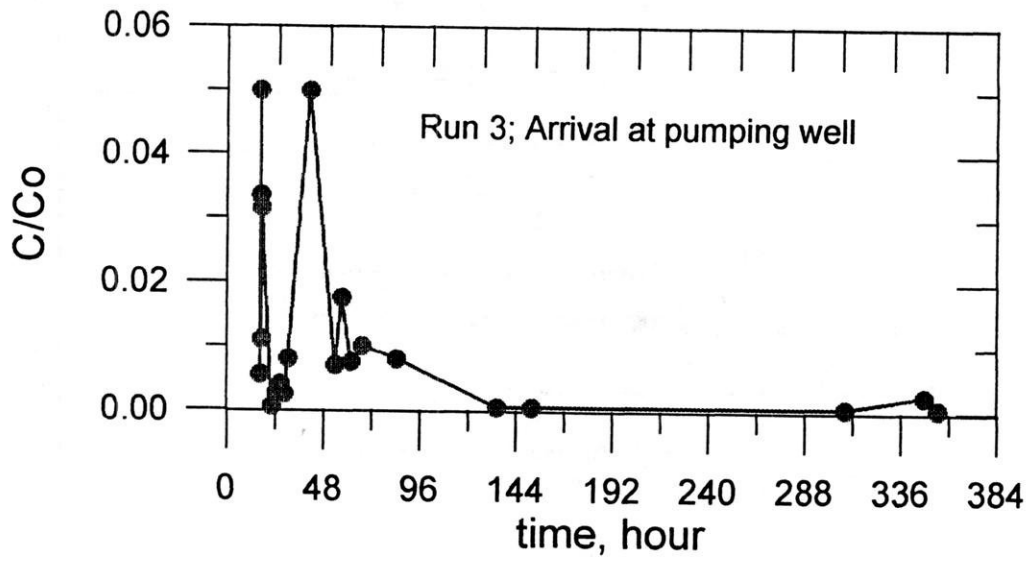


Figure 46. Simulated breakthrough at the withdrawal well.

CHAPTER 5

CONCLUSIONS

Detailed site characterization, hydraulic tests, tracer tests, and preliminary modeling experiments suggest that standard investigative and monitoring techniques may not be appropriate to characterize site-specific transport in fractured-carbonate aquifers.

The hydrogeologic site characterization completed at the Bissen Quarry was designed to determine both "continuum" aquifer properties, determined by standard monitoring techniques (*i.e.* "open-hole" pumping tests), as well as the properties of discrete fractures. Comparison of distributions of hydraulic head and hydraulic conductivity determined by these two approaches suggests that standard hydrogeologic field techniques, including long-interval monitoring wells, are of limited use in providing information on the flow characteristics of fractured-carbonate aquifers at a site-specific scale.

Hydraulic conductivity tests at several scales show that traditional pumping tests are inadequate to characterize the study site for the purposes of groundwater movement and solute transport. The bulk hydraulic conductivity of the dolomite, measured in the open-hole pumping test, ranges from 1.8×10^{-5} to 1.3×10^{-4} ft/sec with a geometric mean value of 3.9×10^{-4} ft/sec. However, short-interval packer tests yield a much larger range of measured values (1.4×10^{-2} ft/sec to 2.3×10^{-8} ft/sec, geometric mean 9.9×10^{-6} ft/sec). Tracer tests yielded horizontal and vertical groundwater velocities on the order of 10's to 100's ft/day. These velocities are consistent with maximum hydraulic conductivities derived from short-interval packer tests and are inconsistent with velocities from traditional pumping tests.

Accurate determination of head distributions is essential to determining flow directions, designing a monitoring system, or designing an effective remediation plan. The distribution of hydraulic head in fractured-rock aquifers can be difficult to characterize since the head distributions in fractures may be very different than the head distribution in matrix blocks. Water levels in open holes provided head measurements integrated over approximately a 30-ft saturated section; these data suggest a dynamic flow system that responds rapidly to recharge events. Data from the multi-level samplers indicates a much more complex three-dimensional distribution of hydraulic head. Determination of flow direction is difficult as the magnitude and direction of the horizontal hydraulic gradient varies across the site and from one discrete fracture to the next. In addition, horizontal gradients within large fractures are quite low. Vertical gradients are larger than horizontal gradients and tend to reverse seasonally. The significant differences in the head distributions determined from the open boreholes and the multi-level samplers shows the necessity of discrete zone monitoring to describe the head distribution in fractured carbonate aquifers. Wisconsin monitoring well code (NR141) specifies that water-table wells have a 3- to 10-ft screen and that open bedrock wells (without screen) must be cased to a minimum depth of 2 feet and open below that. Neither of these standard monitoring well designs would be capable of

providing the detailed head information required for determination of groundwater flowpaths at site-specific scales in settings similar to Bissen Quarry.

The tests conducted at Bissen Quarry during the summer of 1994 suggest that the fracture network at the site is well-integrated both horizontally and vertically. The dominant horizontal flow paths are developed along bedding plane fractures at approximately 92, 82, and 75 ft elevation. The measured horizontal and vertical velocities for all tests are on the order of 10's to 100's of ft/day.

Tracer results indicate that hydraulic data alone are poor predictors of transport at small scales. Even with the detailed, three-dimensional head distribution measured in the multi-level samplers, it was difficult to predict tracer movement. Transport at site-specific scales appears to be dominated by discrete fracture pathways and channels within the fractures. These results suggest that contaminants will be difficult to detect in these settings, especially with standard monitoring wells constructed with long open intervals. Monitoring systems designed to monitor the high-permeability pathways are more likely to intercept contaminants. The measured tracer velocities of 10's to 100's of ft/day suggests that standard monitoring frequencies, such as quarterly sampling, would not detect a contaminant release in a timely fashion.

Using measured data on fracture characteristics, the fracture network models reproduce the data from the preliminary tracer experiment relatively well. Fracture-network models are more appropriate than porous-medium models for simulating flow and transport in these environments; future investigations should collect appropriate data for the use of these models.

REFERENCES

- Abelin, H., L. Birgersson, J. Gidlund, and I. Neretnieks, 1991a. A large-scale flow and tracer experiment in granite, 1. Experimental design and flow distribution. *Water Resources Research*, vol 27, no 12, p. 3107-3117.
- Abelin, H., L. Birgersson, L. Moreno, H. Widen, T. Ågren, and I. Neretnieks, 1991b. A large-scale flow and tracer experiment in granite, 2. Results and Interpretation. *Water Resources Research*, vol 27, no 12, p. 3119-3135.
- Alexander, E.C., Jr., and J.F. Quinlan, 1992. *Practical Tracing of Groundwater with Emphasis on Karst Terranes*, Short Course Manual. Geological Society of America, Boulder, Colorado, 2 vols.
- ASTM, 1995. D5717 *Standard Guide for the Design of Ground-water Monitoring Systems in Karst and Fractured-rock Aquifers*, American Society of Testing and Materials, West Conshohocken, PA. 1998 Annual Book of ASTM Standards, Vol 04.09, p. 439-455.
- Billaux, D., J.P. Chiles, K. Hestir, and J. Long, 1989. Three-dimensional statistical modelling of a fractured rock mass - an example from the Fanay-Augères mine. *International Journal of Rock Mechanics, Mineral Science and Geomechanical Abstracts*, vol 26, no 3/4, 281-299.
- Bradbury, K.R., 1982. *Hydrogeologic relationships between Green Bay of Lake Michigan and onshore aquifers in Door County, Wisconsin*: unpublished Ph.D. Thesis - Geology, Univ. of Wisconsin, Madison, 287 p.
- Bradbury, K.R., 1989. Door County's groundwater: An asset or a liability? *In: Conference Proceedings, Door County and the Niagara Escarpment: Foundations for the future*, K. Hershbell, ed., Wisconsin Academy of Sciences, Arts, and Letters, Madison. p. 36-44.
- Bradbury, K.R., M.A. Muldoon, A. Zaporozec, and J. Levy. 1991. *Delineation of wellhead protection areas in fractured rocks*. U.S. EPA Technical Guidance Document, 144 p.
- Bradbury, K.R., and M.A. Muldoon, 1992. *Hydrogeology and groundwater monitoring of fractured dolomite in the Upper Door Priority Watershed, Door County, Wisconsin*. Wisconsin Geological and Natural History Survey Open File Report, WOFR 92-2, 84 p.
- Bradbury, K.R., and M.A. Muldoon, 1993. Preliminary comparison of a discrete fracture model with a continuum model for groundwater movement in fractured dolomite. Final administrative report to the Wisconsin Department of natural Resources in fulfillment of DNR Contract # NRB96011. 39 p.

- Bradbury, K.R., and Muldoon, M.A., 1994. Effects of fracture density and anisotropy on wellhead protection area delineation in fractured-rock aquifers. *Applied Hydrogeology*, vol 2, no 3, p. 17-23.
- Cacas, M.C., E. Ledoux, G. de Marsily, B. Tillie, A. Barbreau, E. Durand, B. Feuga, and P. Peaudecerf, 1990a. Modeling fracture flow with a stochastic discrete fracture network, Calibration and validation, 1. The flow model. *Water Resources Research*, vol 26, no 3, p. 479-489.
- Cacas, M.C., E. Ledoux, G. de Marsily, A. Barbreau, P. Calmels, B. Gaillard, and R. Margritta, 1990b. Modeling fracture flow with a stochastic discrete fracture network: calibration and validation, 2. The transport model. *Water Resources Research*, vol 26, no 3, p. 491-500.
- Cady, C.S., S.E. Silliman, and E. Shaffern, 1993. Variation in aperture estimate ratios from hydraulic and tracer tests in a single fracture. *Water Resources Research*, vol 29, no 9, p. 2975-2982.
- Chamberlin, T.C. 1877. *Geology of Wisconsin, Volume 2. Survey of 1873-1877*: Wisconsin Geological and Natural History Survey, Madison, Wisconsin. p. 335-389.
- Cherkauer, D.S, P.F. McKereghan, and L.H. Schalch, 1992. Delivery of chloride and nitrate by ground water to the Great Lakes: Case Study for the Door Peninsula, Wisconsin. *Ground Water*, vol 30, no 6, p. 885-894.
- Cooper, H.H., and C.E. Jacob, 1946. A generalized graphical method for evaluating formation constants and summarizing well field history. *American Geophysical Union Transactions*, vol 27, p. 526-534.
- Davis, S.N. , D.J. Campbell, H.W. Bentley, T.J. Flynn, 1985. *Ground-water Tracers*. Cooperative Agreement CR-810036, Robert S. Kerr Environmental Research Laboratory, Ada, Oklahoma, National Well Water Association, Worthington, Ohio, 200 p.
- Dershowitz, W, A. Herbert, and J. Long, 1989. *Fracture Flow Code Cross-Verification Plan*. Stripa Project Technical Report 89-02, Swedish Nuclear Fuel and Waste Management Company, 64 p.
- Dershowitz, W, G. Lee, J. Geier, S. Hitchcock, and P. LaPointe, 1993. FRACMAN, Version 2.306: Interactive Discrete Feature Data Analysis, Geometric Modeling, and Exploration Simulation: User Documentation. Golder Associates, Seattle, Washington.
- Dronfield, D.C., and S.E. Silliman, 1993. Velocity dependence of dispersion for transport through a single fracture. *Water Resources Research*, vol 29, no 10, p. 3477-3483.

- Dunham, R.J., 1962. Classification of carbonate rocks according to depositional texture. In: *Classification of Carbonate Rocks*, W.E. Ham, ed., American Association of Petroleum Geologists, Memoir 1, p. 108-121.
- Garabedian, S.P., D. R. LeBlanc, L.W. Gelhar, and M.A. Celia, 1991. Large-scale natural gradient tracer test in sand and gravel, Cape Cod, Massachusetts 2. Analysis of spatial moments for a nonreactive tracer, *Water Resources Research*, vol 27, no 5, 911-924.
- Gianniny, G.L., M.A. Muldoon, J.A. Simo, and K.R. Bradbury, 1996. *Correlation of high-permeability zones with stratigraphic features in the Silurian dolomite, Sturgeon Bay, Wisconsin*. Wisconsin Geological and Natural History Survey Open File Report, WOFR 1996-7, 102 p. and 1 plate.
- Hegrenes, D., 1996. *A Core Study of the Sedimentology, Stratigraphy, Porosity and Hydrogeology of the Silurian Aquifer in Door County, Wisconsin*. Unpublished M.S. Thesis, University of Wisconsin-Milwaukee, 156 p.
- Hess, K.M., S.H. Wolf, and M.A. Celia, 1992. Large-scale natural gradient tracer test in sand and gravel, Cape Cod, Massachusetts 3. hydraulic conductivity variability and calculated macrodispersivities, *Water Resources Research*, vol 28, no 8, p. 2011-2027.
- Hsieh, P.A., A.M. Shapiro, C.C. Barton, F.P. Haeni, C.D. Johnson, C.W. Martin, F.L. Paillet, T.C. Winter, and D.L. Wright, 1993. Methods of characterizing fluid movement and chemical transport in fractured rock, in Chaney, J.T. and J.C. Hepburn (eds.) *Field Trip Guidebook for Northeastern United States*, Geological Society of America, Annual Meeting, October 25-28, Boston, Massachusetts, 30 p.
- Hvorslev, M.J. 1951. Time-lag and soil permeability in groundwater observations: U.S. Army Corps of Engineers, Waterways Experiment Station Bulletin No. 36, Vicksburg, MS, 50 p.
- LaPointe, P.R., and J.A. Hudson, 1985. Characterization and interpretation of rock mass joint patterns. *Geological Society of America Special Paper 199*, 37 p.
- Laslett, G.M., 1982. Censoring and edge effects in areal and line transect sampling of rock joint traces, *Mathematical Geology*, vol 14, no 2, 125-140.
- Leap, D.I., and P.M. Belmonte, 1992. Influence of pore pressure on apparent dispersivity of a fissured dolomite aquifer. *Ground Water* vol 30 no 1, p. 87-95.
- LeBlanc, D.R., S.P. Garabedian, K.M. Hess, L.W. Gelhar, R.D. Quadri, K.G. Stollenwerk, and W.W. Wood, 1991. Large-Scale natural gradient tracer test in sand and gravel, Cape Cod, Massachusetts 1. Experimental design and observed tracer movement. *Water Resources Research*, vol 27, no 5, 895-910.



b89072246382a

- McDonald, M.G., and Harbaugh, A.W., 1988. A modular three-dimensional finite-difference ground-water flow model: Chapter A1, Book 6, Modeling techniques, Techniques of Water-Resources Investigations of the U.S. Geological Survey.
- Mackay, D.M., D.L. Freyberg, P.V. Roberts, and J.A. Cherry, 1986. A natural gradient experiment on solute transport in a sand aquifer; 1. Approach and overview of plume movement: *Water Resources Research*, vol 22, no 13, p. 2017-2029.
- McKenna, S.A., and L.C. Meigs, 1997. Evaluation of the effects of heterogeneity and matrix diffusion on tracer breakthrough curve tailing (abstract). Geological Society of America, Abstracts with Programs. vol 29, no 6, p. A369.
- Moench, A.F., 1984. Double-porosity models for a fissured groundwater reservoir with fracture skin. *Water Resources Research*, vol 20, no 7, p. 831-846.
- Moltyaner, G.L., M.H. Klukas, C.A. Wills, and R.W.D. Killey 1993. Numerical Simulations of Twin-Lakes Natural-Gradient Tracer Test: A Comparison of Methods, *Water Resources Research*, vol 29, no 10, p. 3433-3452.
- Muldoon, M.A., and K.R. Bradbury, 1990. Monitoring spatial and temporal variations of hydraulic head in a fractured dolomite aquifer (abstract). Geological Society of America, Abstracts with Programs. vol 22, no 7, p. A370
- Muldoon, M.A., 1996. Vertical Variability of Hydraulic Conductivity in a Fractured Dolomite Aquifer, Door County, Wisconsin. (Abstract) EOS, vol 77, no 46, p. F219.
- Muldoon, M.A., 1998. *Supplemental data for tracer studies performed at Bissen Quarry, Door County, Wisconsin, 1993-1997*. Wisconsin Geological and Natural History Survey Open File Report, WOFR 1998-3.
- Muldoon, M.A., J.A. Simo, and K.R. Bradbury, in prep. Correlation of high-permeability zones with stratigraphy in a fractured-dolomite aquifer, Door County, Wisconsin In: *Groundwater Flow and Contaminant Transport in Carbonate Aquifers*, C. Wicks and I. Saskowsky, eds., Geological Society of America Special Paper,.
- National Research Council (Committee on Fracture Characterization and Fluid Flow), 1996. *Rock Fractures and Fluid Flow: Contemporary Understanding and Applications*: National Academy Press, Washington D.C., 551 p.
- Nauta, R. 1987. *A three-dimensional groundwater flow model of the Silurian dolomite aquifer of Door County, Wisconsin*: M.S. Thesis - Geology, Univ. of Wisconsin, Madison, 105 p.

- Neuman, S.P., 1975. Analysis of pumping test data from anisotropic unconfined aquifers considering delayed yield. *Water Resources Research*, vol 11, no 2, p. 329-342.
- Orion Research, Inc., 1991. Instruction manual, Halide Electrodes, models 94-35 and 94-53, Cambridge, Mass, 29 p.
- Paillet, F., R. Crowder, and A. Hess, 1996. High-resolution flowmeter logging applications with the heat-pulse flowmeter. *Journal of Environmental and Engineering Geophysics*, vol 1, no 1, p. 1-11.
- Rouleau, A. 1988. A numerical simulator for flow and transport in stochastic discrete fracture networks. NHRI Paper 39, National Hydrology Research Institute, Saskatoon, Saskatchewan. 204 p.
- Rovey, C.W. II, and D.S. Cherkauer, 1994. Relation between hydraulic conductivity and texture in a carbonate aquifer: Observations. *Ground Water*, vol 32, no 1, p. 53-62.
- Shapiro, A.M., 1988. Interpretation of tracer tests conducted in an areally extensive fracture in a northeastern Illinois dolomite. *In Proceedings of the International Conference on Fluid Flow in Fractured Rock*, Atlanta, GA, May 15-18, 1988. p 12-22.
- Shapiro, A.M., and J.R. Nicholas, 1989. Assessing the validity of the channel model of fracture aperture under field conditions. *Water Resources Research*, vol 25, no 5, 817-828.
- Sherrill, M.G. 1978. Geology and ground water in Door County, Wisconsin, with emphasis on contamination potential in the Silurian dolomite: U.S. Geological Survey Water-Supply Paper 2047, 38 p.
- Shrock, R.R. 1940. Geology of Washington Island and its neighbors, Door County, Wisconsin: Wisconsin Academy of Sciences Transactions, p. 199-227.
- Slichter, C.S., 1905. Field measurement of the rate of movement of underground waters: U.S. Water Supply and Irrigation Paper No. 140, 122 p.
- Sudicky, E.A., 1986. A natural gradient experiment on solute transport in a sand aquifer: Spatial variability of hydraulic conductivity and its role in the dispersion process. *Water Resources Research*, vol 22, no 13, p. 2069-2082.
- Waldhuetter, K.R., 1994. *Stratigraphy, Sedimentology, and Porosity Distribution of the Silurian Aquifer, The Door Peninsula, Wisconsin*. Unpublished M.S. Thesis, UW-Milwaukee, 210 p.

89072246382



B89072246382A

051268
Tracer Study for
Characterization of ...

10-77-9a Mick Day

WATER RESOURCES INSTITUTE
LIBRARY
UNIVERSITY OF WISCONSIN
1975 WILLOW DRIVE
MADISON, WI 53706-1103
608-262-3069

DEMCO